Theta guided sequences in the medial entorhinal cortex

A Thesis

Submitted in partial fulfillment of the requirements

for the degree of

Doctor of Philosophy

by

Arun Neru

ID: 20133243

2019

Certificate

Certified that the work incorporated in the thesis entitled *Theta guided sequences in the medial entorhinal cortex* , submitted by Mr. Arun Neru , was carried out by the candidate, under my supervision. The work presented here or any part of it has not been included in any other thesis submitted previously for the award of any degree or diploma from any other University or institutions.

Dr. Collins Assisi

June 11, 2019

Declaration

I declare that this written submission represents my ideas in my own words, and where others' ideas have been included, I have adequately cited and referenced the original sources. I also declare that I have adhered to all principles of academic honesty and integrity and have not misrepresented or fabricated or falsified any idea/data/fact/source in my submission. I understand that violation of the above will be cause for disciplinary action by the Institute and also evoke penal action from the sources which have thus not been properly cited or from whom proper permission has not been taken when needed.

Arun Neru

June 11, 2019

Acknowledgements

I thank my supervisor Dr. Collins Assisi for giving me the opportunity and independence to pursue PhD in his lab. His insights and valuable suggestions helped me to see the fruition of my PhD.

I thank my RAC members Dr. Pranay Goel, Dr. Raghav Rajan and Dr. Yoganarasimha Doreswamy for their regular and timely suggestions. My sincere thanks to Prof. Shashidharaa, Prof. Sanjeev Galande and IISER Pune for providing financial assistance and infrastructure and to University Grants Commission for my PhD scholarship.

I would like to thank all the past and present members of Computational Neruobiology Lab. I owe my sincere gratitude to my informal co-supervisor Dr. Suhita Nadkarni for regular insights on my work and for maintaining a cheerful lab environment. I, especially, thank Mr. Pranav Kulkarni for developing the simulation software - in silico, and teaching me the know-how. I also thank Shivik, Anup, Gaurang, Rohan, Nishant, Sandeep, Shruti, Prathyush, Bharat, Vidya, Vishnu, and Subadhra for their clever suggestions and scintillating scientific discussions.

I thank all the friends from IISER pune for making me feel like a member of a big family. I would like to thank Boomi, Senthil, and Harsha for all their stress-busting chit-chats. I would thank my batch-mates Niraja, Neelesh, Tanushree, and Kunalika for the wonderful memories they are part of, which I will cherish forever. Special thanks to Bhavani for her moral and financial support.

Last but not in least, I would like to thank my parents and siblings, for standing by me in all the ebbs and flows of my life, for which I am greatly indebted.

Arun Neru

June 2019

Synopsis

Name of the student	**Arun Neru**
Registration Number	**20133243**
Name of the supervisor	**Collins Assisi**
Date of joining	**2-January-2013**
Thesis title	**Theta guided sequences in the medial entorhinal cortex**

Introduction

Spatiotemporal patterns of neural activity encode our sensory world and our perception of it [Wehr and Laurent, 1996]. These patterns encode memories and are invoked as we recall them later [Pastalkova et al., 2008, Jones and Wilson, 2005, Robbe et al., 2006]. The hippocampal formation receive multisensory cortical inputs and send projections to structures involved in affecting behaviour [Cappaert et al., 2015]. It also sends extensive feedback to the cortical input layers and participates in consolidating short term memories. Removal of the hippocampus impairs the acquisition of new memories in humans [Scoville and Milner, 1957]. The neurons of the hippocampal formation are sensitive to spatial locations and uniquely represent spatial trajectories of the animal [O'Keefe, 1976, Frank et al., 2001]. Whenever an animal visits a unique spatial location within an enclosure, a place cell of the hippocampus encode that location with an elevated firing rate [O'Keefe, 1976]. In the medial entorhinal cortex, neurons fire in locations on the enclosure that are arranged on the vertices of a regular hexagonal grid like pattern. These neurons were named grid cells [Hafting et al., 2005]. Sequential responses of place cells and grid cells of the hippocampal formation are also observed when animals navigate non-spatial sensory dimensions [Aronov et al., 2017].

As is true for many other cortical local circuits, a closer look at the entorhinal cortex reveals that the coding properties of neurons are influenced both by the internal architecture and afferent inputs. Given that it is bombarded with noisy sensory inputs and the internal influences on spiking are mostly noisy as well, how do neurons in the medial entorhinal cortex produce the stable sequential activity required for spatially precise firing fields with hexagonal symmetry? A crucial factor that plays a role was suggested by the experiments of Koenig et. al [Koenig et al., 2011], and Brandon et. al [Brandon et al., 2011]. They had transiently stopped theta rhythmic inputs arriving from the medial septum and found that the periodicity of the grid fields was also vanished. The grid cell pattern returned with the recovery of theta oscillation.

Dynamical regimes of medial entorhinal cortex

Using a motif characteristic of MEC, we show two dynamical regimes: An autonomous oscillator and a multistable switch. One of the states reflect self-organized patterns while the other faithfully responds to sensory inputs. The motif comprised two fast-spiking inhibitory interneurons and two stellate cells, with inhibitory interneurons sending inhibition to each other and to stellate cells. The stellate cells had intrinsic conductances that enabled them to rebound spike in response to inhibition. The activity switched autonomously when stellate cell spikes excited postsynaptic quiescent interneurons. The interneuron, in turn, recruited the other stellate cell and the alternating pattern of activity continued. This oscillatory pattern came to a halt when depolarizing drive to both the inhibitory interneurons increased. In this regime, depending on the initial transients, either of the two interneurons remained active continually, inhibiting the other neuron. A transient, external pulse could be used to switch the activity from one interneuron to the other. Thus, as a function of the firing rate of fast-spiking interneurons, the network motif can either be in an autonomous switching regime or in a bistable state where an external pulse can toggle the states.

Theta induced reliability

To model the experimental findings of Koenig et al [Koenig et al., 2011], we implemented a network of stellate cells and interneurons arranged on a ring. The adjacent stellate cells received overlapping inhibition. The adjacent interneurons on the ring were sequentially recruited in time by a traveling pulse of transient input that mimics the grid-like receptive fields as an animal traverses space. We simulated two scenarios: One where the interneurons passively recruited stellate cells, and the other where the stellate cells sent feedback connections to the inhibitory ring in a random manner. When the external, transient pulse recruited successive interneurons arranged on the ring, the switch in the activity of the inhibitory population was registered as rebound spikes in the stellate cell population. When excitatory connections were introduced, we found that the sequential of stellate cell population did not faithfully follow the input. However, when interneurons received theta rhythmic input in addition to the excitatory drive, the network reliably followed the input.

Mechanism of theta induced reliability

How does theta interact with the inputs to generate a reliable sequence? We found that when input arrived at specific phase window of theta it reliably caused a switch in the inhibitory neurons. Further theta rhythmic inhibition to interneurons synchronized the response of postsynaptic stellate cells and relegated them to the least receptive phases of theta. This phenomenon remained robust to varying frequencies of theta. In contrast, in the absence of theta, rebound spikes competed with external inputs and disrupted the sequence that followed.

Flexible routing of reliable information with theta rhythm

Theta created temporal windows where the MEC network reliably respond to input. Here, we modeled a scenario where the local circuit could flexibly respond to either of the two competing inputs that induced a different sequential response in the circuit. Inputs that arrived at the depolarizing phase of theta caused a successful switching

and were represented in the network activity. When both the inputs arrived at the depolarizing phase of theta, the latest input caused a successful switching.

Inheriting phase precession

Next we tackled the related phenomenon of phase precession in the medial entorhinal cortex. Phase precession exemplifies one of the most studied temporal coding schemes in the central nervous system. The spatially modulated neurons of the hippocampal formation, align their spikes to local LFP fluctuations. As the animal moves through the receptive field of a place cell, the neuron fires at progressively earlier phases of theta [OKeefe and Recce, 1993, Skaggs et al., 1996, Hafting et al., 2008]. We show that stellate cells can inherit phase precession from interneurons via rebound spiking. Although phase precession occurs de novo in a novel environment, they become more robust with experience [Feng et al., 2015]. We found that the slope of phase precession induced in the postsynaptic stellate cell was modulated as a function of the shape of the connectivity profile. A learning induced asymmetries in particular direction increased the slope of phase precession.

Discussion

We will examine how our model compares with the experimental findings of Yartsev et al [Yartsev et al., 2011], where they found grid cells that produced grid fields in the absence of theta oscillatory LFP fluctuations. MEC harbors plasticity mechanisms that, when combined with our model, might lead to learning of sequential responses [Haas et al., 2006]. Also, the apparent contradiction of inducing reliability, by relegating stellate cells to a narrow range of phases, and the observed phase precession of spikes of grid cells is dispelled by noting the finer points of phase precession in MEC [Mizuseki et al., 2009], and potential synaptic processes that could alleviate this incompatibility. Our model would suggest that interneurons possess narrower tuning profiles. However recent experiments [Buetfering et al., 2014] have indicated that interneurons' tuning profiles are broadly tuned. We suggest ways our results can be reconciled with this observation.

References

[Aronov et al., 2017] Aronov, D., Nevers, R., and Tank, D. W. (2017). Mapping of a non-spatial dimension by the hippocampal–entorhinal circuit. *Nature*, 543(7647):719–722.

[Brandon et al., 2011] Brandon, M. P., Bogaard, A. R., Libby, C. P., Connerney, M. A., Gupta, K., and Hasselmo, M. E. (2011). Reduction of Theta Rhythm Dissociates Grid Cell Spatial Periodicity from Directional Tuning. *Science*, 332(6029):595–599.

[Buetfering et al., 2014] Buetfering, C., Allen, K., and Monyer, H. (2014). Parvalbumin interneurons provide grid cell–driven recurrent inhibition in the medial entorhinal cortex. *Nature Neuroscience*, 17(5):710–718.

[Cappaert et al., 2015] Cappaert, N. L., Strien, N. M. V., and Witter, M. P. (2015). Chapter 20 - hippocampal formation. In Paxinos, G., editor, *The Rat Nervous System (Fourth Edition)*, pages 511 – 573. Academic Press, San Diego, fourth edition edition.

[Feng et al., 2015] Feng, T., Silva, D., and Foster, D. J. (2015). Dissociation between the experience-dependent development of hippocampal theta sequences and single-trial phase precession. *Journal of Neuroscience*, 35(12):4890–4902.

[Frank et al., 2001] Frank, L. M., Brown, E. N., and Wilson, M. A. (2001). A comparison of the firing properties of putative excitatory and inhibitory neurons from CA1 and the entorhinal cortex. *Journal of Neurophysiology*, 86(4):2029–2040.

[Haas et al., 2006] Haas, J. S., Nowotny, T., and Abarbanel, H. (2006). Spike-timing-dependent plasticity of inhibitory synapses in the entorhinal cortex. *Journal of Neurophysiology*, 96(6):3305–3313.

[Hafting et al., 2008] Hafting, T., Fyhn, M., Bonnevie, T., Moser, M.-B., and Moser, E. I. (2008). Hippocampus-independent phase precession in entorhinal grid cells. *Nature*, 453(7199):1248–1252.

[Hafting et al., 2005] Hafting, T., Fyhn, M., Molden, S., Moser, M.-B., and Moser, E. I. (2005). Microstructure of a spatial map in the entorhinal cortex. *Nature*, 436(7052):801–6.

[Jones and Wilson, 2005] Jones, M. W. and Wilson, M. A. (2005). Theta rhythms coordinate hippocampal–prefrontal interactions in a spatial memory task. *PLOS Biology*, 3(12).

[Koenig et al., 2011] Koenig, J., Linder, A. N., Leutgeb, J. K., and Leutgeb, S. (2011). The spatial periodicity of grid cells. *Science*, 592(Issue: 6029):592–595.

[Mizuseki et al., 2009] Mizuseki, K., Sirota, A., Pastalkova, E., and Buzsáki, G. (2009). Theta oscillations provide temporal windows for local circuit computation in the entorhinal-hippocampal loop. *Neuron*, 64(2):267–280. 19874793[pmid].

[O'Keefe, 1976] O'Keefe, J. (1976). Place units in the hippocampus of the freely moving rat. *Experimental Neurology*, 51(1):78–109.

[OKeefe and Recce, 1993] OKeefe, J. and Recce, M. L. (1993). Phase relationship between hippocampal place units and the EEG theta rhythm. *Hippocampus*, 3(3):317–330.

[Pastalkova et al., 2008] Pastalkova, E., Itskov, V., Amarasingham, A., and Buzsaki, G. (2008). Internally generated cell assembly sequences in the rat hippocampus. *Science*, 321(5894):1322–1327.

[Robbe et al., 2006] Robbe, D., Montgomery, S. M., Thome, A., Rueda-Orozco, P. E., McNaughton, B. L., and Buzsaki, G. (2006). Cannabinoids reveal importance of spike timing coordination in hippocampal function. *Nature Neuroscience*, 9(12):1526–1533.

[Scoville and Milner, 1957] Scoville, W. B. and Milner, B. (1957). Loss of recent memory after bilateral hippocampal lesions. *Journal of Neurology, Neurosurgery & Psychiatry*, 20(1):11–21.

[Skaggs et al., 1996] Skaggs, W. E., McNaughton, B. L., Wilson, M. A., and Barnes, C. A. (1996). Theta phase precession in hippocampal neuronal populations and the compression of temporal sequences. *Hippocampus*, 6(2):149–172.

[Wehr and Laurent, 1996] Wehr, M. and Laurent, G. (1996). Odour encoding by temporal sequences of firing in oscillating neural assemblies. *Nature*, 384(6605):162–166.

[Yartsev et al., 2011] Yartsev, M. M., Witter, M. P., and Ulanovsky, N. (2011). Grid cells without theta oscillations in the entorhinal cortex of bats. *Nature*, 479(7371):103–107.

Contents

List of Figures

List of Tables

Chapter 1

Introduction

The nervous system of the animals has evolved to coordinate stereotypical behaviours that are essential for survival. These are specialized in learning from past environmental variations to bring about adaptive behaviours at opportune moments. To be able to select an appropriate behaviour in a given context, the representation of the external world in the activity of brain must be stable and reproducible [Stangl et al., 2018, Valerio and Taube, 2012, Weiss et al., 2017]. The neurons and synapses of the brain circuits have mechanisms in place that enable sensory experiences to modify the intrinsic properties of neurons [Kim and Linden, 2007, Narayanan and Johnston, 2010], integrative properties of synapses [Buonomano and Merzenich, 1998, Shouval et al., 2002], and synaptic connectivity [Igarashi, 2015] in a direction that potentially improves future behavioural response of the animal. These plasticity mechanisms often rely on precise neural activity of the constituent circuits. Adaptive behaviour requires reliable representations and the ability to transmit these representations across brain regions [Frank et al., 2000, Kim and Lee, 2011, Fujisawa and Buzsáki, 2011, DeCoteau et al., 2007, Benchenane et al., 2010, Barnes et al., 2005].

Rather than acting as a sequence of relays from the peripheral sensors to skeletal muscles, the brain exhibits elaborate patterns of activity by ensembles of neurons. This was anticipated from earlier behavioural experiments with rodents learning mazes [Tolman, 1948]. In a typical task, a rat was released at an entry door of a maze. It generally received a reward at the exit door. Over time, the rat learned to wade through mazes in shortcuts, spending ever lesser time in the alleys leading to dead ends. The animal quickly learned the appropriate turns based on current cues. The behaviourist viewpoint [Skinner, 1974] prevalent around early twentieth

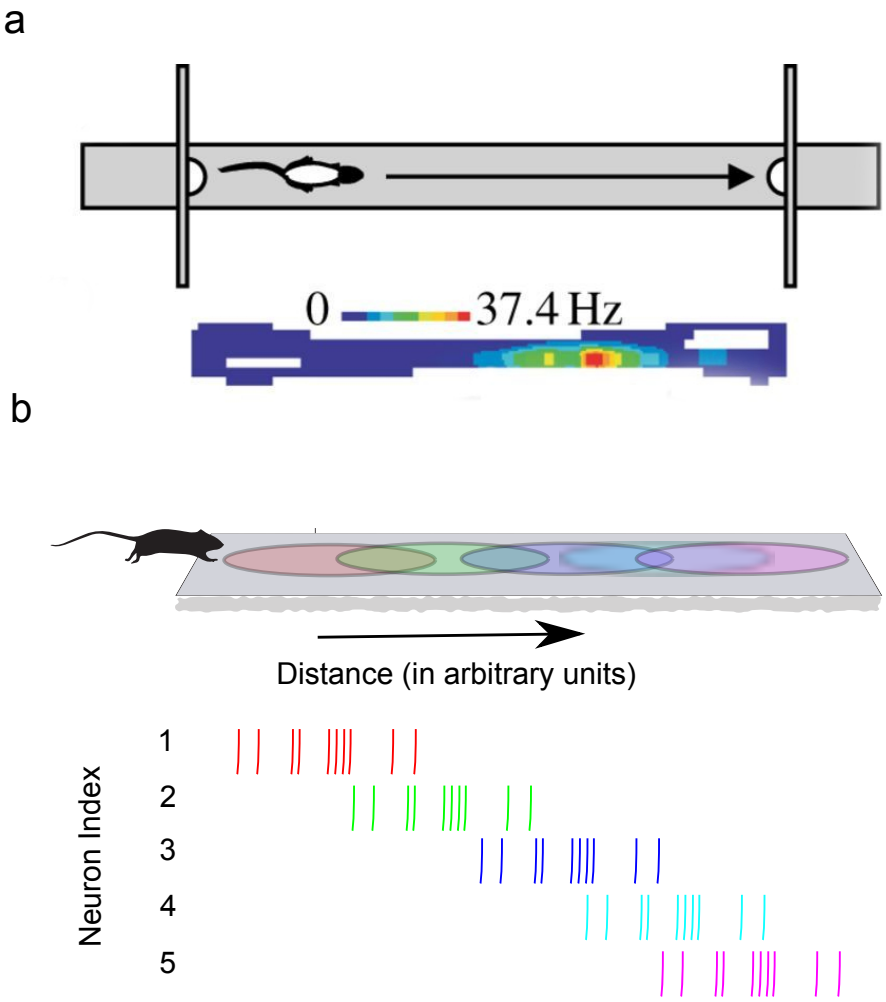

FIGURE 1.1: *Sequence encoding a trajectory.* (a) firing property of a place cell. Upper panel - A schematic of the setup, where a rat is made to run to the other end of a linear track to get a reward, is shown. Lower panel - The firing rate of a single cell recorded from hippocampus, estimated in bins of the the trajectory along the linear track, showing a clear peak in a circumscribed region. From 1 a of [Huxter et al., 2003]. (b) Upper panel - A rat running through five overlapping firing fields (shown as five ellipses of differing colors) of place cells. Lower panel - A schematic illustration, using a raster plot, of sequential activity induced in the place cells as the animal traversed along a trajectory. The vertical lines represent individual action potential spikes generated by the neurons. The colours of the spike train of a place cell is matched to that of the place field. Notice the increased firing rate of the spikes in their respective center of the place field.

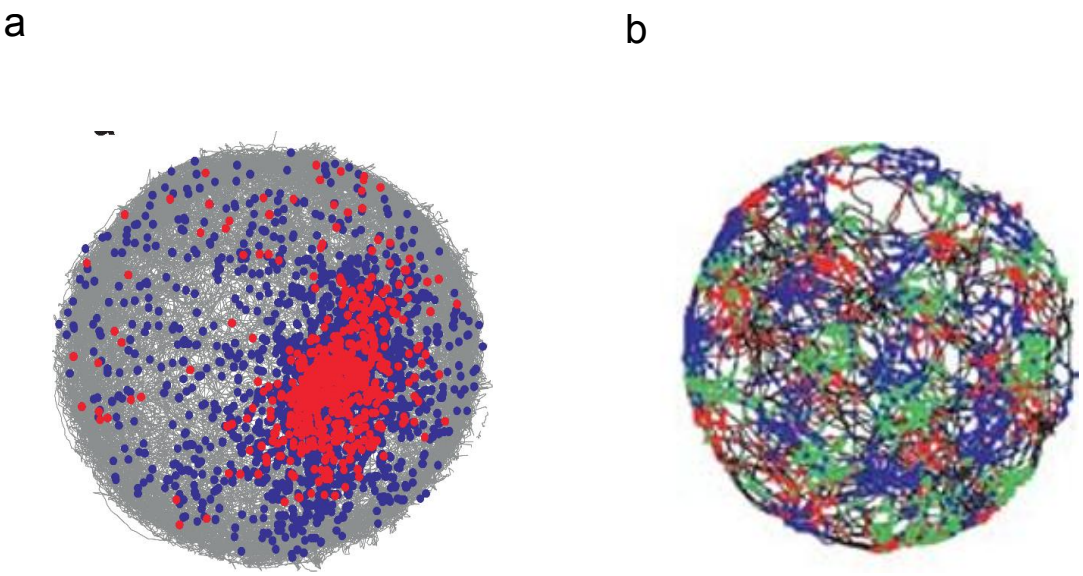

FIGURE 1.2: *Spatial receptive fields of a place cell and a grid cell.* Place cell (a) and grid cell (b) activity as recorded from hippocampus (not shown) [Huxter et al., 2008] and medial entorhinal cortex (not shown) [Hafting et al., 2005] respectively. The black trace represent trajectory of a rat freely moving in a circular enclosure. The color dots mark the location along the trajectory where a simultaneously recorded cell generated action potential spikes. (a) A clearly circumscribed region, called place field, is defined by the firing of a place cell. Both the red and blue dots represent the locations along the trajectory when a simulataneously recorded place cell generated action potential. The red dots represent the spiking that are aligned to the trough of theta oscillation and the blue represent the depolarizing phase. From supplementary figure S5 of [Huxter et al., 2008] (b) The three colored dots represent the firing locations of three simultaneously recorded grid cells from medial entorhinal cortex. The three cells share common orientation and inter grid field distance with shifted location of grid field center with respect to each other. From figure 3 a of [Hafting et al., 2005].

century provided explanations where the strength of stimulus-to-response connection that lead to reward was strengthened while the strength of connections between the stimulus-response pair that was unrewarded was diminished. Behavioural experiments in the early thirties [Tolman, 1948] challenged this viewpoint when they discovered a phenomenon in rats termed 'latent learning'. In these experiments, the rats were not given any rewards, yet when they were given rewards at a later point during the progression of experiments, they found a way to the exit as quickly as control animals trained with rewards from the beginning. These sudden drops in time to exit the maze in unrewarded, freely exploring animals suggested that the animals were building the representation of the maze all along, which they used later when rewards were given. How are these 'cognitive maps' of the world, as they are called, built from sensory input? How are they represented in the brain? Part of the answer to these questions came from experiments performed by John O'Keefe [O'Keefe, 1976].

O'Keefe was recording from neurons in the hippocampus while rats roamed on a raised platform. He found neurons that generated elevated firing rates of action potentials at specific locations on the platform. The hippocampus is distant from the sensory periphery. Neurons in the hippocampus rarely fired in response to simple sensory stimuli. The average response of neurons defined clearly circumscribed regions of space. These neurons were therefore christened, 'Place cells', by O'Keefe. The specific locations were termed 'place fields'(figure 1.1 a). Various models ([OKeefe and Burgess, 2005, Samsonovich and McNaughton, 1997, Schönfeld and Wiskott, 2015]) have been proposed to explain the emergence of place fields since then. Experimental works from several labs have identified complexities and nuances to simple spatially correlated firing of place cells ([Eichenbaum et al., 1999, Eichenbaum, 2014, McNaughton et al., 1996]). Recording simultaneoulsy from many place cells, Wilson and McNaughton identified that place fields of different place cells were distributed throughout the enclosure. Therefore trajectories of animals were represented as sequential activity of place cells with receptive fields situated along the trajectory [Wilson and McNaughton, 1993, Frank et al., 2000] (figure 1.1). Input to the CA1 comes from MEC. To understand the origins of place cell pattern, Hafting et. al [Hafting et al., 2005] started to record the neural activity

from the medial entorhinal cortex. In doing so, they had discovered neurons that fired preferentially at multiple locations. The locations, where the cell fired action potentials, were arranged at the vertices of a hexagonal grid pattern in a two dimensional arena. The cells were therefore named grid cells (figure 1.2 b). Neighboring grid cells have grid fields that are shifted with respect to each other and covered the entire arena.

Apart from its role in spatial navigation, as exemplified by the existence of place cells and grid cells, hippocampal formation is also implicated in episodic memory formation in humans. In the years following 1950, Scolville and Milner encountered patients with epilepsy with sources deep in medial temporal lobe. They had to remove hippocampal regions bilaterally. They had to turn to this recourse when other forms of medication failed to deliver any remedies. These patients showed symptoms of severe memory impairment: their ability to convert sensory experiences into long term episodic memories was diminished, with a complete loss of episodic memory formation and recall in some patients [Scoville and Milner, 1957]. Thus, the hippocampal formation was implicated in forming memories pertaining to personal experiences, helping animals to find their way around, and in forming maps of the external world.

The Medial entorhinal cortex also (MEC) acts as an interface between hippocampus and neocortical circuits. Anatomical [Couey et al., 2013, Gu et al., 2018, Witter et al., 2017] , electrophysiological [Domnisoru et al., 2013, Tocker et al., 2015] and computational [Burgess et al., 2007, Burak and Fiete, 2009, Kropff and Treves, 2008] explorations suggest that the computational role of entorhinal cortex is influenced by the internal organization as well as by the external inputs it receives from afferent structures. How are these precise sequential responses generated despite unreliable sensory inputs and internally generated noise ? This variability arising from afferent sources and local circuits could confound the reliable formation of grid fields. Theta rhythmic input arriving from a central pattern generator that produces and broadcasts oscillatory inputs to the hippocampal formation is shown to play a role in forming stable sequences. How does theta stabilize these representations? Theta rhythm is also implicated in many brain functions, including encoding and recalling memories and linking distinct regions of the brain into phase synchronized cell

assemblies [Fell et al., 2001, Fell and Axmacher, 2011, Klimesch, 1999, Clouter et al., 2017, Wilson et al., 2015]. How is the role of theta rhythm in formation of stable receptive fields related to the other roles attributed to it ? In this thesis, we will try to understand how theta rhythmic drive can stabilize the response of an MEC motif to sequential sensory inputs. Further, we ask whether this relates to the role of theta in connecting regions across the brain. In this chapter, we will describe the prevalence and role of sequential activity in different brain regions. We will review experimental and computational studies that highlight important factors that contribute to sequential activity in the local microcircuits of the MEC. The diverse role of theta rhythms discovered from many different experiments will also be highlighted.

1.1 Sequential Activity in the brain

Local neural circuits of the brain can generate self organized activity in the absence of any inputs from external sensory world. However, they retain their ability to reshape their dynamics in response to salient external inputs in a behaviourally relevant way [Rabinovich et al., 2006]. The self organized activity often takes the form of an elaborate sequential activity, where the participating neuronal populations divide into groups with one group being active (generating action potentials) at any one moment, and the activity switching among the groups in a predictable manner (A certain group X always leading another group Y in the sequence, for example).

Central pattern generators, where rhythmic patterns of neural activity are initiated and maintained without any structured external inputs, provide illustrative examples of internally generated sequential activity patterns[Getting, 1989, Harris-Warrick and Marder, 1991]. Rhythmic motor patterns generated by central pattern generators underlie behaviours that are essential for survival and are either present throughout the lifetime of an animal (breathing, heartbeat, pyloric rhythm, etc) or switched on in response to sensory inputs (swallowing, chewing, sneezing, mating, gastric mill rhythm etc). Elements of the sequences maintain an order with respect to each other even when the patterns were compressed and stretched in time. These patterns emerge as a result of interactions among intrinsic neuronal properties[Adams and Benson, 1985, Friesen, 1994], strength and time courses of synaptic

interactions [Graubard et al., 1983, Dickinson et al., 1990] and the connectivity patterns. Studies on invertebrate microcircuits continue to provide crucial insights into the functioning of neural networks in general.

In cortical circuits, self organized sequential activity is hypothesized to subserve important cognitive and behavioural roles. In area 18 of the visual cortex of a cat, the neurons that respond to similar stimulus features (angle of orientation of a light bar, in this case) were arranged on contiguous patches. When a light bar with a certain orientation was presented to an awake animal, it activated neurons in spatially periodic patches on the cortical surface. When the orientation changed slightly, a similar overlapping patch of neurons was stimulated. In an anasthetized animal, even when there are no visual stimulus present, the patterns of activity were almost indistinguishable from those observed in the awake animal [Kenet et al., 2003]. Thus, the intracortical connectivity without sensory input can lead to self organized sequential activity of neurons.

Sequences of activity in the hippocampal formation are implicated in spatial navigation, encoding and retrieving episodic memories and binding events to contexts [Frank et al., 2000, Eichenbaum, 2014, Buzsáki and Tingley, 2018]. The hippocampal formation receives multimodal sensory information from most of the sensory modalities routed via the association cortices. In the presence of sensory inputs in an awake, freely behaving animal, the hippocampal formation produced sequential activity of population of neurons that encoded the trajectory of the animal.

The network of neurons of the hippocampal formation include the spatially modulated place cells and grid cells. These neurons can also encode non-spatial attributes. Pastalkova et. al, 2018, trained rats to successfully alternate between two arms of a T-arm maze. In between the traversal of the different arms of the maze, the rats were forced to run on a wheel. The animals were sealed off from any external cues during the wheel running. The hippocampal formation generated sequences during the interim wheel running, without any visual or tactile cues. The sequnces so generated were comparable in temporal scale to that of animals exploring the arms of the maze (figure 1.3). These sequences are generated by the neurons most of which also displayed place fields coding for trajectories along the maze. These internally organized sequences predicted behavioural performance of the animal reliably.

In another experiment, rats were trained on a trace eye blink conditioning task. The time duration between the appearance of conditioned stimulus (tone or odor) and a time point, where an unconditional stimulus had been given in the training sessions, was encoded in a sequential activity of hippocampal neurons [Modi et al., 2014].

Hippocampal sequences that encode spatial trajectories can also encode trajectories through other sensory spaces. Aronov et. al [Aronov et al., 2017] had trained rats to deflect the joysticks to increase the frequency of an auditory pure tone played in the background, and to release the joystick once a target frequency was reached. Hippocampal neurons, many of which showed clear place and grid fields in an open environment also participated in encoding the trajectories that were traversed in auditory space as animals manipulated the joystick. The experimenters manipulated the gain of the joystick on the rate of frequency change along the scale; the frequency at times increased faster, and other times is slowed down in its progression to a target frequency. The neural sequences adapted themselves to these changes in gains and reliably encoded the appropriate frequency (figure 1.3). Hippocampal sequences, to be able to encode spatial locations, have to adapt to varying speeds and head directions. As hippocampal sequences are sensitive to sensory modalities other than that involved in navigation, It has been proposed that trajectories in feature spaces of these stimuli can be encoded by hippocampal sequences. The same mechanism that helped the hippocampal sequences to adapt in response to changing velocity of the animal, as hypothesized, will help them in changing adaptively to changing rate of succession of features along the space.

Sequences of the hippocampal formation thus uniquely represent the trajectories of the animal in space and in abstract feature dimensions. They also encode episodes during working and association memory tasks. Sequences in the cortical structures are also implicated in subserving the roles of planning and decision making [Siegle and Wilson, 2014, Jones and Wilson, 2005b, Jones and Wilson, 2005a, van der Meer and Redish, 2011].

1.2 Mechanism of sequence generation

Various mechanisms have been proposed to generate sequential activity in diverse brain regions. These models were constrained by anatomical configurations of the local and afferent inputs and biophysical properties of constituent neurons. Mechanisms to generate sequences in small network motifs have been studied extensively in central pattern generators of invertebrates [Getting, 1989]. The sequential activity in those circuits could arise either by coupling a rhythmic bursting neuron to a recurrently connected microcircuit [Selverston et al., 1998] or as a consequence of synaptic interactions within a small motif [Skinner et al., 1994]. Inhibitory interactions mediate the emergence of sequential activity pattern in many central pattern generators. For example, two neurons connected via mutual inhibition can generate alternating activity patterns due to intrinsic cellular properties (rebound spiking due to Ih, for example), and integrative properties of synapses [Skinner et al., 1994, Wang and Rinzel, 1992]. Slow temporal processes can order neuron in a mutually inhibitory network generating a sequential activity pattern [Assisi et al., 2011].

1.2.1 Lessons from Anatomy and Physiology

The entorhinal cortex is a cortical structure that surrounds the three layered hippocampal formation. Similar to cortical structures it is divided into six layers , but unlike cortical columns where the inputs are provided to deeper layers, the inputs to entorhinal cortex arrive at superficial layers (layer II and layer III) [Cappaert et al., 2015]. The deeper layers of entorhinal cortex, receive input from hippocampal formation and send projections to many neocortical sites. The deeper layers also receive inputs from few cortical sites (infralimbic and prelimbic cotical regions innervate both MEC and LEC in almost equal proportions, whereas retrosplenial cortex and piriform cortex send inputs that are targeted at layer V neurons MEC and LEC respectively) [Ohara et al., 2018].

Multimodal inputs from association cortices are relayed to the entorhinal cortex at perirhinal and postrhinal cortex, before reaching hippocampus proper. There is

a functional segregation of inputs arriving at entorhinal cortex. The perirhinal cortex receives processed inputs relevant for computing properties of objects and landmarks and redirects it mainly to the lateral entorhinal cortex. The postrhinal cortex receives processed inputs relevant for path integration that it directs to the medial entorhinal cortex [Kerr et al., 2007, Burwell and Amaral, 1998]. The sensory inputs to perirhinal and postrhinal cortex also go directly to the entorhinal cortex. They show similar segregation when directly innervating entorhinal cortex: those sensory pathways that are purported to process majorly visual information streams are targeted to medial entorhinal cortex and those that process object or landmark properties are streamlined to lateral entorhinal cortex. However, some behavioural studies with lesions specifically to the lateral or medial entorhinal cortex [Cauter et al., 2012] and anatomical evidence showing extensive cross-talk between LEC and MEC [Burwell and Amaral, 1998] suggested that the neuronal representation of these structures might overlap. When complexities in the behavioural tasks were introduced, the representations of the lateral and medial entorhinal cortex indeed show overlapping representations [Keene et al., 2016].

The MEC and LEC receive diverse inputs. However, their internal circuit organizations are similar [Witter et al., 2017]. Both the structures posses principal neurons that interact with inhibitory interneurons found abundantly in superficial layers. The medial entorhinal cortex has two principal neuron types that are selectively sensitive to either calbindin or reelin (protein biomarkers). Reelin positive stellate cells, the most predominant of principal neuron types (Four additional subtypes can be distinguished [Winterer et al., 2017]), interacts with each other mainly via parvalbumin positive, fast spiking interneurons [Couey et al., 2013]. Likewise, in the lateral entorhinal cortex, reelin positive fan cells [Nilssen et al., 2018](absence of basal dendrite differentiate them morphologically from stellate cells) interact with each other via 5Hta3 expressing interneurons.

These anatomical observations suggest that the difference in coding properties of neurons in MEC and LEC could arise due to their major differences in afferent inputs and to lesser extent local circuit structures.

1.2.2 Lessons from Modeling studies

Since the discovery of grid cells, various models have been proposed to explain the emergence of spatially periodic firing fields of grid cells. They can be broadly classified based on the level in the neural organization at which they assumed the emergence of the hexagonal pattern: 1) Models where hexagonal periodicity emerges due to integrative properties of individual neurons [Burgess et al., 2007], 2) Models where hexagonal symmetry emerges due to network interaction [McNaughton et al., 2006, Guanella et al., 2007, Navratilova et al., 2011, Burak and Fiete, 2009], and 3) Models where hexagonal symmetry is learned from statistical properties of feed forward inputs [Kropff and Treves, 2008, Weber and Sprekeler, 2018, D'Albis and Kempter, 2017]. We will briefly mention few comparative descriptions of the oscillatory interference model and the continuous attractor models as they pertain to the current thesis. Comprehensive review of different models of grid field generation can be found in other references [Zilli, 2012, Giocomo et al., 2011].

Oscillatory interference model and the continuous attractor model both assume that the function of mEC is to integrate velocity components along different directions to update the location of the animal with respect to local landmarks [Burgess et al., 2007, Burak and Fiete, 2009]. The main difference between these two models arises in the way in which the velocity signal is implemented and integrated.

In oscillatory interference model, velocity is implemented as a change in the instantaneous frequency of membrane potential oscillations. The moment by moment changes of velocity in a particular direction is translated into frequency changes of an oscillation. These oscillation interferes with a fixed frequency oscillation from the somatic oscillator. When the peak of this interference cross a threshold, the neuron generates spikes [OKeefe and Recce, 1993, Lengyel et al., 2003, Burgess et al., 2007]. The interaction of a fixed frquency and velocity dependent frequency leads naturally to spatially periodic, sparse firing patterns. Thus integration of the velocity occurs at the level of a single cell. It is hard to maintain independent oscillations across different dendrites of a neuron, as they would synchronize even with a weak electric coupling [Remme et al., 2010]. However, the independent oscillations can be maintained by external networks [Zilli and Hasselmo, 2010].

In continuous attractor models, the velocity information is implemented in both the firing rate gain of neurons of interconnected network, as well as in the extent of bias in a neural sheet in the direction corresponding to the direction of the animal movement [Zhang, 1996, Samsonovich and McNaughton, 1997, Song, 2005, Navratilova et al., 2011, Burak and Fiete, 2009]. With faster movement of the animal in a certain direction, for example, a subset of neurons in the network are made to fire faster which in turn introduces stronger bias in the propagation of activity along appropriate direction in the neural sheet. [Guanella et al., 2007, Burak and Fiete, 2009]. The recent findings due to Gu. et. al, demonstrating a map-like architecture of mEC reveals that developmental plasticity mechanisms could bring about connectivity schemes [Gu et al., 2018] required for generation of attractor states. In one set of experiments performed with rats entering virtual linear environments, the entering of grid like receptive fields in the virtual linear track was correlated with ramp like depolarization of membrane potential in the stellate cells of the medial entorhinal cortex [Domnisoru et al., 2013]. The stellate cells are the most predominant cell type in layer II MEC, and are shown to form grid like activity pattern for a freely behaving animal [Rowland et al., 2018]. The ramp like increase seems to suggest that it might be the increase in firing rate of a single cell when the activity bump moves across a continuous attractor sets.

Studying correlations between temporally adjacent stellate cells, Tocker et al. concluded that the correlation in depolarizations are occuring in time scales shorter than synaptic transfer [Tocker et al., 2015]. Considering the existence of projections from deeper layers, they suggested that these depolarizations might arise due to feedforward inputs projected from deeper layers of medial entorhinal cortex. The recurrent excitation prevalent in layer III and V, as compared to layer II where it is sparse, make the deeper layers better candidates for path integrating attractors [McNaughton et al., 2006].

Apart from these experiments favoring either of the available models about grid field formation, there are other experiments that elucidated crucial factors that determine the periodicity of the grid cells. One such experiment showed the essential role of fast-spiking inhibitory interneurons of the medial entorhinal cortex. Blocking

the GABAergic inhibition from fast-spiking interneurons that target the somatic region of the principal neurons of mEC, disrupted the precise firing of the grid cells, whereas blocking dendrite targeting somatostatin interneurons left the grid cell firing intact [Miao et al., 2017]. The parvalbumin-positive, fast-spiking interneurons are believed to include speed cells that code exclusively and almost linearly the speed of the animal [Kropff et al., 2015]. These interneurons are also strongly modulated in their firing due to theta rhythmic input from medial septum [Gonzalez-Sulser et al., 2014, Justus et al., 2016]. The theta rhythmic input has also been shown to be carrying speed information in its amplitude [Vanderwolf, 1969, Hinman et al., 2011]. Thus, at higher velocities the amplitude of theta and the extent of theta rhythmicity in the interneurons both increases.

Experimental manipulations that decoupled the visual cues from the internal representation of place fields, grid fields and head direction cells across hippocampal and parahippocampal formation found cohesive nature of these representations [Hargreaves et al., 2007]. The head direction cells that are least modulated by theta rhythm are the first cells to break away from this cohesive bond across structures when confronted with conflicting visual cues [Kornienko et al., 2018]. Thus, theta oscillations, found ubiquitously across these structures, can bind these separate regions together. Theta rhythm has also been shown in coupling regions involved in subserving various behavioral and cognitive demands [Jones and Wilson, 2005b, Kim and Lee, 2011, van der Meer and Redish, 2011]. Feedforward inputs from regions that are coupled to the local circuit via rhythmic oscillation at theta frequency might play a very crucial role in generating stable receptive fields that are cohesive across these widely separated regions of the hippocampal formation.

1.3 Why stability of sequences matter

Stable formation of sequential activity in the hippocampal formation and associated structures is necessary for the animal to perform adaptively in various tasks. For example, in a homing task, animals were trained in darkness to use path integration to find their way back to home cages. Errors in heading direction the animal made

were correlated with misaligned head direction activities in the population of neurons encoding head direction. Thus, reliable representation in the form of dynamic cell assembly sequences representing changes in head directions might help animals to guide their navigation [Valerio and Taube, 2012].

The orientation of the grid-like periodicity is anchored to the borders of the enclosure an animal is exposed to. In a disorientation behavioral task, rats were released into a square enclosure with identical opposite corners. One of the corners was always rewarded. The sessions were divided into blocks of trials that were separated by single trials where the animal was rotated at the beginning of that trial. After this intermittent disorientation, the cohesive population of grid cells and the head direction cells retained either of the two possible representations: the original one before the training sessions or the other representation rotated by 180 degrees with respect to the original representation. The new representation after disorientation remained unperturbed till the next disorienting spin. To get to reward locations available at one corner of the room, the animal relied on the reliable representations across previous trials, rather than the representation that succeeded the jerky, disorienting, vestibular motion of the animal. The performance following disorientation dropped significantly, if, in preceding trials, the misaligned representations were reliably represented. Thus, recourse to reliable memories of the past is essential for guiding behaviors [Weiss et al., 2017].

These observations suggest that animals actively maintain stable representations that are easily perturbed by stronger manipulations. The extent of stable representation is reflected in the performance in behavioral tasks.

Experimental findings suggest factors that might shape the precise spatial firing of grid cells. They include the excitatory drive from the hippocampal formation [Bonnevie et al., 2013], active dendritic properties of principal neurons [Schmidt-Hieber et al., 2017] of medial entorhinal cortex and theta rhythmic oscillatory drive from the medial septum [Koenig et al., 2011, Brandon et al., 2011]. In the remainder of this chapter, we will focus on the role of theta rhythm in stability.

1.4 Theta rhythm: An overview

Rhythmic fluctuations in local field potentials are observed across brain structures in a variety of brain states [Buzsáki and Draguhn, 2004]. Theta is the most prominent of such temporal patterns observed in the hippocampal formation as an animal actively explores its environment [Vanderwolf, 1969]. Theta rhythmic oscillations are generally observed in mobile animals [Vanderwolf, 1969], while for human beings it is recorded from immobile patients undergoing source identification of epileptic seizures [Arnolds et al., 1980]. It is also one of the most variable rhythms with its frequency varying across species (6-10Hz in rodents, 4-6Hz in carnivores [Buzsáki et al., 2013])and within a species with different states of the animal [Bohbot et al., 2017, Korotkova et al., 2018]. Until recently, It was generally agreed among the neuroscience community that the frquency of theta rhythm is lower in humans (1-4 Hz [Buzsáki et al., 2013, Arnolds et al., 1980]) when compared to other mammalian species (5-10Hz). A recent study conducted in walking humans has unearthed a faster theta rhtyhm which is comaparable to that of actively exploring animals [Aghajan et al., 2017]. There are many potential intrinsic theta oscillators within the hippocampal formation. However, hippocampal theta is largely driven by inputs from the medial septum [Buzsáki, 2002, Vertes and Kocsis, 1997, Gonzalez-Sulser et al., 2014]. The medial septum host a variety of neuronal types that generate and modulate theta rhythmic activity in the hippocampal formation: Glutamatergic neurons with recurrent projection within the medial septum help in initiating the theta rhythm. GABAergic neurons in MS carry theta frequency inputs to the hippocampal formation. These inputs are crucial for maintaining theta across hippocampal structures [Fuhrmann et al., 2015]. Cholinergic inputs from medial septum play a modulatory role on MEC theta frequency [Carpenter et al., 2017]. The major target of theta rhythmic input is parvalbumin-positive interneurons of the hippocampus and the medial entorhinal cortex [Unal et al., 2015]. Afferent fibers that carry proprioceptive and vestibular movements [Tsanov, 2017] enable the medial septum to transform self-movement signals into changes in theta frequency and amplitude. These transformations are suggested to be useful for path integration and inter-regional communications [Hinman et al., 2016]. For example, at a higher velocity of the animal,

medial septal inputs increase the LFP frequency and theta rhythmicity in individual neuronal spikes. Momentary inactivation of the medial septum by pharmacological agents disrupted this mapping between velocity and theta frequency [Hinman et al., 2016]. Interestingly, blocking theta rhythmic input from medial septum disrupted the spatially periodic, regular firing fields of grid cells, underscoring the importance of theta rhythmic drive in the reliable formation of receptive fields [Koenig et al., 2011].

Theta has been implicated in many functional roles with three broad categories: 1) Spatial coding: shaping tuning properties of spatially modulated cells of the hippocampal formation. 2) Learning and memory: Theta is hypothesized to induce plasticity mechanisms of relevance to episodic memory formation and spatial learning. 3) Communication across regions: Phase coherent theta oscillations across regions has been linked to efficient communication that subserves behavioral or cognitive demands. We will briefly review each of them.

1.4.1 Role of theta in spatial coding: Phase precessing theta sequences

As an animal traverses through a place field, the corresponding place cell starts spiking when it enters the field. The firing rate increases toward the center. Averaged across trials, the firing rates generally fit a Gaussian profile that defines the tuning curve of the place cell. In addition to the firing rate, precise spike time provided additional location information when measured against a background of theta oscillation. As the rate advances through the place field, the phase of theta at which spikes occur also advances to earlier phases [OKeefe and Recce, 1993, Skaggs et al., 1996, Maurer and McNaughton, 2007] (figure 1.4).

Phase precession has been observed in both the hippocampus and in the medial entorhinal cortex [OKeefe and Recce, 1993, Hafting et al., 2008, Reifenstein et al., 2012]. The phase precession in MEC is independent of hippocampal CA1 phase precession [Hafting et al., 2008]. Phase precession is observed in linear tracks [OKeefe and Recce, 1993, Skaggs et al., 1996] and along two dimensional trajectories [Skaggs et al., 1996]. It can be observed even in a single traversal of the animal along a grid field [Hafting et al., 2008, Reifenstein et al., 2012].

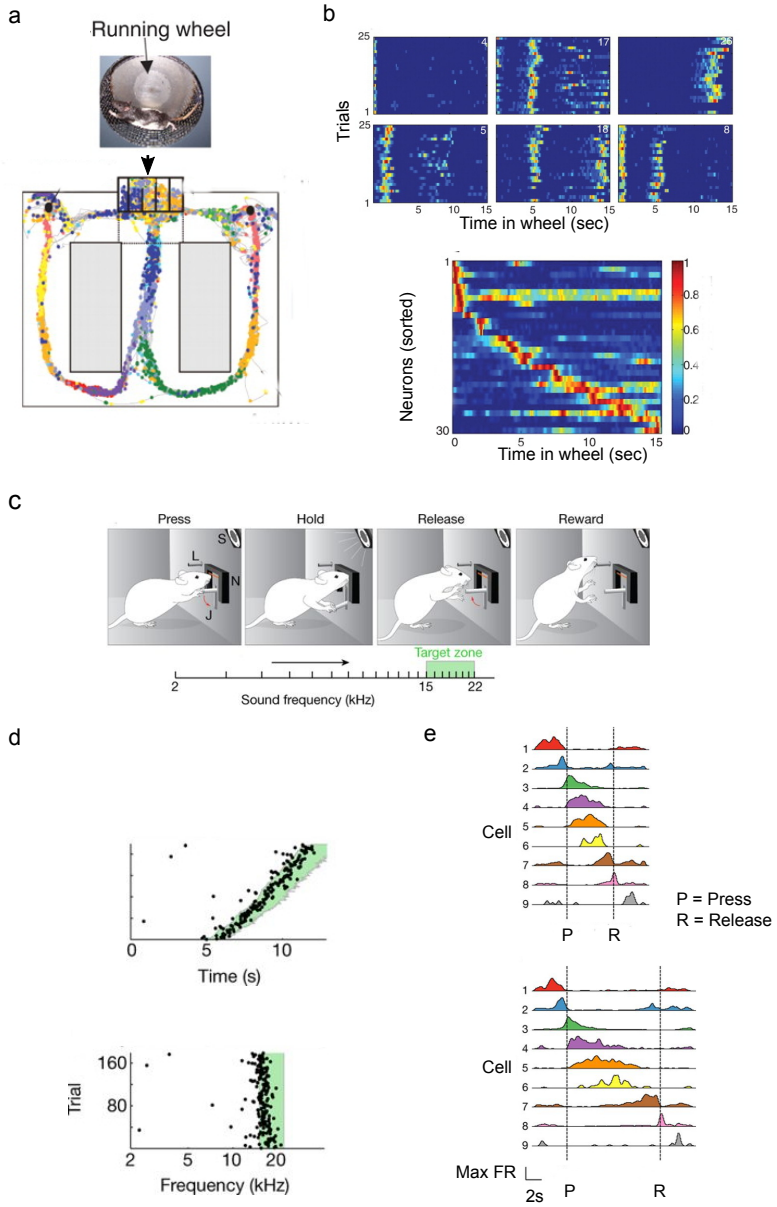

FIGURE 1.3: *Internally organized sequential activity patterns.* (a) A sequential activity in a delayed alternation (pnemonic) task [Pastalkova et al., 2008]. Upper panel - A rat is made to run on a wheel (where external visual and tactile inputs are sealed off) in between traversal along the maze to a stipulated reward location from where it is sent to the wheel in the center. Lower panel - The schematics of the eight shaped maze is shown with trajectories of the animal and spiking responses of select place cells with clearly defined place fields overlaid. From figurer 1a and 1b of [Pastalkova et al., 2008] (b) Upper panel - Reliable firing of six neurons, during wheel running, across trials (28 shown here), each occupying distinct moments/episodes during the fifteen seconds of wheel running before the animal entered the middle stem of the maze. Lower panel - The firing rate map of the neurons sorted based on the latency to peak firing rate, showing that the sequential activity fills the duration of the wheel running. From figure 1d and 1e of [Pastalkova et al., 2008]. (c) Nonspatial sequences of hippocampal formation [Aronov et al., 2017]. The behavioral task. The rat was trained to press a lever, which triggered the playing of pure tones of increasing frequencies, and the rat was supposed to hold on pressing the lever till a pure tone of desired frequency is reached when it has to release the lever to get a reward. The range of frequencies of pure tones is shown below arranged on a logarithmic scale. From figure 1a of [Aronov et al., 2017] (d), The rat learned the task for various gains in the rate of change of frequency of the tones. Upper panel - The press release occurred at varying times across trials as a result. Lower panel - But the release of the lever coincided reliably with the desired frequency. From figure 1d of [Aronov et al., 2017] (e) The sequential activity encoded the trajectory of the frequencies of tones an animal experienced. The sequence adapted itself such that neurons reliably coded for frequencies irrespective of the change in the rate of frequencies. Upper panel - fast switching of activity of neurons when the frequency change was faster. Lower panel - slower switching of activity of neurons when the frequency change was slower. From figure 1e of [Aronov et al., 2017]

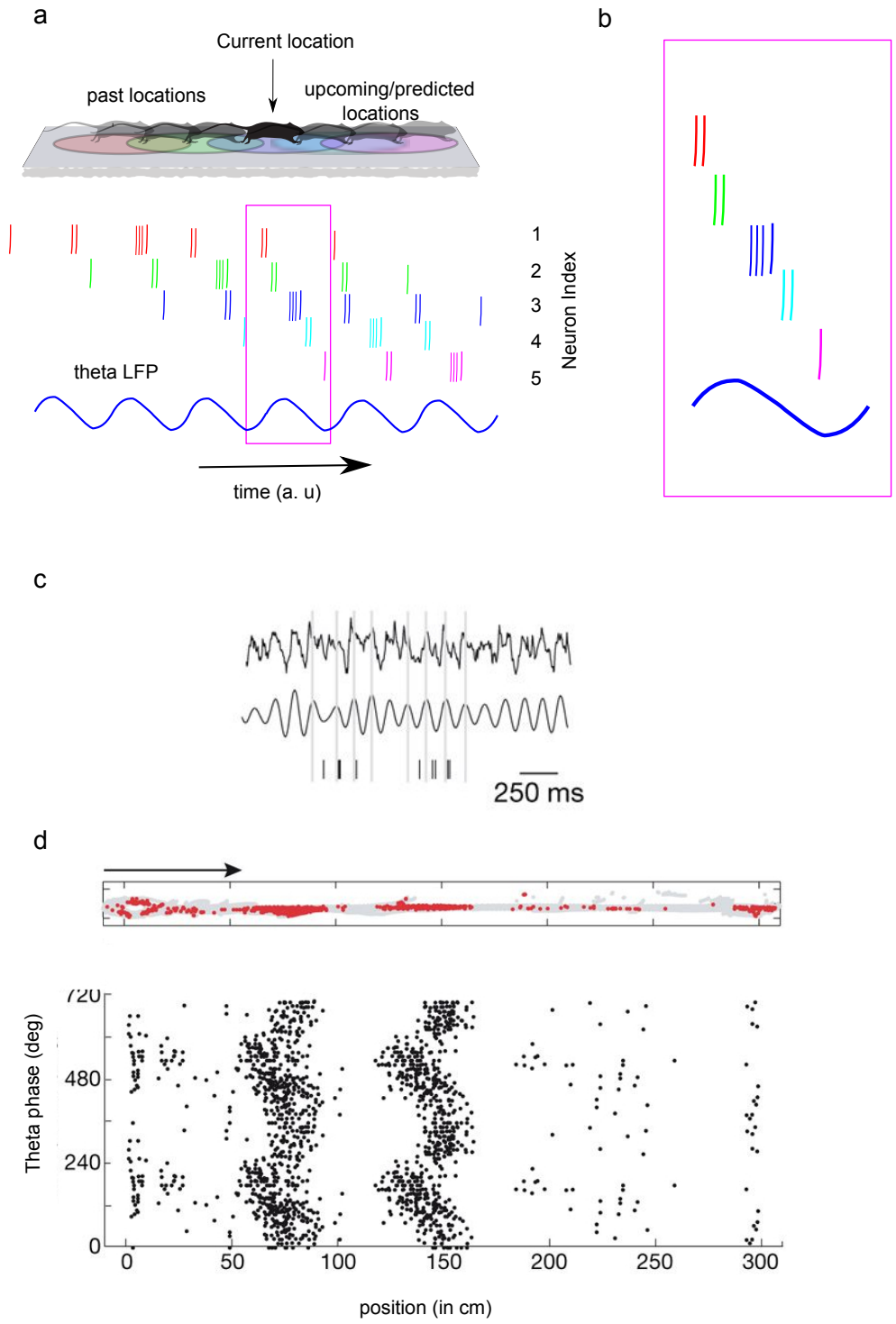

FIGURE 1.4: *Theta phase precession in the hippocampal formation.* (a) Upper panel - A schematic of a rat running along a linear track. Lower panel - The sequential activity of place cells with overlapping place fields along the track is shown along with the background LFP oscillation in theta frequency (blue oscillatory curve). For an individual neuron, the spikes occur at progressively earlier phases as the rat traverse through its place field. (b) The phase precession, in a cycle of theta oscillation, is represented as compressed sequences of neurons whose order is similar to the order of appearance of firing fields. (c) Phase precession in a single traversal of a trajectory for a grid cell from MEC. Upper panel - raw LFP trace. Middle panel - LFP bandpass filtered. Lower panel - The spiking of an individual neuron. From figure 1c of [Hafting et al., 2008]. (d) Upper panel - repeated traversals in the forward directions of a rat are shown in gray. The red dots mark the locations along the trajectories where a single grid cell from MEC fired action potentials. Lower panel - The phases of spikes, with reference to background LFP oscillation, of a single grid cell, pooled over many trials is shown. The negative slope of the phase of the spike as a function of position within a field indicates phase precession. From figure 1d and 1g of [Hafting et al., 2008]

Various mechanisms to generate phase precession and theories of its functional role have been proposed. [OKeefe and Recce, 1993, Bose et al., 2000, Bose and Recce, 2001, Lengyel et al., 2003, Mehta et al., 2002, Navratilova et al., 2011, Lisman and Redish, 2009, Robbe et al., 2006]. In the oscillatory interference model, for example, phase precession of the somatic oscillation arises naturally as a consequence of interference of two oscillators at the soma.

1.4.2 Role of theta in learning and memory

An important role proposed for theta mediated phase precession is to process behavioral time scale spike patterns to enable activity-dependent plasticity mechanisms [Mehta et al., 2002, Robbe et al., 2006, Dragoi and Buzsáki, 2006]. When neurons with overlapping place fields or grid fields generate phase precessing spikes in successive cycles of theta they appear as a compressed sequence that preserves the order of appearance of place fields. This sequence unfurls in a single cycle of theta. Theta mediated compression of sequences is thought to enable activity-dependent plasticity mechanisms that rely on the precisely ordered pre and postsynaptic neurons [Mehta et al., 2002, Yamaguchi et al., 2007]. When phase precession is selectively inhibited in the hippocampus using cannabinoids, rats were unable to use recently experienced trajectories to guide their future explorations [Robbe et al., 2006].

In freely behaving animals neuronal spike patterns are modulated by theta rhythmic oscillations. When such theta modulation was mimicked by electrically stimulating axonal fibers connected to the soma of CA1 neurons, the extent of LTP was maximally enhanced as compared to LTP induced by continuous spikes at higher frequencies. For example, a spike pattern comprising bursts of 4 spikes at 10-millisecond intraburst spike interval delivered at a regular interval of 200 ms elicited almost 40 percent increase in the synaptic strength, while the bursts at a regular interval of 2 seconds induced strength increase not exceeding 10 percent [Larson et al., 1986].

Finer temporal control of the stimulus protocol, in another set of experiments, revealed the crucial role of theta phase in gating induction of LTP using bursty spike

patterns. A burst of spikes at 200 *Hz* delivered at the depolarizing phase of theta oscillations induced reliable LTP. The LTP so induced can be effectively reversed by another burst delivered at the hyperpolarizing phases in subsequent cycles [Hölscher et al., 1997].

These experiments point out that the complicated machinery involved in long term plasticity mechanisms believed to underlie learning are tuned to phase-locked bursts that are generated in vivo in freely behaving animals.

1.4.3 Role of theta in interregional communication

Phase coherent oscillations have been hypothesized to facilitate efficient information transfer across brain regions [Fries, 2016, Akam and Kullmann, 2014]. Local LFP oscillations reflect the synchronous changes in the excitability of the population of neurons. When the phases of the LFP in two regions are synchronized it implies that inputs arrive at the most excitable phases [Fell and Axmacher, 2011].

In a working memory task [Jones and Wilson, 2005b], rats were trained to remember a location cue that was associated with a reward at a different location. The post-learning accuracy of the task performance was nearly 80 percent. As the animal navigated from the cued to the rewarded location, the hippocampus and the mPFC showed increased coherence without any perceptible change in the power of theta frequency LFP oscillation. This increase in coherence was lower or absent when the animal incorrectly headed to the unrewarded location or was forced to move along a trajectory that was invariably rewarded.

In another set of experiments [Kim and Lee, 2011], rats were trained to topple either of two objects (toys), indicating their preference to the experimenter to get a reward. They had to choose one of the objects irrespective of the order in which it was placed. The rats were also supposed to choose the first object in one context and the second object in another context. Hippocampal neurons showed clear receptive fields distinguishing the places and contexts in the early sessions when the animals were still learning the task. In later trials, prefrontal cortical neurons developed spatial receptive fields, that reflected the type of event (For example, entering to a platform where the decision is taken) irrespective of the context. Interestingly theta

coherence between the hippocampus and the medial prefrontal cortex was maximal post-learning near the locations where the animal was making a choice.

A similar increase in coherence is also observed between the hippocampus and the ventral striatum [van der Meer and Redish, 2011].

A plethora of other experimental studies, including the above mentioned, suggest that theta rhythm couples regions in a behavior dependent manner and facilitate efficient communication between the involved regions. However, the mechanism that brings two or more regions into phase synchronized states is mostly unknown [Varela et al., 2013, Remondes and Wilson, 2013, Fujisawa and Buzsáki, 2011, Wilson et al., 2013].

1.5 Our Work

In Chapter 2, we find two qualitatively different regimes in which the local motif of MEC can operate: The autonomous switching and switching induced by external input that toggled the activity among interneurons. We show, in the regime of externally driven dynamics that theta rhythmic input stabilizes the response of the local network motif, which we explore in Chapter 3. Moreover, this explains losing of periodic firing fields of the grid cells of the medial entorhinal cortex. The mechanism by which this is achieved is also explored in chapter 3. Briefly, Theta created temporal windows wherein the weak inputs arriving at the proper phases induces successful switching in the activity of local competitive circuits, while those arriving at other phases fail to do so. This also allowed us to contemplate a way in which theta might facilitate inter-regional communication which is dealt with in Chapter 4. Finally, I discuss how our work fits within the current knowledge in the field emanating from experimental and theoretical work in systems neuroscience.

Chapter 2

Dynamical regimes of medial entorhinal cortex

2.1 Introduction

Almost all the sensory information directed to the hippocampus is routed via the entorhinal cortex, a six-layered cortical region that surrounds hippocampus proper [Witter et al., 2017]. Distinct anatomical connections and functional divisions motivated neuroscientists to divide the entorhinal cortex into the medial and lateral entorhinal cortex [Burwell and Amaral, 1998]. Medial entorhinal cortex harbors circuits that are involved in processing information related to spatial navigation and episodic memory. For example there are spatially modulated grid cells [Hafting et al., 2005], head direction cells coding for orientation of the animals head [Sargolini et al., 2006], neurons that increase their firing rate almost linearly with increasing velocity of the animal [Kropff et al., 2015], cells that fire in response to borders of the enclosure the animal is put in [Solstad et al., 2008], and neurons that encode the duration of episodes [Robinson et al., 2017]. The different kinds of neurons with clearly defined receptive fields in varying contexts continue to be discovered [Diehl et al., 2017, Høydal et al., 2019].

Stellate cells of the medial entorhinal cortex are the most prominent excitatory cells found in layer II of the medial entorhinal cortex, where the concentration of pure grid cells is most abundant. One-fourth of the stellate cells are grid cells [Rowland et al., 2018]. They send direct projections to the dentate gyrus and CA3 of the hippocampus. Stellate cells are easily distinguishable from pyramidal cells, the

other type of excitatory cells found in layer II, by their morphology (large soma size and star-like appearance of dendrites) and electrophysiological properties [Alonso and Klink, 1993]. In response to depolarizing inputs, stellate cells generate sustained membrane potential oscillations at theta frequency. Upon further depolarization, they show mixed-mode oscillations wherein subthreshold oscillations are interspersed with action potential spiking responses [Dickson et al., 2000].

A series of biophysical experiments teased apart the ionic currents that made the subthreshold oscillations in response to depolarization possible [Magistretti and Alonso, 1999, Magistretti et al., 1999, Dickson et al., 2000]. Modeling studies also articulated the details of how subthreshold oscillations are generated [Dickson et al., 2000, Fransén et al., 2004, Rotstein et al., 2006]. Membrane potential oscillations are mediated by the interaction of two ionic currents that are active below the spiking threshold. One of the currents, called I_h, is due to non-specific cation channels that are activated by hyperpolarized membrane potentials. They increase the membrane potential when open. This hyperpolarization activated depolarizing property of the current along with the kinetic scheme endows a resonant property to stellate cells at theta frequency [Dickson et al., 2000]. To generate sustained membrane potential oscillations, the resonating I_h currents needs to be amplified by a persistent sodium current. These are non-inactivating, depolarization activated depolarizing currents that are quick to reach their steady-state as a function of membrane potential as opposed to I_h currents [Magistretti and Alonso, 1999]. The mechanism of membrane potential oscillation mixed with spiking response is illustrated in figure 2.1 and figure 2.2.

Another characteristic electrophysiological feature of stellate cell is the sag response to an inhibitory/hyperpolarizing input pulse. Instead of reaching a lower membrane potential asymptotically, the membrane potential, after a delay, bounces back to a relatively more depolarized state. For strong enough inhibitory pulses, this delayed depolarization with the help of amplifying I_{NaP} current, can reach the threshold and lead to a spike. This rebound spiking property of I_h is observed in anesthetized animals in vivo and is hypothesized to be capable of forming grid patterns of grid cells [Shay et al., 2016].

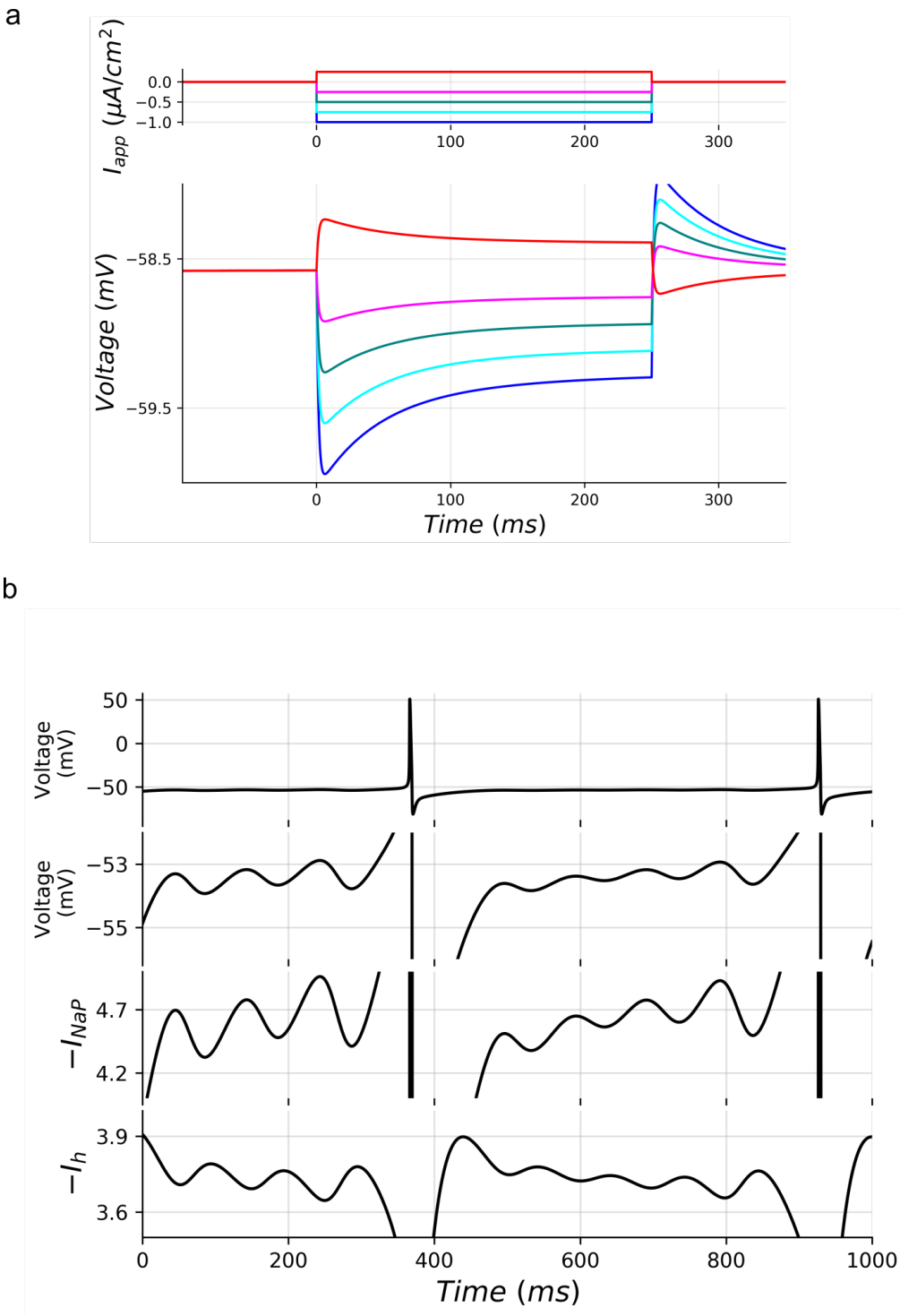

FIGURE 2.1: *sag response and mixed mode oscillation in a stellate cell.* (a) A biophysical model comprised of conductances mediating I_h, leak current shows the characteristic sag response (upper trace) in response to step hyperpolarizing currents of various amplitudes. When spiking currents (I_{Na} and I_K) and persistent sodium current, I_{NaP} , are added to the biophysical model, it exhibited mixed mode oscillation where the membrane potential oscillations are interspersed with spikes. (b) The voltage response (first and second row) showing the spiking and membrane potential oscillations. The low amplitude oscillations of the membrane potential, upon a closer look (second row), reveals the steady increase in the amplitude of the membrane potential and the coincident of the spike with the peak of the membrane potential oscillation. The ionic currents involved in mediating the mixed mode oscillations are shown in the third and fourth row of the panel. Third row - I_{NaP} current. Fourth row - I_h current

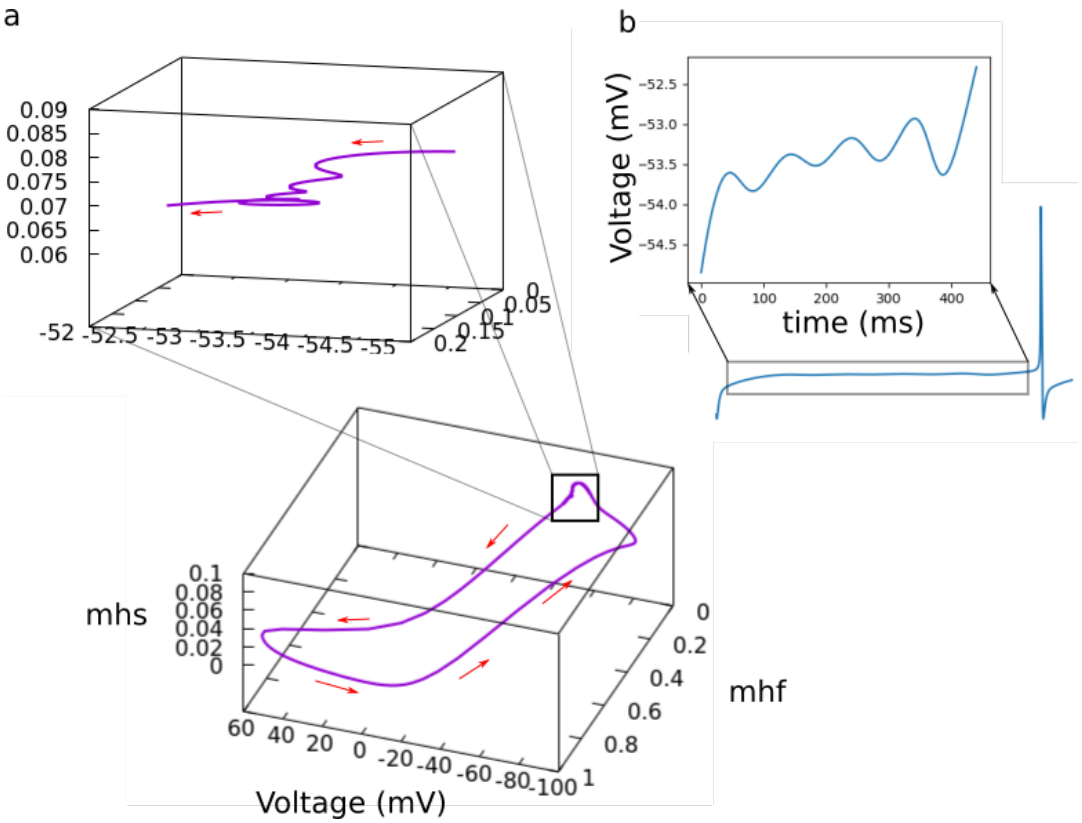

FIGURE 2.2: *Mechanism of mixed mode oscillation in the stellate cell model.* (a) Trajectory of the system exhibiting mixed mode oscillation behavior is shown in The $Voltage - mhf - mhs$ volume/hyperplane. mhf is the gating variable (taking the values from 0 to 1). mhs is the gating variable of the slow component of the I_h current. The subthreshold regime is shown in the inset (shown expanded in the upper panel): The slower increase in the strength of $I_{hs}(slowcomponentofh - current)$ progressively brings the peaks of subthreshold oscillations to spiking threshold upon which the system leaves the regime of subthreshold oscillation to that of spiking dynamics. The faster-time scale spiking currents, in turn, return the system to a state from where it evolves toward the subthreshold regime again. Such switching of activity between slower, low amplitude oscillations and faster large amplitude oscillations (spikes) is referred to as mixed mode oscillation [Rotstein et al., 2008]. (b) A stellate cell expressing mixed mode oscillation.

Fast spiking, parvalbumin-positive, inhibitory interneurons of the medial entorhinal cortex are shown to be essential for spatial coding [Miao et al., 2017] and they send GABAergic projections exclusively to perisomatic regions of the stellate cells [Fuchs et al., 2016]. The medial septum, one of the main sources of theta for hippocampal formation, target the fast spiking interneurons of the MEC with GABAergic innervations of inhibitory neurons of medial septum [Gonzalez-Sulser et al., 2014]. As a consequence, the inhibitory interneurons of MEC are strongly modulated by theta. Stellate cells with sparse, if any, excitatory interactions among them, interact with each other mainly via these inhibitory interneurons [Couey et al., 2013]. There are also reports of mutual inhibition [Wouterlood et al., 1995] among inhibitory interneurons which is rarely utilized in models to explain the grid-like patterns produced by stellate cells.

Here we built a small network motif composed of stellate cells and fast spiking interneurons with all the crucial electrophysiological properties mentioned above incorporated into them, to understand the major dynamical regimes of functional relevance in the medial entorhinal cortex.

2.2 Results

2.2.1 Oscillatory and bistable dynamics of a MEC network motif

Layer II of the MEC consists of two distinct microcircuits with characteristic patterns of connectivity within and sparse connections across circuits [Witter et al., 2017, Nilssen et al., 2018]. Stellate cells and fast-spiking parvalbumin positive interneurons [Couey et al., 2013, Buetfering et al., 2014] form one circuit while pyramidal cells and 5HT3A interneurons form the other [Witter et al., 2017, Nilssen et al., 2018]. This di-synaptic circuit motif, where principal neurons interact via an inhibitory intermediary, is prevalent throughout the EC [Couey et al., 2013, Fuchs et al., 2016, Nilssen et al., 2018]. To understand how a network's architecture affects its dynamics we simulated a simple network motif (Figure 2.3 b), a building block of the MEC, that consisted of biophysically detailed models of stellate cells [Acker et al., 2003, Rotstein et al., 2006] and inhibitory interneurons [Wang, 1996].

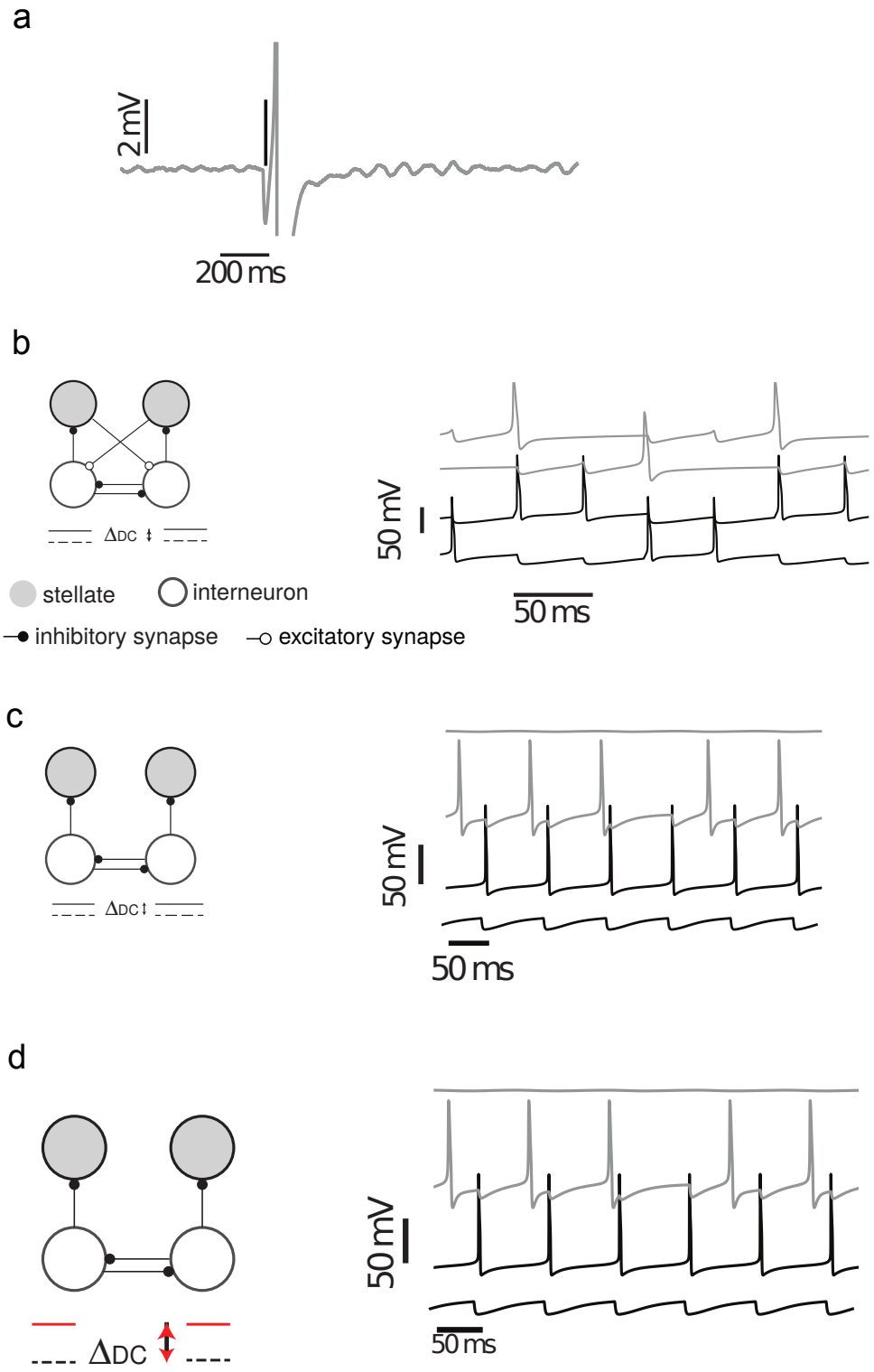

FIGURE 2.3: *Oscillatory and bistable dynamics in MEC.* (a) shows the rebound spiking response of a stellate cell to a single inhibitory spike. The time of the inhibitory spike is shown by the vertical line. In the absence of inhibition, the membrane potential of the stellate cell showed subthreshold oscillations. (b) A supra-threshold input applied to the inhibitory interneurons caused a rhythmic switching of activity in the network motif. Stellate cells spiked (gray traces) when the inhibitory interneuron (black traces) transitioned from activity to silence. ΔC is the constant applied current above a baseline given to both the inhibitoy interneurons. (c) Switching failed in the absence of excitatory input; continuous firing of one interneuron (black trace) passively recruited the stellate cell (in gray trace) while the other interneuron (black trace) and corresponding stellate cell remained silent. (d) Increasing the strength of applied current (ΔC) resulted in failure of switching with fast spiking interneuron completely silencing the other interneuron.

Stellate cells show subthreshold membrane potential oscillations and generate rebound spikes when released from inhibition [Alonso and Klink, 1993] (Figure 2.3 a). We modeled these properties using a hyperpolarization activated depolarizing current (I_h) [Dickson et al., 2000, Shay et al., 2016] and an amplifying persistent sodium current (I_{NaP}) [Magistretti and Alonso, 2002] in addition to leak and spiking currents (I_L, I_{Na} and I_K). We modeled interneurons using modified sodium and potassium currents that allowed it to spike at high frequency [Wang, 1996]. In our simulations, both interneurons (Figure 2.3) received supra-threshold input. However, since they inhibit each other, only one of the neurons spiked while the other remained silent. Successive inhibitory spikes from an interneuron activated depolarizing I_h currents in the postsynaptic stellate cell. This eventually drove the stellate cell to spike. Excitatory drive from the stellate cell activated the other interneuron of the pair that, in turn, silenced the first one. The activity of this motif switched rhythmically. The interneurons alternated between episodes of spiking and quiescence and oscillated out of step with each other. Rebound spikes by stellate cells marked every transition from spiking to quiescence (Figure 2.3 b) and may serve as a viable mechanism to generate periodic firing fields of grid cells [Shay et al., 2016]. Excitation due to rebound spiking caused rhythmic switching. When we removed excitatory inputs from stellate cells to the interneurons, only one interneuron remained active even though the interneurons reciprocally inhibited each other (Figure 2.3 c). Transitions in the activity of inhibitory interneurons can drive other stellate cells to fire, potentially leading to a pattern of activity where different neurons are sequentially activated. As the input to inhibitory interneurons increased so did its spiking frequency [Wang, 1996]. At higher frequencies, the time between inhibitory spikes was too short for the post-synaptic neuron to fire a rebound spike and cause a switch in the activity pattern (Figure 2.3 d). In this parameter regime, depending on the initial conditions, either one of the interneurons continually generated action potentials while the other interneuron remained quiescent due to regular inhibitory postsynaptic potentials arriving at a faster rate.

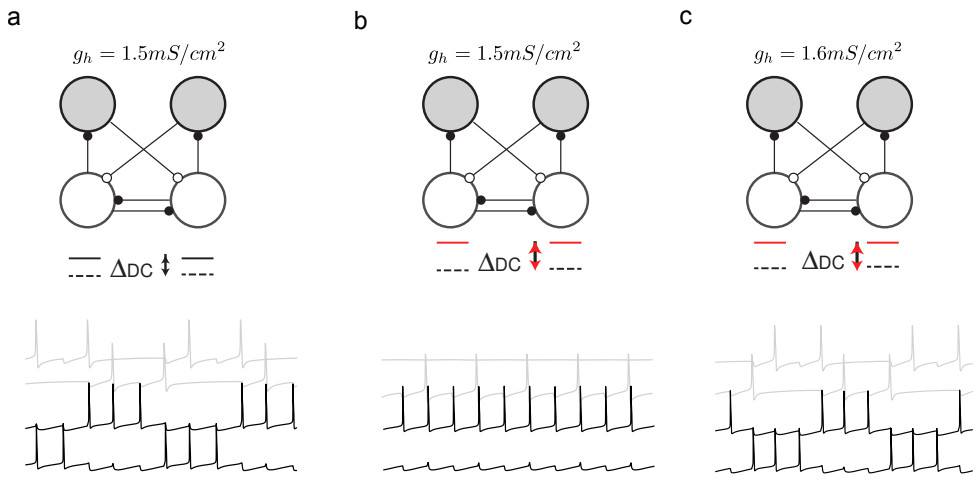

FIGURE 2.4: *Modulation of I_h conductance switches regimes.* For (a) and (b) the value of I_h conductance was fixed at $1.5mS/cm^2$. The conductance is increased slightly for (c). Increased applied current ΔC disrupted the autonous switchig activity which is recovered by increasing the I_h conductance.

2.2.2 Modulation of I_h conductance leads to the transition of regimes

The two dynamical regimes - oscillatory alternative spiking regime and bistable regime, are resulting from the interaction of properties of connectivity (mutually inhibitory interaction), synapses(fast inhibitory time scales), and intrinsic properties of individual neurons of the motif. Modulatory factors can impinge on any of these to affect the dynamical behavior of the network motif. For example, in the previous section modulating the gain of inhibitory neurons or the strength of excitatory connections from stellate cells to inhibitory interneurons can induce the transition of the behavior of the network motif from an autonomous oscillator to a bistable system or vice versa. The conductance of I_h current responsible for rebound spiking can also provide another way for modulatory control of the regimes as switching is induced by rebound spiking stellate cells. For example, in figure 2.4 a and 2.4 b, an increase in firing rate brought about by increased depolarization to both the interneurons lead to the transition from oscillatory activity pattern to the bistable regime. When the conductance value of I_h current is slightly increased, the autonomous oscillatory activity is recovered.

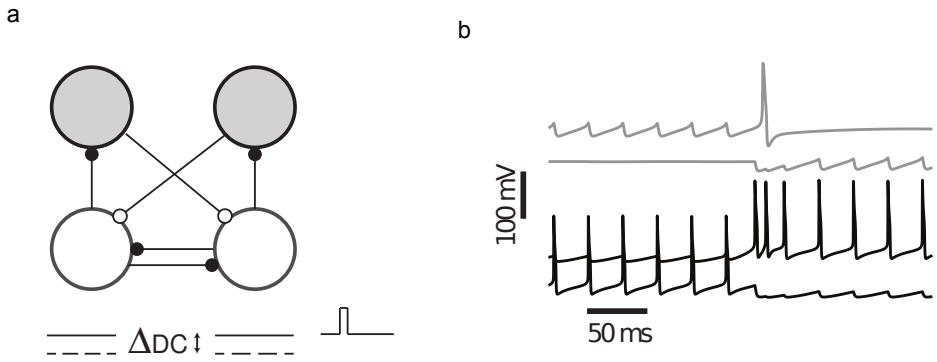

FIGURE 2.5: *Transient pulse toggles states in the bistable regime.* (a) the network motif is same as before and the applied current is such that it allows continuous firing of only one interneuron (Figure 2.4 c). A transient pulse is given to the silent interneuron. (b) Switching in the activity of inhibitory interneurons caused by the external pulse. The post synaptic stellate cell is released from inhibition upon this switch.

2.2.3 Transient pulse toggles states in bistable regime

The symmetric competitive interaction between the inhibitory interneurons leads to a bistable state at high firing rate, where depending on the initial condition one of the neurons reigned in firing continuously while the other one received regular inhibitory postsynaptic potentials impeding its ascent to spiking threshold. The network acted as a bistable switch where one of the interneurons remained active until a transient external perturbation toggled the switch (Figure 2.5). When inhibitory input to one of the stellate cells ceased, it emitted a rebound spike that marked the transition from one state of the network to the other (Figure 2.5). Thus, depending on the parameter regime, the motif simulated here can act as an autonomous oscillator (Figure 2.3 b) or as a switch (Figure 2.5) whose state could be toggled between activity and quiescence by a transient external perturbation.

2.3 Discussion

Our results show that a network motif based on the architecture of MEC operates in two modes, one where it switches autonomously between states and the other where it shows bistable states. A transient pulse can be used to toggle between the states. For a region of the brain known to exhibit self organized activity patterns

as well as gating neocortical inputs to the hippocampus via the perforant pathway, having two modes where it exploits the internal structure to generate autonomous switching and switch among states with transient pulses suggest a way in which it can perform such functions.

Autonomous switching is caused by rebound spiking of stellate cells that fired in response to inhibition from the active interneuron of two mutually inhibiting interneurons. The connectivity of the network is such that the stellate cell sends excitatory projections to an interneuron that it does not receive inhibition from. Anatomical studies suggest the existence of such a connectivity scheme [Schmidt et al., 2017]. The resulting dynamics can be extended to sequential activity if more inhibitory and stellate cells are added via feedforward connections from stellate cells to inhibitory interneurons. Asymmetry in stellate to inhibitory interneurons can enforce sequential spiking akin to velocity dependent asymmetries in continuous attractor models [McNaughton et al., 2006]. In continuous attractor models, the varying velocity inputs are integrated by modulating the asymmetry in a neural sheet. Thus asymmetric connectivity in our network motif (extended to include more neurons) correspond to the activity of the neural population integrating the position of an animal moving with constant velocity.

Continuous attractor models(CAN) of the circuits of medial entorhinal cortex (mEC) often incorporate a strong recurrent excitation [McNaughton et al., 2006, Guanella et al., 2007], which has little experimental support to it. The excitatory neurons of entorhinal cortex (mEC), on the other hand, send sparse mutual excitatory connections among them [Couey et al., 2013]. Their interaction is mainly inhibtory, which is mediated by the fast spiking interneurons of the mEC. Later models of CAN [Burak and Fiete, 2009], however, revealed that pure inhibitory interaction among the grid cells can generate hexagonal pattern. The inhibitory connections enforced in those models can be justified by assuming that there is a dedicated inhibitory interneuron for each pair of excitatory neurons. This simplification fails when relative numbers of excitatory and inhibitory neurons and their convergent (many-to-one) and divergent (one-to-many) synaptic connections are taken into consideration. Thus, models like ours where inhibitory neurons are explicitly included would be able to address these concerns. Also, mechanisms of generation of gamma

rhythm explicitly invoke the role of a population of fast spiking inhibitory neurons [Wang, 1996, Shipston-Sharman et al., 2016]. Thus, a large scale implementation of our model has the potential to generate gamma rhythmic activity as well.

Our work modeled a scenario where the system could be moved between competing states. Bistable or multistable states abound in nervous systems of many species of animals, where active processes operating at the cellular and network level mediate quick transitions by a transient pulse-like input. In CPGs involved in swimming behavior of marine mollusk *Clione limacina*, certain inhibitory interneurons are endowed with membrane ion channels that allow the neurons to remain at either of the two membrane potential values, a low resting membrane potential and a depolarized plateau potential that are separated by 40-50 mV. Transient depolarizing or hyperpolarizing pulses result in quick switching from the resting membrane potential to a plateau potential or from a plateau potential to the resting potential. Different phases in the swimming pattern of the mollusk are recruited by the different membrane potentials of the inhibitory neuron. Thus the membrane level implementation of bistability allows for dynamic reconfiguration of circuits to subserve drastically different patterns of behaviour [Arshavsky et al., 1985]. A similar phenomenon is observed where switching to one of the two states of the membrane potential of a neuron allows it to participate in either pyloric or gastric mill rhythms in the stomatoganglion of lobster [Weimann et al., 1991]. A network level implementation of a bistable switch is potentially implemented by two regions of the mesopontine tegmentum on either side of the region [Lu et al., 2006]. These two regions send GABAergic innervation to each other, and one of the regions send glutamatergic innervation to the basal forebrain, the medulla and spinal cord. These glutamatergic innervations bring paradoxical state characteristic of REM sleep.

An increase in the firing rate of interneurons resulted in a change from an autonomous oscillator to a bistable system in our model. The switching of dynamical patterns using changes in the gain of neurons is suggested by [Zhang and Abbott, 2000]. A presynaptic neuron sends projection to a group of neurons of a circuit resulting in a fine balance of excitation and inhibition. A gradual change in the firing rate of the presynaptic neuron disrupts the fine balance of strong excitatory and inhibitory synaptic potentials in the postsynaptic neurons. This disruption of balance

can lead to a drastic change in the drive to those neurons to cause a switch in activity regime. Our model suggests that a similar switch can be achieved in a small motif where the gain modulation is combined with intrinsic properties of biophysically realistic neurons.

Changes in conductance values of I_h current, induced transition from one regime to another (for increasing values of I_h, the dynamics shifted from bistability to autonomous switching). I_h currents are shown to be modulated by the neurotransmitter, acetylcholine. For example, muscarinic receptor activation leads to a reduction of I_h current and a shift in the steady state activation curve such that the current is diminished at depolarized membrane potentials [Heys and Hasselmo, 2012, Pastoll et al., 2012]. Our results suggest that neuromodulatory signals can cause changes in dynamical patterns of activity via changing conductance values and channel properties of I_h current mediating channels.

Chapter 3

Theta Induced reliability

3.1 Introduction

Oscillatory electrical activity at the scale of populations of neurons characterizes various states of the brain in health and disease [Buzsáki and Draguhn, 2004, Steriade, 2001]. Brain oscillations cover a wide range of frequencies with oscillators closer in frequency space rarely occurring together in a particular region of the brain, demarcating distinct oscillators [Buzsáki and Draguhn, 2004]. These rhythmic fluctuations have been implicated in subserving many cognitive, mnemonic and behavioral performance of animals of various species [Colgin, 2013, Buzsáki and Draguhn, 2004]. For example, oscillations tune the response profile of neurons towards inputs at a given frequency band while shutting the inputs in other bands [Akam and Kullmann, 2010]. Oscillatory LFPs can also work as reference frames against which neurons can align their spikes when coding for a feature of a stimulus [Panzeri et al., 2010]. Combined with the firing rate of neurons that selectively increases in response to certain stimulus features, the phase of the spikes provides complementary coding capacity. A clear example is the phase and rate coding of spatial locations by the neurons of hippocampal formation [O'Keefe, 1976, Skaggs et al., 1996]. Another important function attributed to local population level oscillatory activity is providing a stable representation of information in the presence of noise.

Theta rhythm is a slow oscillation, of 6 to 12 Hz frequency, in local field potential recordings of depth electrodes or EEG recordings at the scalp-level. These oscillations increases in power or gain prominence as an animal engages in exploratory locomotion and cognitively demanding tasks [Colgin, 2013, Buzsáki, 2002]. It is

observed in many regions of the brain, but is more pronounced, and is well studied in the hippocampal formation [Colgin, 2013]. The medial septum is an important source of theta rhythm for the entire hippocampal-entorhinal axis [N et al., 1979, Vertes and Kocsis, 1997, Gonzalez-Sulser et al., 2014]. Accordingly, when pharmacological agents that inactivate neural activity were momentarily infused into the medial septum, the power of theta rhythm across all major subfields of hippocampal formation is reduced [Mitchell et al., 1982]. As a consequence, individual neurons also expressed reduced rhythmicity at a lower frequency [Koenig et al., 2011].

In a pair of experiments [Koenig et al., 2011, Brandon et al., 2011], rats were made to forage in a square enclosure while single-unit recording and local population level electrical activity in the form of LFP was being recorded simultaneously. Medial septum mediated theta rhythmic activity in both the hippocampus as well as in the medial entorhinal cortex were reduced transiently upon inactivation of the medial septum. The power of theta rhythm was brought back to normalcy once the effect of the pharmacological agent died down (figure 3.1 a). The hippocampus and medial entorhinal cortex harbor a milieu of neurons that encode features relevant for navigation and memory [O'Keefe, 1976, Fyhn et al., 2004, Hafting et al., 2005, Sargolini et al., 2006, Solstad et al., 2008, Stensola et al., 2012]. Of these, the periodic firing fields of grid cells, that covers the arena an animal forages in, was vanished once theta input from the medial septum was disrupted. Grid cells recovered their firing fields eventually, as the effect of the pharmacological agent was reduced and the power of theta rhythm was high enough (figure 3.1 b). This transient disruption is specific to the hexagonal periodicity of grid cells, leaving intact the sparse and unique place fields formed by place cells of the hippocampus. The non-spatially modulated head direction cells and border cells of the medial entorhinal cortex were also unaffected.

There was a reduction in firing rate in the absence of medial septal inputs. Later works [Bonnevie et al., 2013] showed that the periodic firing of grid cells requires excitatory input from the hippocampus proper. Can the disruption of firing fields of grid cells on MS inactivation be attributed to the reduced firing rate of individual neurons? Various observations from these experiments suggested that the disruption was not due to the reduced firing rate of the neurons. The firing rate of grid

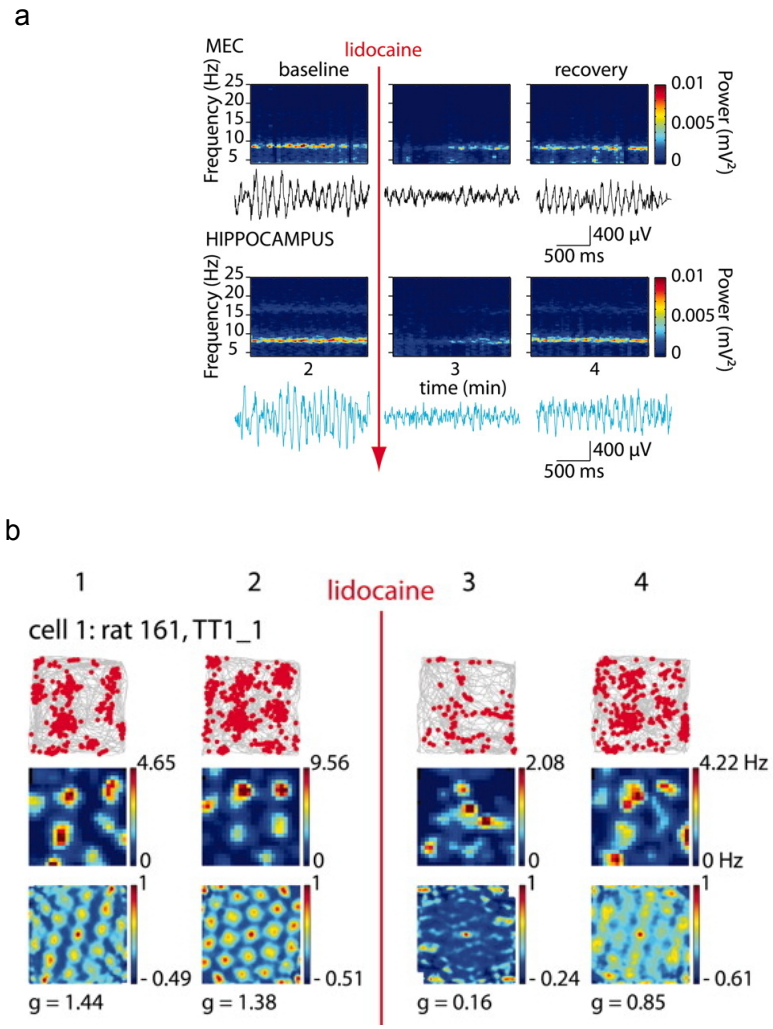

FIGURE 3.1: *Theta is required for stability.* (a) Application of lidocaine to medial septum momentarily reduced the power of the theta rhythmic oscillations in MEC and hippocampus. Once the effect of lidocaine died down, the power of the oscillation, as reflected in the spectrogram and in raw trace, recovered to normalcy. From figure 1B of [Koenig et al., 2011]. (b) The blocking of medial septum also disrupted the ability of grid cells to fire in a periodic manner in the grid fields. right panel. The grid fields formed before the medial septum (upper panel - spiking response overlaid on top of trajectories of the animal, middle panel - firing rate map, lower panel - autocorrelation of firing rate map.) display periodicity characteristic of grid cells. Left panel. Momentary disruption of grid field formation after lidocaine application and the recovery of them later. From figure 2A of [Koenig et al., 2011].

cells recovered independent of the recovery of spatial periodicity. Nongrid cells (place cells, head direction cells, border cells, etc), some of which have a spatially modulated (non-hexagonal) firing fields, have a comparable reduction in the firing rate upon removal of theta rhythm, nevertheless, maintained their receptive fields intact throughout. Thus an explanation of mere reduction in firing rates causing a disruption in the grid cell firing does not explain these experimental findings. The oscillatory drive from the medial septum must be involved in crucial ways to stabilize the periodic firing fields of grid cells.

In the previous chapters, we have seen how the network motif of the medial entorhinal cortex operates in two different regimes: Autonomous oscillator and multistable system with external input working as a toggling mechanism among the stable steady states. In this chapter, we find out that with realistic topological constraints the network fails to follow switching in the direction facilitated by the external input. Instead, the network dynamics is a mix of internal dynamics and the external inputs that fluctuate noisily to render useless any coding provided by individual neurons. In the presence of oscillatory drive from inhibitory innervations of the medial septum, the network regains its stable response behavior to external inputs in spite of noisy background variations across trials. Our results corroborate the experimental findings of Koenig et al [Koenig et al., 2011] and Brandon et al [Brandon et al., 2011], demonstrating the disruption of the periodic firing of grid pattern in the absence of rhythmic medial septal inputs.

3.2 Results

3.2.1 Feedback excitation from stellate cells disrupt reliable response to external input

In a network motif comprising mutually inhibiting interneurons and stellate cells, where transient external pulse reliably switched activity in the interneuron population, we introduced random excitatory connections from stellate cells to inhibitory interneurons (compare figure 3.2 a and b). The response of the MEC network, as a result of this feedback excitation, did not consistently follow the external drive

(compare figure 3.2 c and d). Interneurons received competing depolarizing inputs, one from the transient external drive and the other due to stellate cell spikes. The background noise and the history of activation determined which interneuron won this competition and silenced all others. This led to unreliable switching and considerable trial-trial variability in the activity of inhibitory interneurons. Therefore, the firing of stellate cells, that mark the shifts in interneuron activity, was also unreliable across trials (figure 3.2 d, bottom trace in gray background).

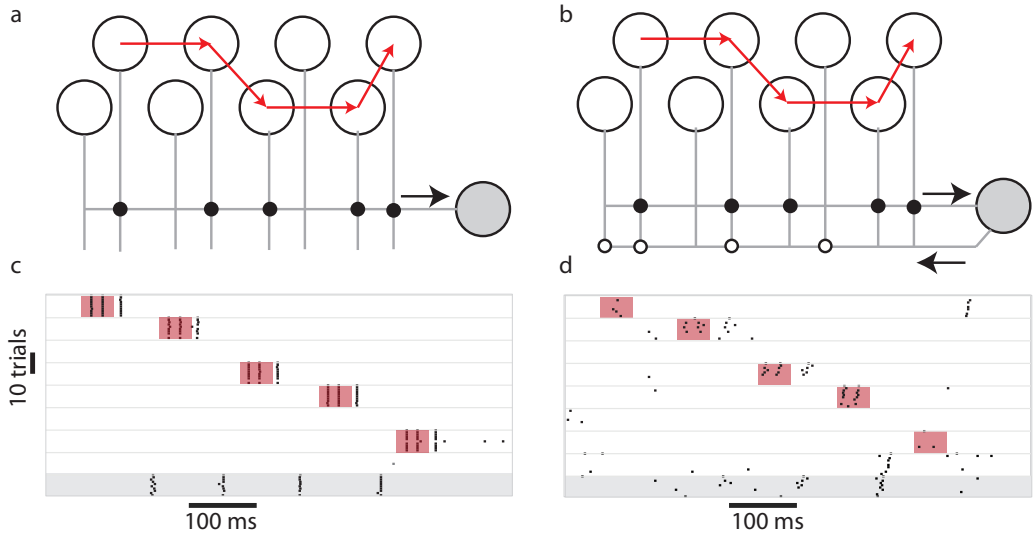

FIGURE 3.2: *Stability of input driven sequences.* (a) Network with sequential suprathreshold depolarizing pulses (temporal order of the input is shown by the red arrows) driving a subset of interneurons that were connected to a single postsynaptic stellate cell (filled gray circle). The response of the interneurons over 10 trials is shown as a raster plot in (c). The stellate cell (bottom raster shaded in gray) responded reliably over multiple trials. When feedback excitation from the stellate cell to a randomly selected subset of interneurons (b) was introduced, the response of the interneurons to the sequential input was perturbed and stellate cells did not spike reliably. The duration of the inputs is marked by the colored boxes in (c) and (d)

3.2.2 Model building

Our network is comprised, as before, of interneurons and stellate cells. We have constrained our topology based on properties reflected in the firing of stellate cells as observed in various experiments [Hafting et al., 2005, Ray et al., 2014, Rowland et al., 2018, Krupic et al., 2015, Barry et al., 2012, Shilnikov and Maurer, 2016, Yoon et al., 2016, Wernle et al., 2018]. Stellate cells are the most predominant of principal neurons found in medial entorhinal cortex. A signinficant proportion of the stellate cells are spatially modulated, with as much as one fourth of them expressing hexagonal

firing fields of a grid cell [Hafting et al., 2005, Ray et al., 2014, Rowland et al., 2018]. The grid fields are segregated into anatomical modules along dorsoventral axis such that any two grid cell from a single module have almost identical grid field size and inter grid field distance. The only difference between them is that the centre of firing fields occupy different locations. Thus, among the stellate cells from the same module, with their overlapping, phase shifted hexagonal firing fields, they cover the entire arena an animal is actively exploring. Rather than being rigid frames, these hexagonal firing field yield to many experimental manipulations that deform the symmetric hexagonal pattern. The concensus from these expermental findings is that the spatial contiguity of the hexagonal pattern arises as a result of network level interactions, rather than being mediated by independent, cellular level integration of afferent inputs. Specifically, our model assumes that the overlapping firing fields of stellate cells are brought forth by overlapping inhibitory inputs they receive. This assumption augurs well with the experimental manipulations that find the phase differences between any two grid cells unperturbed , even when their individual grid patterns are sheared [Krupic et al., 2015], stretched [Barry et al., 2012] and reoriented by perturbations originating from external cues [Wernle et al., 2018]. Figure 3.3 a shows the overlapping receptive fields of four stellate cells. The periodic triangular lattice of the receptive fields can be used to form a torus such that any point in space can be mapped to a point in that unit torus. This mapping captures the essential spatially symmetric pattern of grid cells. For example, all the places where the firing of population of grid cells are identical are specified by one location on the torus. Any arbitrary trajectory an animal traverses can be mapped to a recurring trajectory on the unit torus [Shilnikov and Maurer, 2016]. Any straight line trajectories on any of the two primary axes of the triangular lattice corresponds to a mapping on a cirlcle such that the trajectory is represented as a wave of neuronal activity traversing along the circle. We wanted to model the scenario where the animal is traversing along the linear trajectory along the primary axis. When combined with the assumption that the overlapping activity of two stellate cells are due to overlapping inputs, this yielded a neuronal network model where adjacent stellate cells, on a conceptual ring, that fire in close temporal and spatial proximity were receiving connection from overlapping group of interneurons. A single interneuron connects to adjacent

stellate cells with the strength that follows a gaussian profile. As in the chapters before, the interneurons are connected to each other in all-to-all manner (Figure 3.3 b). The neighborhood relationship between interneurons was therefore inherited from their connections onto the stellate cell layer and the sequential order of external pulses. Stellate cells extended random excitatory inputs onto the interneuron layer. The wave like propagation along a cirlcle that a linear trajectory of the animal is mapped to is implemented with sequential activation of inhibitory interneurons with a transient input.

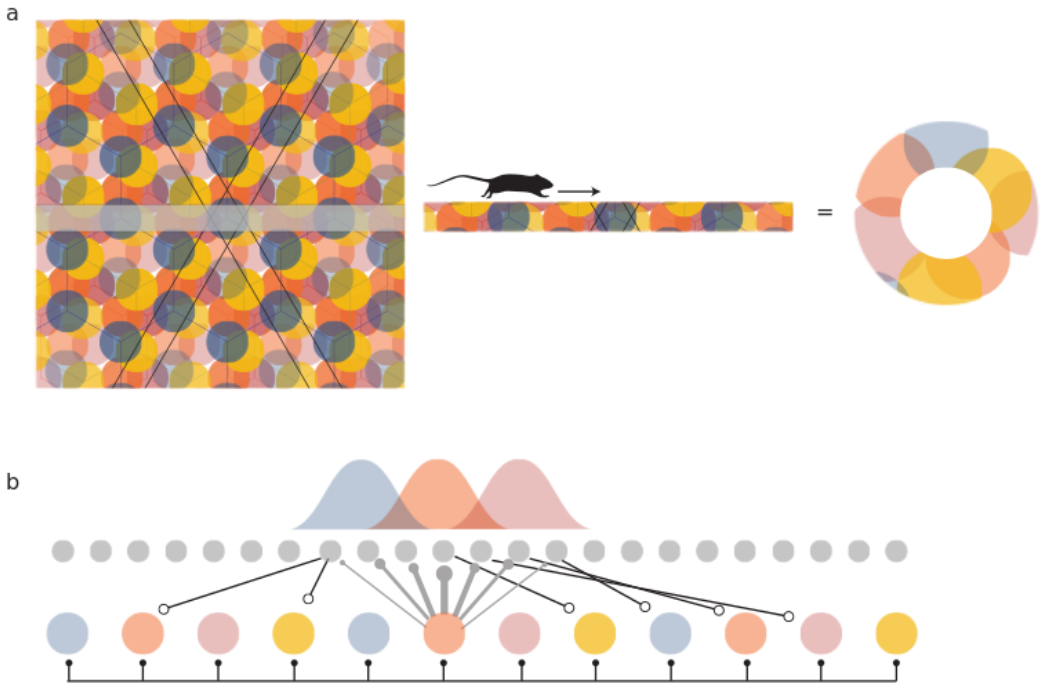

FIGURE 3.3: *Construction of network topology.* A schematic representation of the overlapping grid-like receptive fields of 4 grid cells is shown in the left panel of (a). As the rat traveled along a linear trajectory (marked in the figure as straight line paths), the grid field repeated periodically (middle panel of (a)). This can be mapped to a circle (right panel of (a)). Stellate cells in the network (gray filled circles in (b)), received inhibitory input from the interneuron layer (coloured circles). The strength of the inhibitory input followed a Gaussian profile (distribution shown in (b)). Each stellate cell connected to a randomly selected group of interneurons.

3.2.3 Theta subdues trial to trial variability

The response of a subset of 20 stellate cells from the ring network to a temporally varying input that sequentially excites the interneurons on the ring is shown in the raster plot of figure 3.4 a. In the presence of random noise across trials, the response of the network was not reliable across trials and did not always follow the input.

The activity of one of the neurons from this network, averaged across 10 trials, in the form of firing rate, is shown in figure 3.4 c. As the sequential external pulses were given assuming neurons were arranged on a circle, each neuron received a suprathreshold input at regular intervals. The neuron was just as likely to fire when an input was present as when it was absent.

Reliable responses of principal neurons in the EC and the hippocampus are often contingent upon the presence of theta oscillations. One source of theta to the MEC is a central pattern generator in the medial septum [Vertes and Kocsis, 1997] that extends GABAergic connections to the inhibitory interneurons and periodically modulates its firing rate [Gonzalez-Sulser et al., 2014]. We implemented theta rhythmic modulation of the MEC network by periodically (6-12Hz) driving the entire population of inhibitory interneurons (See methods for details). The pulse like input that was used to drive the neurons remained the same as in earlier simulations (See figure 2 and methods). Neighboring interneurons were recruited in successive cycles of the theta oscillations (125ms apart). We found that the presence of theta oscillations ensured that only those neurons receiving an external input fired and suppressed the activity of all the other interneurons.

The output generated in response to a sequential input pattern was stable across noise trials (figure 3.4 b). The firing rate map (figure 3.4 c, solid line) calculated for one neuron as an animal traversed a linear track (figure 3.4 c, schematic) is shown. Assuming that the animal moved at a uniform velocity, it encountered each grid field (alternately, received an external input) after a fixed interval of time and reliably generated a sequence of spikes in response to the input. Note that uniform velocity is not a prerequisite for stable stellate cell responses as we will explain in the next section.

3.2.4 Theta induced reliability persists over a range of frequencies

Theta oscillations span a range of frequencies from 6 to 12 Hz in rodents. Do changes in theta frequency compromise the reliability of the network responses? As theta frequency increased, the time between inhibitory bursts and rebound spikes remained nearly the same since this was determined by the time scale of the rebound kinetics

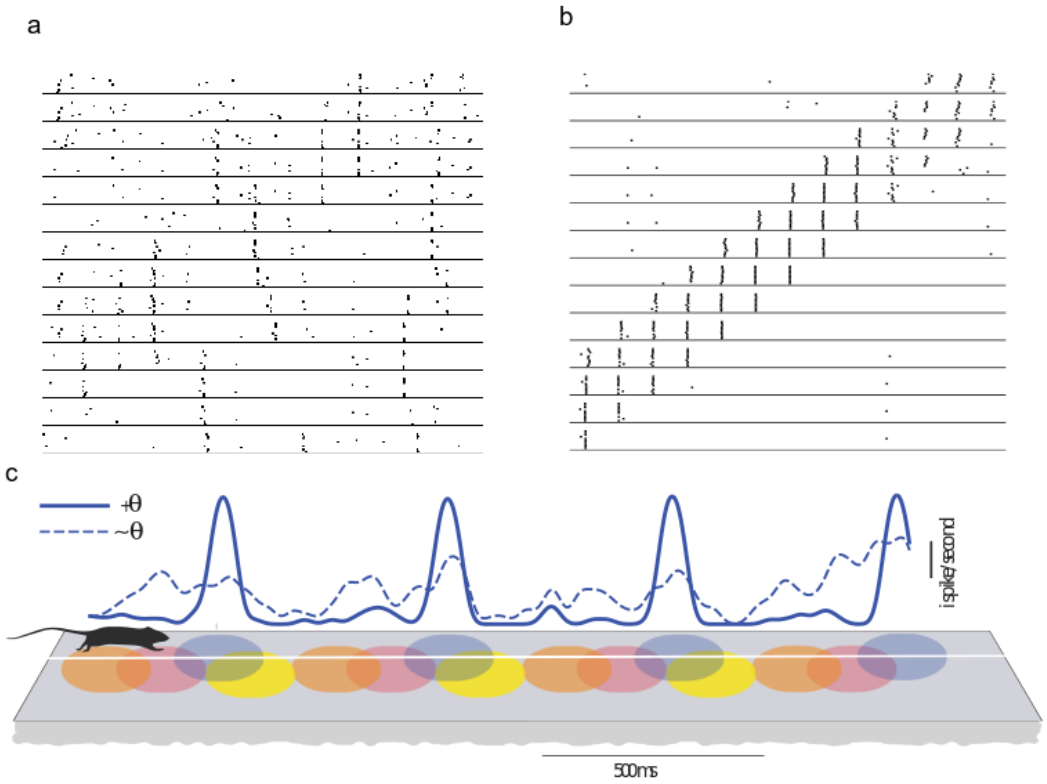

FIGURE 3.4: *Theta mediated stability of an MEC network* The response of the stellate cells in the absence of theta drive to the inhibitory interneuron layer is shown as a raster plot in (a). When theta oscillations (8Hz) were present, stellate cells evoked a reliable response over ten trials (b). The mean firing rate convolved with a moving Gaussian window is shown in (c) when theta oscillations were present (solid line) or absent (dashed line). The schematic below shows the grid fields of a rat running at a uniform velocity. The temporally periodic spiking pattern of stellate cells appears as a spatially periodic response.

of stellate cells. Therefore, the phase at which stellate cell spikes occurred started to shift systematically as the frequency increased (figure 3.5 a, b). As long as the shifted stellate cell spikes stayed within a phase window where the inhibitory neurons were sufficiently hyperpolarized by the theta drive, the network responses continued to follow the external input. At frequencies 12Hz stellate cell spikes invaded the receptive phases of the theta oscillations and began to interfere with the ability of the network to follow an external input. This caused an increase in the standard deviation of the spike time distribution (figure 3.5 a) and a further deterioration of the network's response. We calculated the reliability across trials measured as the pairwise dissimilarity between spike trains (see methods). This measure showed greater reliability (lower spike distance - circles in figure 3.5) for theta between 6-12 Hz compared to a network that was not driven by theta oscillations (triangles in the box plot of figure 3.5 c). Changes in theta frequency can signal changes in the animal's behavior. For example, theta frequency is linearly related to the animal's velocity [Jeewajee et al., 2008] and can change dynamically with changes in velocity. As the animal's velocity increased, it encountered grid fields more rapidly. This translated in our model as an increased rate at which external pulses arrived at neighboring interneurons. We found that the network responded reliably to external inputs despite velocity dependent changes in frequency (figure 3.5 d). Our simulations also show that stable sequences are generated despite dynamic changes in the frequency of theta that can speed up or slow the onset of activity in successive neurons (figure 3.5 d).

3.3 Discussion

Our work shows that theta might play a role in stabilizing the response of the MEC network to sequential inputs by reducing the influence of internal distractors. Our approach differs from the way in which the experimental observations of Koenig et. al [Koenig et al., 2011] and Brandon et. al [Brandon et al., 2011] has been interpreted in the literature until now. The requirement of theta oscillations for the stable generation of grid cells has been taken as evidence for the oscillatory interference

model of grid field formation (See Introduction) [Burgess et al., 2007]. The proponents of the continuous attractor model dispute the role of theta by arguing that the stabilizing properties of medial septal theta arise due to its excitatory glutamatergic inputs rather than the rhythmic GABAergic inputs [Moser et al., 2014, Moser et al., 2017]. More experiments need to be performed in order to understand the mechanism of the emergence of hexagonal periodicity in MEC. But the requirement of external inputs impinging on layer II MEC for the stable emergence of the grid field has been gaining evidence from neuroanatomical and system neuroscience studies [Witter et al., 2017, Tocker et al., 2015, Dordek et al., 2016, Bonnevie et al., 2013]. Our work emphasizes the stabilizing role of theta for such externally generated inputs. Theta rhythm is thought to generate periodic temporal windows for local computations at certain phases of the rhythm [Mizuseki et al., 2009]. Also, any increase in the velocity of the animal is associated with a monotonous increase in the frequency and amplitude of theta rhythm across the hippocampal formation [Hinman et al., 2016]. Medial septal inactivation, which disrupts periodic firing fields of grid cells[Koenig et al., 2011, Brandon et al., 2011], disrupts this transformation of speed signals into increased frequency and amplitude of theta rhythm [Hinman et al., 2016]. These observations emphasize the role of theta rhythm in generating a reliable response to inputs arriving at commensurate frequencies that vary as a function of the velocity of the animal. But, the local circuits should be able to generate a reliable response for a wide range of frequencies at which the phase locked external inputs arrive. Our work demonstated that it is possible for a local circuit made of biophysically realistic stellate and interneurons with mutual inhibitory interactions to reliably respond to a wide range of frequencies. How does theta rhythmic drive to the local circuit generated reliable response? What properties of the local circuit allowed it to respond reliably to external inputs phase locked to theta rhythmic drive? We will try to answer these questions in the next chapter.

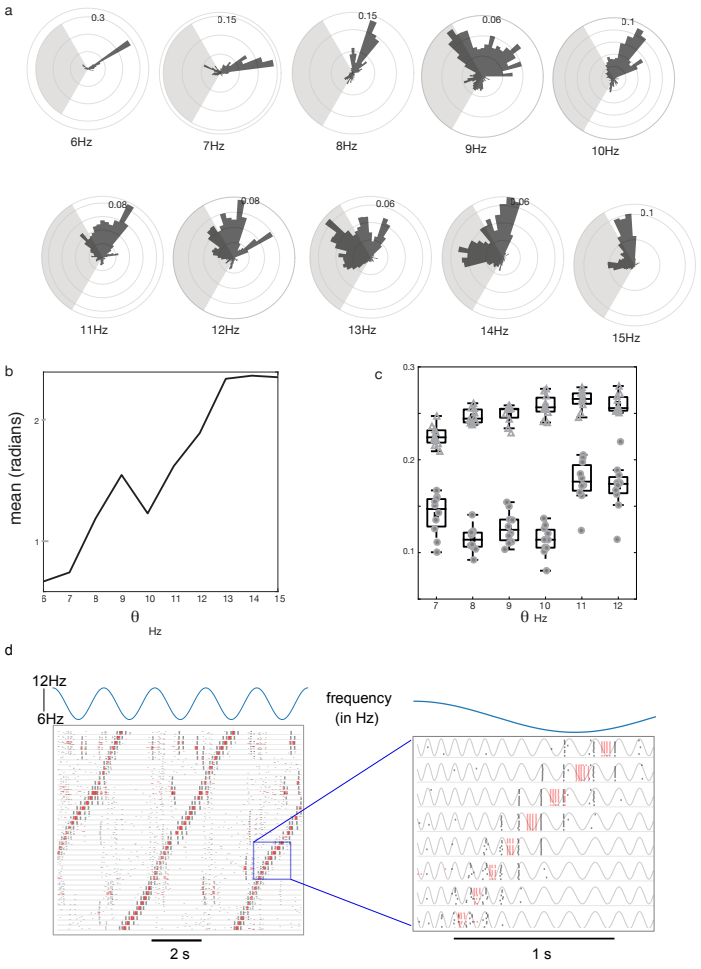

FIGURE 3.5: *Reliability across a range of theta frequencies.* (a) Polar plots showing the distribution of phases of stellate cell spikes for a range of theta frequencies from 6Hz to 15Hz. (b) The circular mean of the phase distribution of spikes plotted against theta frequency. (c) box plot of the spike distance in the presence (filled circles) and absence (triangles) of theta as a function of the rate at which input pulses stimulated successive interneurons. (d) Raster plot showing the response of the neurons (40 stellate cells - black lines, 40 interneurons - red lines) across ten trials (as in Figure 4d and 4e). Theta frequency varied periodically (0.5Hz, blue trace above the raster plot) between 6.0 and 12.0Hz. A magnified version of the raster plot on the left shows spikes against a background of frequency modulated theta oscillations

Chapter 4

Mechanism of theta induced reliability

4.1 Introduction

The hippocampal formation encodes neuronal representations of the external world that are relevant for navigation and memory. The firing rate of pyramidal cells of the hippocampus, for example, encode the location of an animal as it enters these circumscribed regions, known as place fields, and the firing rate of the recorded cell monotonically increases towards the center of the field [O'Keefe, 1976]. Apart from this symmetric firing rate, information about the location of the animal is also encoded in the phase of theta rhythm at which the individual place cells fire. As the animal traverses the place field of a neuron, the spiking systematically shifts from the trough of theta to near the peak of theta as it exits the field [OKeefe and Recce, 1993]. Grid cells of the medial entorhinal cortex fire at the vertices of a hexagonal grid [Fyhn et al., 2004, Hafting et al., 2005]. Like place cells, the phase of grid spikes also precesses with respect to theta rhythmic LFP [Hafting et al., 2008]. When combined with firing rate coding, phase precession increases the information content of the place cell response about the location of the animal significantly. Such temporal coding referenced to internally generated, behaviourally modulated rhythms abounds in nervous systems [Panzeri et al., 2010, Kayser et al., 2009]. One of the crucial roles attributed to oscillations observed in various regions of the brain is to stabilize neuronal activity patterns in the presence of noise [Kayser et al., 2009].

The stabilizing role of temporal coding with oscillations is seen in the auditory

cortex. Information about auditory stimuli is represented in spatially distributed cell assemblies that evolve over time. These spatiotemporal patterns are locked to slow oscillations (4-8Hz) that are concurrenty observed. Including information about the phases at which cell assemblies and temporal patterns of neurons occur improves the representation of auditory stimulus. Slow oscillations provide separate channels for information representation in a wide variety of neuronal systems. When naturalistic noise was added to a fixed stimuli that did not vary across trials, the coding represented by the firing rate across spatiotemporal scales deteriorated; However, phase code provided by a slow oscillatory background drive persisted and increased the information content, even more than when there was no noise [Kayser et al., 2009].

Reduced reliability in the absence of slow theta rhythmic drive in the medial entorhinal cortex provides another example of the role of oscillations in stabilizing neural responses. How do slow oscillations bring about a reliable neuronal response in the presence of destabilizing noisy background activity?

Diverse experimental observations suggest a few potential ways by which oscillations can cause reliable neuronal response across trials. Oscillations in local circuits modulate the gain of neurons thereby affecting their spike timing [Tiesinga et al., 2004]. External inputs can increase the amplitude and can reset the phase of the oscillations in the target regions [Rizzuto et al., 2003]. Thus, gain modulation and phase resetting can lead to precise neuronal spiking from the onset of the stimulus. Oscillations are often generated in a central pattern generating circuits and are broadcast to many target regions. The synchronized oscillations along with long-range connections can bring about phase synchronized oscillations across the regions mediating efficient information transmission. Oscillations can directly influence the precision of action potentials as well. Slow oscillations are particularly suited for reducing the impact of noise on precise neuronal spike patterns. The hyperpolarizing phase of the oscillation curtailed the accumulating jitter in the timing of action potentials of individual neurons mainly by reducing membrane potential variations.

Phase synchronized oscillations might ensure phase locked inputs arriving at the local circuits. Yet, it is not sufficient to explain how the local circuit responds reliably to the external inputs. Accumulating jitter alone would not explain the loss of grid

cell periodicity when theta oscillation in the medial entorhinal cortex is removed. The firing fields do not become more diffuse but often fire at different locations compared to the original vertices of the hexagonal pattern. Therefore, the mechanisms mentioned above cannot explain the loss of grid cell periodicity when theta rhythms are removed.

We show that theta achieves reliable receptive field formation via two mechanisms: 1) It creates temporal windows where a phase locked afferent input can induce a reliable switching in a local competitive circuit, and 2) it synchronizes and relegates the stellate cells to the hyperpolarizing phase where they are unable to induce any activity in the recurrent circuit they are part of.

4.2 Results

4.2.1 Theta create temporal windows of heightened switching ability of local circuits

How do theta oscillations affect the network such that it responds selectively to an external input and not to the distractors, namely, competing excitatory spikes from stellate cells? As pointed out in chapter 2, the mEC network motif can operate in two different regimes: The activity in the local circuit is shifted intrinsically due to asymmetries present in the network (oscillatory regime) or the switching is externally induced by pulse like inputs that toggled the activity from one interneuron to the other. We continued our discourse further on with the regime where the external pulses arriving sequentially, commensurating at theta frequencies, distinctly toggled the activity of the local interneuron population. With the feedback excitation from stellate cells, the toggle can either be achieved via the external input or via feedback excitation. To understand the effect of theta oscillations on the network, we first simulated a simple network (Figure 4.1 a) where the two interneurons received different constant depolarizing inputs. The neuron receiving the higher input continually spiked while the other neuron was kept quiescent due to continuous inhibition. In order to toggle the activity of this network, we stimulated the quiescent neuron with a transient pulse. For sufficiently strong pulses, the neuron's activity switched for

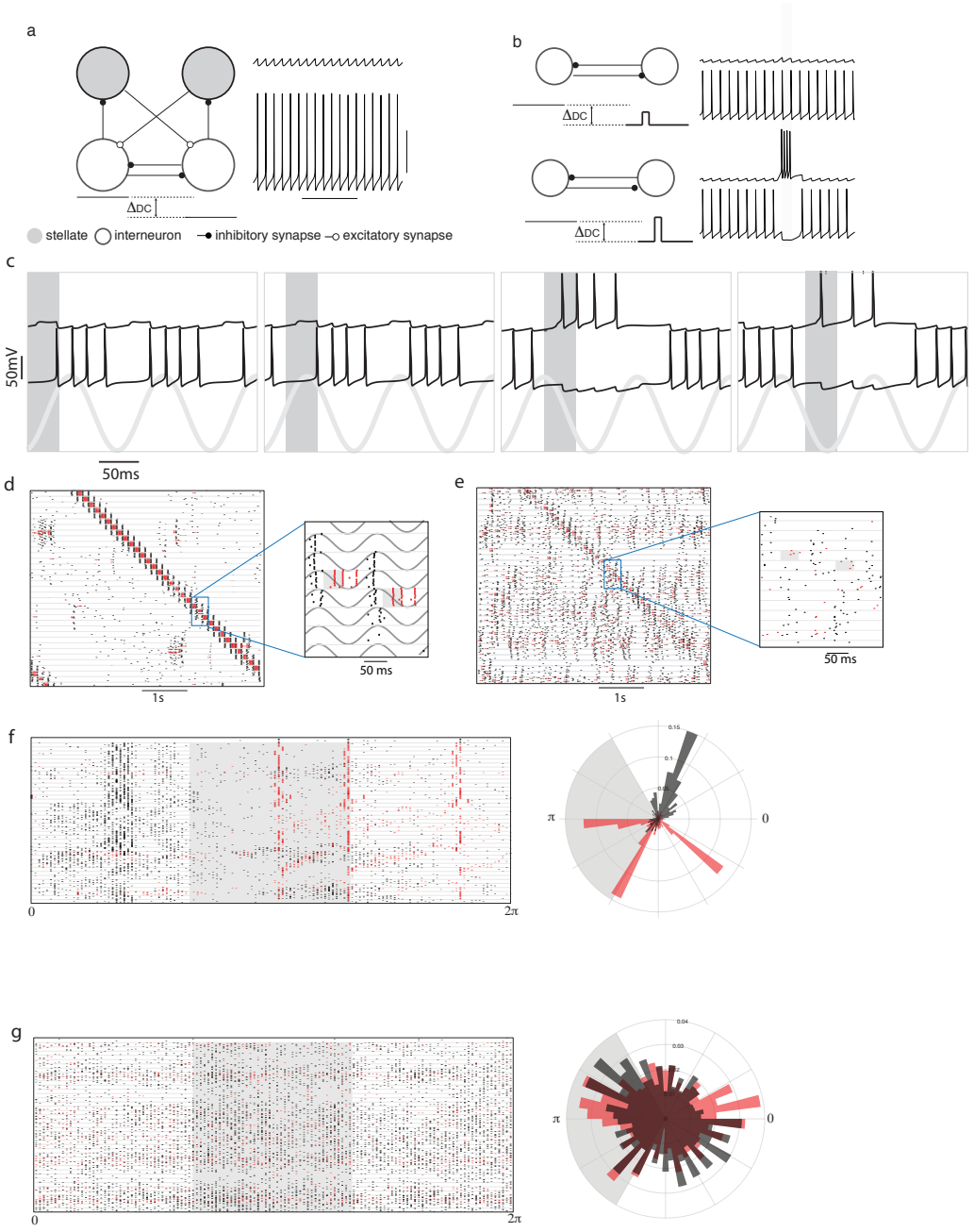

FIGURE 4.1: *Mechanism of theta induced reliability.* (a) Membrane potential of inhibitory interneurons when they received different suprathreshold inputs. The neuron receiving the higher input fired continually (bottom trace) while the other remained silent (top trace). (b) The same network motif as (a) (stellate cells not shown) was simulated. A weak transient pulse was given to the interneuron receiving the lower DC input (top panel of (b)). The stimulated interneuron (top trace) did not switch. A strong pulse caused a successful switch (bottom two traces). (c) Theta rhythmic drive was given to both the interneurons. A weak pulse (duration of the pulse is marked by the gray bar) caused a switch when it occurred in some phases of the theta oscillation (bottom gray trace) but not during others. (d) raster plot showing the reliable response of a subset of 20 interneurons (red line) and 20 stellate cells (black lines) from a larger network of 80 neurons, to an external input (marked as a gray bar in the magnified raster plots). The response of the same network in the absence of theta oscillations is shown in (e). Each row in d and e shows the response of a neuron across 10 trials which are plotted between the horizontal lines in the raster plots (f) Left. The raster plot shows the phase (with respect to the theta oscillation) at which stellate cells (black lines) and interneurons (red lines) spiked. The gray area marks the phase of the oscillation when the stimulus was present. Right. Polar plot showing a histogram of the phases where spikes occurred. The external input is marked in gray. (g) shows the response of the network when theta oscillations were absent. The phase was defined in terms of the input pulse that sequentially and periodically stimulated neighboring interneurons.

the duration of the input (Figure 4.1 b, bottom traces). Weaker pulses, on the other hand, did not evoke a transient switching response (Figure 4.1 b, top traces). We then stimulated the interneurons with a periodic theta drive that modulated the firing rate of the interneurons. Interneurons were maximally depolarized at the trough of theta and were most likely to spike then. When a weak pulse arrived at the quiescent neuron during the depolarizing phase of the theta oscillation, it successfully toggled the network. However, inputs that arrived at other phases did not cause a switch (Figure 4.1 c). Therefore, theta created periodic temporal windows where the activity of the network could be switched from one interneuron to another.

4.2.2 Theta synchronizes stellate cells to fire at phases where local circuits are more resistant to switching

In a larger network, we found that when the input arrived at the receptive phases of theta, the stimulated interneurons responded reliably to the input and the locus of activity of the network followed the input (Figure 4.1 d). However, merely creating periodic windows where external inputs can drive the network is not sufficient to generate reliable activity. Excitatory spikes from stellate cells can also occur during this receptive phase and perturb the response of the network to an external input. We found that when theta oscillations were present, the stellate cell spikes were tightly synchronized (Figure 4.1 d). These spikes always followed a burst of activity in the presynaptic interneurons (Figure 4.1 d inset, Figure 4.1 f). The interneurons were locked to the trough of theta oscillations, while stellate cell spikes occurred at a later phase due to the time taken to generate a rebound spike when released from inhibition. The stellate cell spikes occurred when the interneurons were hyperpolarized and were impervious to feedback excitatation from stellate cells (Figure 4.1 d,f). The input-triggered response of the network revealed the segregation of time between the inhibitory interneuron spikes and the stellate cell responses following a transient input (Figure 4.1 d). When theta was present and the external input occurred at a receptive phase, it was followed by a reliable burst of interneuron spikes, followed by the activity of stellate cells. In the absence of theta, stellate cells fired after each burst of interneuron spikes (Figure 4.1 e and the inset). However, the

stellate cell spikes were broadly distributed throughout the time between successive inputs to the network (Figure 4.1 e and Figure 4.1 g). Thus, stellate cells could effectively perturb the activity of the network in a manner that derailed its response to an external drive.

4.3 Discussion

Our work showed that theta can bring about reliability by the way it affects the gain and precision of interneurons and stellate cells in a recurrent local circuit. By modulating the gain of interneurons embedded in a competitive network and in a regime where a single active interneuron (or a group of neurons – not sharing any mutual inhibition) suppressed the activity of others, theta created temporal windows where a weak input can easily switch the activity from the winning interneuron to a silent one. Without a theta oscillation, the weak input faced competition from internal dynamics that stochastically varied across time and trials leading to an unstable and unreliable sequential response across trials. It is known that the precision of spikes is induced in the presence of strong synaptic inputs. Our work shows that the role of theta oscillation in bringing about reliability or loss of reliability occurs in the external input regime. Another crucial phenomenon that theta utilized in bringing stable responses is rebound kinetics of stellate cells that match the timescale of theta. By locking the spikes of interneuron to the most excitable phase of theta, theta sequestered the spiking response of stellate cells, which spiked after a delay due to rebound, to the least excitable phase.

One interesting question that might arise is that why can't the system adapt to subdue noises without invoking theta or any other oscillations? One answer is that noise is inevitable in a dissipative non-equilibrium system. It starts to play an interesting role once the nonlinearities and dynamics away from fixed points starts to kick in, which happens often in biological systems [Haken, 2008]. It might also happen that organisms actively maintain sources of noise to tackle uncertainties in the external world. For example, noisy representations allow for stable behaviour in the presence of volatile state of the world [Duffy et al., 2019]. Counterintutively, noisy fluctuations can even bring about reliable responses. Correlated noise, which

can easily be provided by divergent pathways of recurrent curcuits, induces synchronized firing in neurons sharing the frequency at which they resonate, leading to synchronized firing that oscillates at a frequency set by intrinsic properties of neurons [Ermentrout et al., 2008]. The synchronized population response of the near homogenous neurons, in turn, can provide a reference frame for encoding spatial information in a reliable manner.

In our model the external input utilized the temporal window created by theta oscillatory drive to induce reliable response. This same mechanism can be used to multiplex inputs arriving at the medial entorhinal cortex wherein the local circuit can flexibly switch responding from one target input to another. We explore this in detail in the next chapter.

Chapter 5

Flexible routing of reliable information with theta rhythm

5.1 Introduction

Local regions of a brain are often specialized to perform certain subsets of computations. For any adaptive behaviour or cognitive task, many regions of the brain act in concert as demanded by specific circumstances. As circumstances change, distinct ensembles of neuronal populations engage with each other. Given that the ebb and flow of the external world is mostly unpredictable, animals, remarkably learn to actively invoke brain wide configurations of active cell assemblies that best serve moment by moment demands.

One dominant hypothesis that explains the dynamic configurations is that oscillations, and particularly phase-locked oscillations of synchronously firing neurons across brain regions facilitate the transmission of information within specific bands [Fries, 2016]. Coherent oscillations across brain structures have been observed over a wide range of frequencies [Siegle and Wilson, 2014, Womelsdorf et al., 2007, Landau et al., 2015]. Slow oscillations, like the theta rhythm, are also implicated in bringing cell assemblies together and facilitating information transmission. Various physiological and behavioral experiments add increasing evidence to the role of theta oscillatory phase locking in coupling regions serving a task/behavior [Jones and Wilson, 2005b, Kay, 2005, Klimesch, 1999, Doppelmayr et al., 1998]. Theta oscillatory coupling has been implicated in successfully encoding memories [Klimesch, 1999], improving performance associated with learning [Jones and Wilson, 2005b, Kay, 2005],

successfully recalling memories invoking learned network configurations in a task-dependent manner [Klimesch, 1999].

In an olfactory learning tasks, rats were trained to discriminate between two odors that arrived at regular time points in random order. The rats were supposed to report the arrival of a conditioned odor stimulus by pressing a lever to get a reward. After a few weeks of training, the rats improved their performance significantly more than chance. As the performance fluctuated in a session spanning many trials, coherent oscillations in theta frequency regime emerged between the olfactory bulb and the hippocampus waxing and waning in step with performance fluctuations. The theta frequency oscillation also coincided with the increased sniffing frequency that preceded odor arrival in a trial [Kay, 2005].

Coherence in theta frequencies is also observed between the hippocampus and the medial prefrontal cortex in working memory tasks and in learning context-dependent behaviors. Learning induced changes occur both at the single cell level as well as at the level population of neurons: the mPFC neurons started to spike in a correlated manner to theta rhythmic LFP of the hippocampus and the phase coherence between mPFC-LFP and hippocampal LFP increased [Jones and Wilson, 2005b].

Optogenetic activation at a theta rhythmic frequency (8Hz) of neurons from the basolateral amygdala innervating medial entorhinal cortex immediately following contextual fear conditioning enhanced the retention of memories [Wahlstrom et al., 2018]. Such activation also entrained hippocampal-entorhinal LFP theta oscillations suggesting an important role for theta oscillations in facilitating information transfer from brain structures to the hippocampus via medial entorhinal cortex.

Buzsaki [Buzsáki, 2006] suggested three possible ways by which phase coherent inputs can arrive at a local circuit: 1) A strong central pattern generator generating a sustained oscillation at a certain frequency can force the target regions to oscillate at that frequency, 2) The oscillations in a local target region can induce a cascade of activities with characteristic time delays in its postsynaptic targets, and 3) Bidirectional connections across two regions with neurons that have resonant properties can generate sustained phase locked oscillations with only weak influences.

In the MEC network we simulated, we show that the same mechanism that allowed weak phase locked inputs to cause reliable switching in the local circuit can

also allow theta rhythm to flexibly listen to one of the competing inputs that try to cause switching in the local circuits.

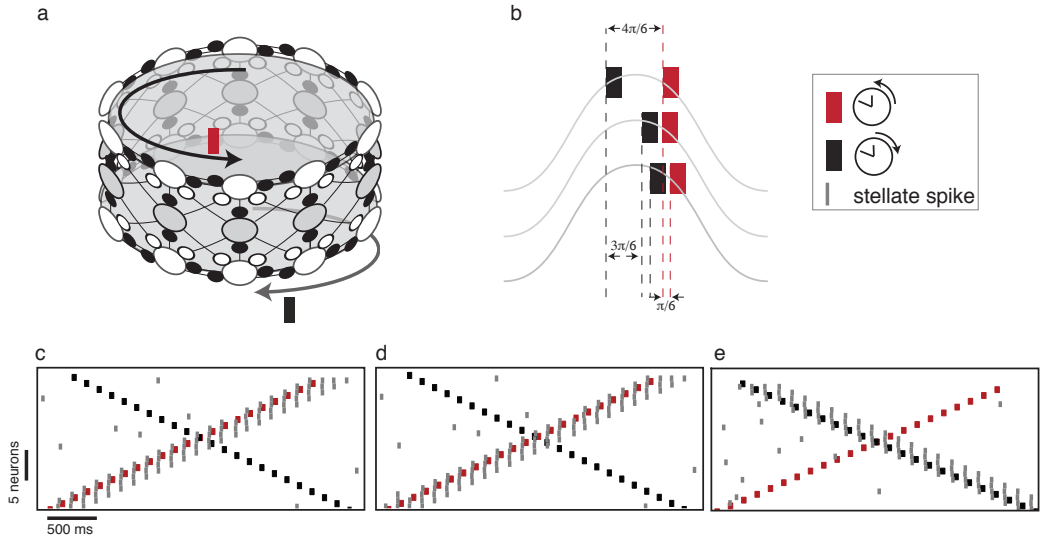

FIGURE 5.1: *Theta gates transmission of competing inputs.* (a) Topology of the network. Two sets of interneurons arranged on different rings (top and bottom empty circles) inhibit the same stellate cell population (middle ring with filled circles). Two separate input pulse trains are given to the two inhibitory population. The input to upper ring followed a counterclockwise activity pattern while input to the lower ring followed a clockwise sequence. (b) The phase of each input within a single cycle of theta for three different cases. The response of the network to these patterns of input are shown in (c), (d) and (e). The peak of the oscillation corresponds to the maximally hyperpolarized phase of theta (c) The input arriving at the depolarizing phase (red) elicited a spike (gray line) in the post-synaptic stellate cell while the one arriving during the hyperpolarized phase elicited none (this case corresponds to the top trace in (b)) (d) Both the inputs arrive at the depolarizing phase. The input that caused a maximum depolarization (red) elicited a successful response (this case corresponds to the middle trace in (b)). (e) The inputs to both the clockwise and the counter-clockwise rings were shifted. This switched the stellate cell from following the counter-clockwise input to following the clockwise input.

5.2 Results

5.2.1 Theta oscillations gate the transmission of competing inputs

When theta oscillations were present, the network reliably followed external inputs that arrived at the receptive phase of theta. Here we examine the response of the network when competing external inputs occur at different phases of the theta cycle. We simulated a network consisting of two groups of interneurons connected to the same pool of stellate cells. All the interneurons were coupled to each other. Each group of interneurons extended inhibitory connections to the stellate cells forming two separate ring networks (Figure 5.1 a). The upper ring of interneurons received

a transient pulse that traveled in a counterclockwise direction while the lower ring received an input that traveled clockwise. The two input streams, clockwise and counterclockwise, competed to elicit a response in the same pool of stellate cells. We kept the amplitude of both the inputs constant and varied their phase relationship with respect to an external common theta oscillation.

In the first of the cases tested (Figure 5.1 b), one of the inputs (clockwise) arrived when the interneurons were near their most hyperpolarized phase while the second input (counterclockwise) arrived at the depolarizing phase. Predictably, the second input succeeded in eliciting a sequence of spikes in the upper ring of interneurons that entrained the stellate cells and inhibited all the other neurons. We then varied the phase of the clockwise input such that the pulse occurred progressively closer to the phase of the counterclockwise input (Figures 5.1 b, Figure 5.1 d and Figure 5.1 e). When the input crossed a particular phase of the theta oscillation (Figure 5.1 b bottom row and 5.1 e), it elicited spikes in inhibitory interneurons of the lower ring. This inhibited all the other interneurons including the neurons on the upper ring of the network. Therefore, even though the counterclockwise inputs occurred during a depolarized phase of theta, the response of the network followed the clockwise inputs because it occurred earlier and also during the depolarized phase of the theta cycle. Thus, the mechanism whereby the network selects between inputs is determined, not only by coherent theta gain modulation of inputs, but also by the temporal order and the phase at which the inputs occur. Thus, theta oscillations can serve as a gate that permits a particular temporal ordering of stellate cell responses while prohibiting a different temporal ordering in the same group of cells.

5.3 Discussion

In our model the distractor inputs were phase locked to theta albeit at the least excitable phases. If the distractor inputs arrived at random phases it might compete with the target inputs and render the response of the network relatively unstable.

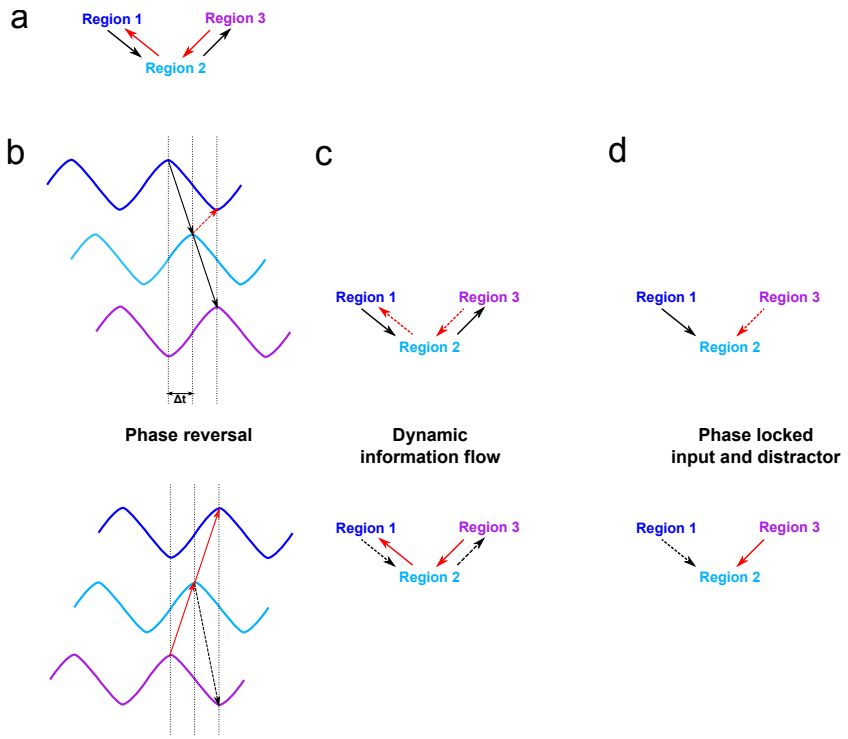

FIGURE 5.2: *Phase reversal imply phase locked distractors.* (a) Three hypothetical regions of a brain are shown with the arrows representing the potential direction of information transmission. Region 2, for example, is bidirectionally connected to both region 1 and region 2. (b) Upper schematics. Local LFP oscillations from the three regions indicate the flow of information as would be facilitated by mechanisms elaborated in the previous sections and chapters. lower schematics. Local oscillations after phase reversals. (c) Upper schematics. Flow of information corresponding to the LFP phase relationship shown in the left panel. Information is relayed from region 1 to region 3 via region 2. Lowe schematics. Flow of information for phase reversed LFP relations. Information is routed in the opposite direction, i.e, from region 3 to region 1 via region 2. (d) As the information is changing the direction of its flow, the local circuits of region 2 flexibly switch from listening to region 1 (upper schematics) to region 3 (lower schematics). Note that the distractor inputs still arrive phase locked to the LFP oscillation.

The mechanism whereby local circuits ignore inputs multiplexed to the least excitable phases of theta is termed temporal division multiplexing [Akam and Kullmann, 2014]. Our model, like temporal division multiplexing, suffer from distractors arriving at randoml phases. While theta rhythmic modulation in our model is able to relegate the intrinsically generated rebound spikes of stellate cells to least excitable phase of theta, it has no control over the externally generated distractor inputs.

There might be a scenario under which the distractor inputs might be packaged into the least receptive phases of rhythmic oscillations. It is exemplified by the phenomenon of phase reversals in a constellation of coherent neural assemblies across brain structures [Adey, 1960, Naya, 2001]. An illustration (figure 5.2) demonstrate the possibility of phase locked distractors arriving at the hyperpolarized phase of an oscillation. The information transfer in certain bidirectionally connected regions of the brain is shown to be flexible in its direction [Naya, 2001]. Thus, when information is flexibly reversed in a path involving at least three distinct regions of the brain, one of the region (not in the edge) has to switch flexibly between responding to one or the other of the adjacent regions. When the regions involved are exhibiting phase coherent oscillations, the distracting inputs to the target region are locked to a phase of the common oscillation.

Chapter 6

Inheriting Phase precession

6.1 Introduction

Phase precession of place and grid cells of the hippocampal formation provides one of the most robust temporal codes known in systems neuroscience [OKeefe and Recce, 1993]. The first set of spikes the place cell generates, as an animal visits the corresponding place field, is aligned to the trough of a theta cycle. Subsequent spikes, as the animal moves through the place field, are aligned to phases of the LFP oscillation. These spikes occur at progressively earlier phases until the animal exits the place field. Phase precession never exceeds 360 degrees. Thus, knowledge of the phase of LFP for a spike of place cell, provides more information about the location of the animal within the place field, than only knowing its firing rate which is nearly symmetric with respect to the center of the place field [OKeefe and Recce, 1993, Skaggs et al., 1996]. The place of the animal is encoded more accurately when this phase information and receptive field information are combined [Jensen and Lisman, 2000].

Another interesting consequence of phase precession can be gleaned when more place cells with overlapping place fields are considered [Foster and Wilson, 2007]. An animal traverses overlapping place fields over a time scale of seconds. With theta phase precession, neurons with neighboring place fields fire sequentially in a cycle of theta rhythm that matches the order in which the corresponding place fields are visited [Mehta et al., 1997, Feng et al., 2015].

Compression of place cell sequences within each theta cycle can enable rapid learning of the trajectories. Spike timing dependent plasticity (STDP), discovered in

hippocampal slices, is sensitive to spike times of the order of milliseconds. A presynaptic neuron spiking a few milliseconds earlier than a postsynaptic neuron causes strengthening of the synapse connecting the two neurons. When the presynaptic spike occurs after a postsynaptic spike, the strength of the synapse decreases [qiang Bi and ming Poo, 1998]. Millisecond differences in the compressed sequences can strengthen the forward synapses thus storing the information of the path travelled as asymmetric connections [Arai et al., 2014].

6.1.1 Mechanism of emergence of phase precession

More than two decades after the discovery of phase precession in place cells in the hippocampus, the mechanisms that lead to phase precession still remain unknown. Models of phase precession are typically of two kinds. Those that require spatial input and those that don't.

Models receiving phase locked spatial input

Spatial information in the neurons of the hippocampal formation can be jointly inferred from the firing rate and the phase of the theta oscillation. The models that generate a phase precessing spike pattern sometimes utilize the information of either the firing rate or assume phase locked spatial inputs that arrive at a fixed phase (not precessing phases) and activate successive neurons with overlapping place fields [Tsodyks et al., 1996, Bose et al., 2000].

In the model due to Tsodyks et. al [Tsodyks et al., 1996], the phase locked input in each cycle of theta activates a single neuron in a chain of neurons asymmetrically connected in one direction. The activated neuron triggers a cascade of activity in the direction of the asymmetry. This activity is terminated by the hyperpolarizing phase of theta oscillation. In the next cycle of theta, the next neuron in the chain is triggered at the same phase. Thus at every cycle of theta successive neurons in the chain are activated. As a consequence, in subsequent cycles the phase of the neuron shifts to an earlier phase.

In another model [Bose et al., 2000], the phase locked inputs, in the beginning of place field of a pyramidal cell, activate a transient activity in a motif comprising

the pyramidal cell and an interneuron (or group of interneurons). The end of the place field is determined by the end of this transient activity which orchestrates the phase precession across cycles of theta without any further spatial input to the motif. The interneuron of the motif receives pacemaker input at the frequency of the background oscillation. Outside the place field, the interneuron is enslaved to the pacemaker input (which is inhibitory), whereas inside the place field, the dynamics of the network involves the interaction between pyramidal cell and inhibitory neuron with pyramidal cell spike leading the inhibitory spike.

Models receiving non rhythmic spatial input

In a model due to Mehta et al [Mehta et al., 2002], an asymmetric ramp depolarization is combined with theta paced inhibition onto the soma of pyramidal cells. This ramp increases over successive cycles of theta. Pyramidal cells are thus released from theta paced inhibition at progressively earlier phases resulting in precessing spikes.

In another [Chadwick et al., 2016] model the interneurons are phase locked to the external theta drive outside the place field. Inside the place field the place cells provide enough depolarization to nudge the interneurons to produce spikes that drift with respect to the background oscillation. Thus, with strong enough excitatory drive inside a place field the interneurons can be made to phase precess to a range of phases below 360 degree. Phase precessing interneurons, in turn, can recruit pyramidal cells to phase precess.

Models that does not require spatial input

In the oscillatory interference model, interaction between two oscillators can explain both the firing rate code of the place/grid cells and the phase code exemplified by phase precessing spikes. One of these oscillators coincides with the background theta oscillation while the frequency of the other oscillator is slightly higher than the background theta oscillation. The frequency of the faster oscillator is also proportional to the velocity of the animal. For an animal running along a linear track with

constant velocity, phase precession can arise as a consequence of the interaction between a slow oscillator and a fast oscillator. The combined nested oscillation of the two oscillators exhibit two time scales: 1) an envelope oscillation of slow frequency (the frequency equalling the difference between the frequencies of the two oscillators) and 2) A faster oscillation (the frequency equalling the average of the frequencies of the oscillators, hence faster than the slowest oscillator) that induces spiking in the grid cell that precess with respect to the slower background oscillation.

Continuous attractor model can explain the emergence of phase precession when intrinsic conductances are added to individual neurons. In a model due to Navratilova et. al [Navratilova et al., 2011], continuous attractors were configured such that a bump like activity was generated and maintained without any external input in a set of neurons arranged on a ring. A velocity input from an animal moving in one of the two directions was fed to one of the two separate rings of neurons that received input from equivalent neurons in the original ring. These neurons sent back their projections to the ring attractor with an offset (clockwise or counterclockwise), as a function of the direction input they received. As these neurons received both head direction information as well as positional information, they were called conjunctive grid cells. Theta rhythmic input to these conjunctive cells allowed them to fire action potentials only at a part of a theta cycle. They caused a movement of 'bump' of activity in one direction along the ring due to their offset. As the hyperpolarizing phase of theta terminated this moving 'bump' of activity, at successive cycles of theta the bump of activity would start from arbitrary neurons on the ring. However, the activity resumed from locations along the ring where a recent firing activity has occurred due to a depolarizing membrane potential dynamics of stellate cell that followed a spiking activity. This enabled the ring attractor to resume activity at the hyperpolarizing phase of theta from recently fired stellate cells, resetting the moving bump of activity in a partial manner. As the resetting of activity is only partial, and the moving bump of activity will proceed from this point onward in the next cycle of theta, the neuron would start firing at earlier phases of theta.

We have, in the previous chapters, induced spatially modulated activity in stellate cells that are recruited by inhibitory interneurons, to explain the reliability due to theta. Experimental observations [Schmidt et al., 2017, Ego-Stengel and Wilson,

2007, Frank et al., 2001] and modeling studies [Bose et al., 2000, Chadwick et al., 2016] hint at the possibility that interneurons of mEC due to their intrinsic nature alone or from their interaction with excitatroy neurons can display phase precessing spikes. In this chapter, we explore the role of phase precessing interneurons in inducing phase precession in stellate cells, and how asymmetry in inhibitory connections affect the extent of phase precession.

6.2 Results

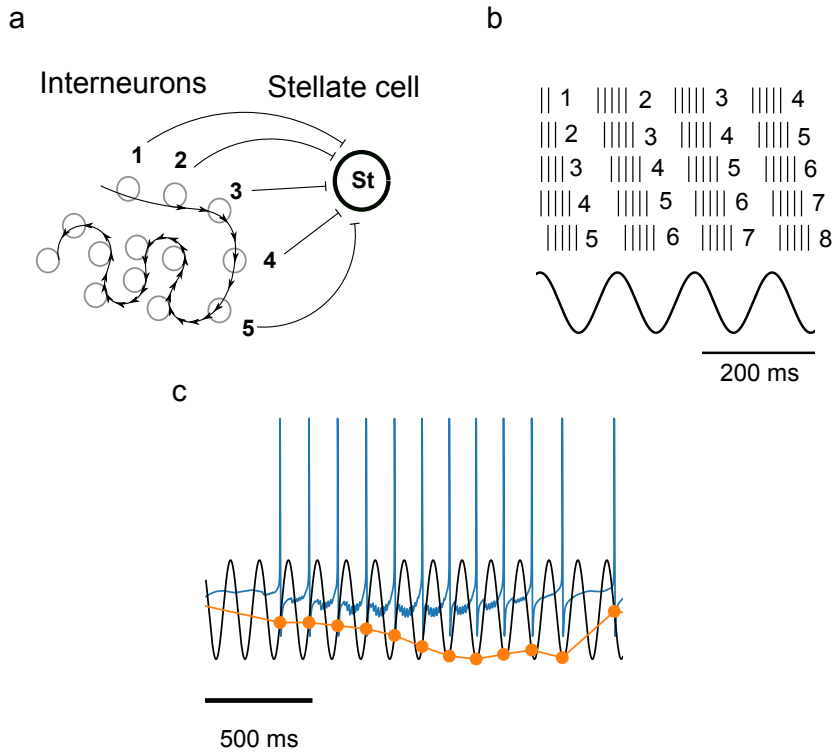

FIGURE 6.1: *Interneurons pass on phase precession to stellate cells.* (a) A stellate cell is connected to 5 interneurons. (b) The interneurons spikes are generated to simulate (see methods) phase precessing interneurons. Each interneuron produced burst of spikes at 80 Hz. Neuron next in the sequence were phase shifted with respect to each other. At every cycle of theta the sequence is generated from overlapping neurons that are shifted by one neuron in the ring or line. (c) Stellate cells rebound spikes are shown with the theta rhythm. The phase of the spikes are precessing monotonously.

6.2.1 Phase precessing inhibitory interneurons recruit stellate cells to phase precess

Previous models have suggested that the interneurons can actively participate in phase precession [Bose et al., 2000, Chadwick et al., 2016]. Active participation of

interneurons in generating phase precession can be mediated ether by a temporal mechanism [Bose et al., 2000], or can be initiated with excitatory place input from pyramidal neurons to inhibitory interneurons [Chadwick et al., 2016]. Instead of explicitly simulating any of these models, we have assumed that interneurons phase precessed using either of these or other mechanisms. To check if postsynaptic stellate cells can inherit phase precession from interneurons, we simulated the network shown in figure 6.1 a. A single stellate cell received inputs from a set of interneurons that were sequentially recruited at the successive cycles of theta (figure 6.1 a and b). Each interneuron fired in successive cycles at progressively earlier phase (figure 6.1 b). Does the phase precessing interneurons induce phase precession in the stellate cells? We found that the phase of the spikes as measured against the background oscillation shifted to earlier phase values in the successive cycles of theta (figure 6.1 c).

6.2.2 Asymmetry in inhibitory connectivity increases slope of phase precession

The weights of the inhibitory synapses onto stellate cell fit a symmetric Gaussian profile. Such a Gaussian, symmetric, inhibitory connectivity profile (figure 6.2 a - red trace) transferred the phase precession from inhibitory interneurons to stellate cells. Next we asked what effect, if any, different possible asymmetries have on the phase precession. We tried two different skewed connectivity (figure 6.2 a, green trace and figure 6.2 b, blue trace - compare with the symmetric inhibitory connectivity (red trace)) All connectivity profiles induced phase precession in the target stellate cell (figure 6.2 b). The asymmetry in one of the directions introduced steepest phase precession compared to the other profiles tested (fig 6.2 b - the green trace compared to the blue and red traces).

6.3 Discussion

We have shown that stellate cells can be recruited to phase precess by interneurons of the medial entorhinal cortex. We have also shown that introducing asymmetry

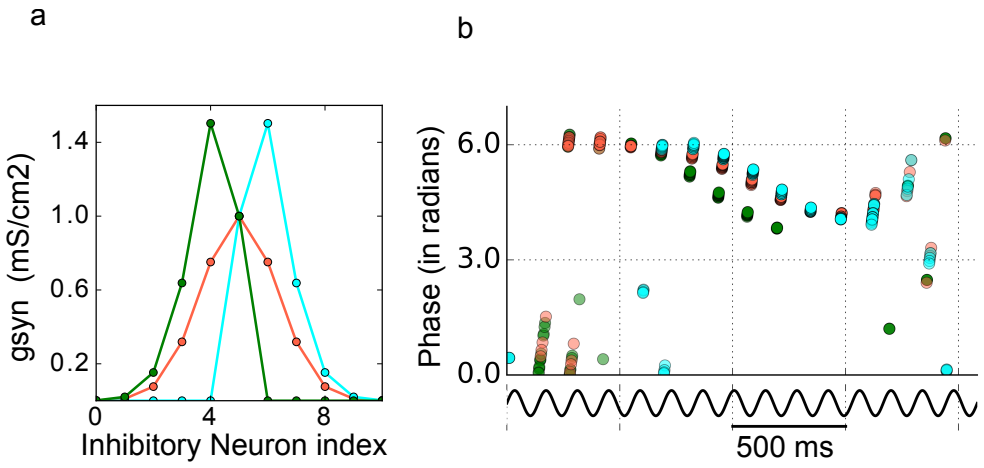

FIGURE 6.2: *An asymmetry in the connectivity increases the slope of phase precession.* (a) the profile of connection strength of inhibitory synapses from a line of interneurons onto a single stellate cell (not shown). The index of the interneurons are shown in the x axis. The strength of inhibitory conductance is shown in the y-axis. (b) All connectivity profiles, symmetric or otherwise, induced phase precession. Phase as a function of time is shown. The slope of phase precession is increased for the asymmetric connectivity.

in the inhibitory-excitatory connections resulted in steeper phase precession of stellate cells. This asymmetry can result from activity dependent plasticity mechanisms. Haas et. al [Haas et al., 2006], has observed in slices of entorhinal cortex a plasticity mechanism in the inhibitory synapses of principal neurons. This inhibitory plasticity is sensitive to the relative timing of the presynaptic and post synaptic spikes. Repeated traversals of a grid field by an animal on a linear track can induce asymmetric connections from inhibitory neurons to excitatory neurons due to spike timing dependent plasticity of the inhibitory synapses. Our result would suggest that the asymmetry so induced must impact the slope of phase precession. Feng et. al [Feng et al., 2015] observed in CA1 region of the hippocampus that a large number of neurons lacked a clear phase precessing temporal pattern that only got stabilized in the subsequent laps through a linear track. Plasticity mechanisms that introduce asymmetry might explain the strengthening of phase precession with experience observed in the hippocampal formation.

Chapter 7

Discussion

We showed that the MEC interneurons are receptive to external inputs only within cyclic windows defined by theta oscillations. Further, theta oscillations corralled stellate cells to spike synchronously at a phase where inhibitory interneurons were hyperpolarized and less receptive to excitatory inputs. This prevented stellate spikes from depolarizing randomly connected postsynaptic inhibitory interneurons that could compete with external inputs to other neurons. This mechanism to generate reliable sequences can also be harnessed to ensure that the entorhinal cortex selectively gates inputs such that some inputs that arrive at specific phases are transmitted to postsynaptic targets while others are blocked.

7.1 Biophysical models and degeneracy of stellate cell electrophysiology

We have utilized the timescales of rebound spikes of the stellate cells mediated by I_h currents to explain theta induced reliability of local circuits with respect to sequential external input patterns. Though we have used biophysical model incorporating the dynamics of ion channels mediating subthreshold oscillations and spiking activity [Rotstein et al., 2006, Fransén et al., 2004, Dickson et al., 2000], we haven't incorporated many other ion channels that are found in stellate cells of medial entorhinal cortex [Pastoll et al., 2012]. Especially, incorporation of calcium currents and calcium dependent potassium currents would enhance formation of doublets and cause burst of spikes in response to depolarizing currents [Fransén et al., 2004, Mittal and

Narayanan, 2018]. These channels also modulate the subthreshold oscillations [Mittal and Narayanan, 2018], afterhyperpolarization and delayed after potential (DAP) [Klink and Alonso, 1993], and are found to be altered in an artificial rat model of Alzheimer's disease [Heggland et al., 2019]. Theta time scale of DAP enables one of the continuous attractor models [Navratilova et al., 2011] to recover the bump of activity after a hyperpolarizing phase of theta to ultimately lead to phase precession of spikes across theta cycles. We have, in our model, chosen a set of parameters that are fixed for all the stellate cells used in our simulations. Variability arised mainly as a result of conductance based synaptic noise we have incorporated in our model. But a recent study found many-to-many mapping of ion channel properties to electrophysiological properties of stellate cells [Mittal and Narayanan, 2018]. It also argued for incorporating heterogeneties in channel properties in modeling studies that try to understand the function of mEC microcircuits, as the properties of ion channels and integrative properties of neurons of mEC are variable in nature [Pastoll et al., 2019]. Although we haven't explicitly incorporated heterogeneity in our large scale simulations, our result from small motif is an attempt in extending the realm of degeneracy and robustness from cellular neurophysiology to microcircuits (see Modulation of I_h conductance leads to the transition of regimes and Figure 2.4). Also the sag ratio, of all the electrophysiological properties studied, seem to be modulated independently by most number of ion channels and is mostly correlated with other electrophysiological properties of stellate cells [Mittal and Narayanan, 2018]. Thus rebound spiking, robust to perturbations of ion channel properties, would render the response of stellate cells stable in the presence of theta rhythmic drive.

7.2 Phase locked spatial inputs to interneurons

The most abundant inhibitory interneurons in the MEC express parvalbumin, and they concentrate their GABAergic synapses onto stellate cells (and intermediate pyramidal neurons) [Wouterlood et al., 1995, Fuchs et al., 2016, Berggaard et al., 2018]. Buffering et al. [2014], determined that these neurons are broadly tuned to spatial locations as opposed to grid cells that fire sparsely and at periodic locations in

space. The phases of the grid cells that provided inputs to an interneuron were uncorrelated. The authors suggested that the spatially uncorrelated inputs from grid cells imparted aperiodic firing fields to interneurons. Their finding adds to the observation that parvalbumin-positive fast-spiking interneurons in the hippocampus and neocortical circuits are broadly tuned [Tremblay et al., 2016, Royer et al., 2012]. However, these regions are also endowed with a subset of fast-spiking inhibitory interneurons that are tuned to spatial receptive field [Wilent and Nitz, 2007, Ego-Stengel and Wilson, 2007, Najafi et al., 2018]. Earlier experiments predating the discovery of grid cells also found that the fast-spiking inhibitory neurons of the entorhinal cortex display retrospective coding properties [Frank et al., 2001]. Thus, there is a possibility that a subset of interneurons does indeed code for grid-like fields.

In the same study [Buetfering et al., 2014], the probability of finding a pair of principal neurons and an interneuron, such that the pyramidal neuron spikes are followed by interneuron spikes within few milliseconds, is increased manyfold if they are recorded from the same tetrode instead of from different tetrodes (133 out of 3538 pairs for the same electrode. 30 out of 9414 pairs for different electrodes). Thus, spatial proximity increases the likelihood that the interneurons will be activated by the principal neurons. The organization of the grid cells in a small neighborhood within a local MEC circuit is such that their relative anatomical location with respect to each other resembles the relative phases of their respective grid fields in a two-dimensional arena where they are defined [Gu et al., 2018]. This functional map is predominantly studied for principal neurons without any knowledge about their local wiring. Another study provides complementary wiring information: Serial block electron microscopy in a tissue block from the MEC reveals that axons protruding from an excitatory neuron make dense excitatory synapses onto adjacent inhibitory interneurons along the axonal path before they innervate excitatory neurons. Any one of the local interneurons receiving these dense excitatory inputs, in turn, makes inhibitory connections with myelinated axons onto the nearby excitatory neuron that is directly excited by its presynaptic neuron [Schmidt et al., 2017]. This cellular level feedforward network is hypothesized to provide a substrate for efficient information transmission. Taken together, the functional map from phase-shifted grid fields to grid cells in MEC [Gu et al., 2018] and a local feedforward inhibitory circuitry the

principal neurons are embedded in [Schmidt et al., 2017], suggest a convincing possibility of the inhibitory interneurons coding for grid cells. This grid-like property could be inherited from local principle neurons or both of the neurons can inherit the grid field firing property from grid cells of deeper layers of MEC.

We have, in our model, provided spatial inputs to inhibitory interneurons. Anatomical evidence listed above suggests that inhibitory neurons could be tuned to code for grid cells. Apart from layer II MEC, layer V neurons [Sargolini et al., 2006] and subiculum [Boccara et al., 2010] also include grid cells in their local circuitry. Layer V MEC, which receives input from the hippocampus as well as the superficial layers of the MEC, is the only known output of the hippocampal formation that sends projections across neocortical sites. Layer V neurons also send ascending fibers to the superficial layers of MEC. Projections from deeper layer (Layer V) neurons ramify onto neurons throughout superficial layers. Of these, synapses onto inhibitory interneurons comprise 44 percent of the total target connections[Ohara et al., 2018]. This suggests that the inhibitory interneurons of layer II might even receive spatially modulated external inputs as used in our model.

By implementing the interneurons and excitatory stellate cells explicitly, our model has the potential to address other questions related to the circuit level functioning of medial entorhinal cortex. The interaction of excitatory and inhibitory neurons can generate grid cell firing that coexist with theta-nested gamma oscillations. An independent modulation of power and phase alignment of gamma rhythms can be achieved to increase the efficiency of information transfer to downstream neurons without affecting the grid field firing [Shipston-Sharman et al., 2016]. Solanka et. al, 2015, [Solanka et al., 2015] have shown that perturbation of interneurons with spatial inputs can disrupt the firing of interneurons in a hexagonal pattern while keeping the grid fields of most of the excitatory neurons intact. Thus, only a subset of excitatory interneurons and interneurons need have grid like firing patterns.

Another characteristic feature of our model is that the inputs arrived locked to theta rhythmic drive and caused a reliable switching in the activity of local circuits. The implication of this assumption is that inputs arriving on a cycle by cycle basis can induce grid-like patterns in target neurons. This is particularly observed in a recent experiment due to Zutshi et. al [Zutshi et al., 2018], where they optogenetically

activated pyramidal neurons that excited most of the neuronal types in the MEC which included the inhibitory interneurons as well. When the pyramidal neurons were rhythmically excited at theta frequency, the recurrent excitation onto other cell types momentarily disrupted the grid cells ability to fire in hexagonal vertices. As the excitatory impact waned within a cycle of theta, the external inputs arriving in a small remaining window were sufficient to induce reliable grid field formation in the MEC circuit. Thus, cycle by cycle integration of external inputs from other cortical inputs or deep layers of MEC converging onto superficial layers of MEC is sufficient to generate spatially modulated firing fields of grid cells.

Thus our model that includes theta rhythmic spatial inputs to interneurons arriving phase-locked to theta is supported by various experimental observations.

7.3 Stability in the absence of theta oscillations

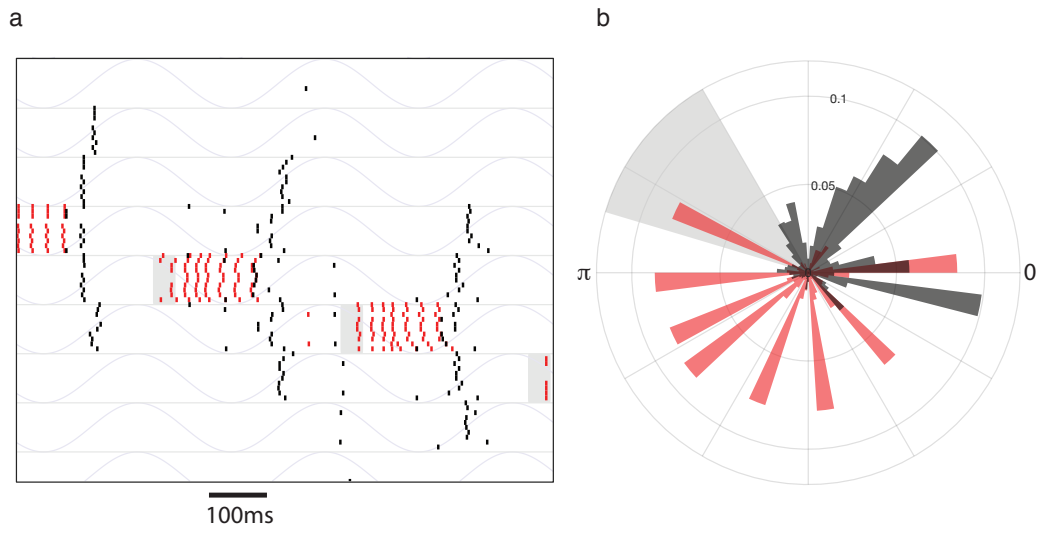

FIGURE 7.1: *Response of the network to a slow oscillation (2 Hz).* The input (shown in gray) toggles the activity of interneurons that continue to generate a burst of spikes (a). Rebound spikes by stellate cells occurred at a phase that did not perturb the sequence. (b) histogram of the phase at which the stellate cells (dark bars) and the inhibitory interneurons (red bars) generate spikes.

Our model suggests that stable sequential activity is contingent upon the presence of theta oscillations. In the absence of theta, multiple traversals over a given region of space failed to evoke a reliable response that is required to form grid-like receptive fields. However, recordings from Egyptian fruit bats show that grid-like

receptive fields can be formed in the absence of continuous theta oscillations [Yartsev et al., 2011]. This seems at odds with our model and experiments in rodent MEC where excising theta reversibly perturbs the grid-like structure of the receptive fields of MEC neurons [Koenig et al., 2011]. One way to reconcile these contradictory observations is to assume that the MEC network in bats receives large amplitude inputs compared to smaller amplitude inputs in rodents. This can lead to a stable response even in the absence of theta oscillations (Figure 4b, bottom traces). However, given that the MEC is a hub that receives multiple inputs, relying only on the amplitude of the input would impair its ability to selectively respond to some inputs while ignoring others that are equally salient. An additional layer of control can multiplex between similar inputs. Multiplexing is typically implemented using oscillations [Akam and Kullmann, 2010, Akam and Kullmann, 2014]. We used theta oscillations to modulate the gain and amplify inputs arriving at some phases while attenuating the effect of others. This phase dependent gain modulation does not require a continuous fixed frequency oscillation. Interestingly, even though bats lack a persistent oscillatory signal like theta in rats, they generate fluctuating low frequency local field potentials to which a significant proportion of principal cells are locked [Eliav et al., 2018]. Can our model network use these low frequency inputs to generate a reliable output? We showed that reliability of our model network responses progressively deteriorates in the high theta frequency regime ($>$ 11Hz) (Figure 5c). At low frequencies, the interneurons fire over a longer duration corresponding to a widened window of depolarization. The hyperpolarizing phase of the theta oscillation tends to shut the response of the interneurons and triggers a rebound excitation in stellate cells (Figure 7a). Stellate cell spikes continue to occur during the hyperpolarizing phase of theta oscillations (Figure 7b) and do not perturb the inhibitory network. Therefore, network responses to low frequency oscillations are reliable.

Bats show a large variability in the frequency of local field potential fluctuations unlike theta oscillations in rodents that vary over a smaller range. In our model network the input driven switch from one interneuron to another is rapid due to inhibitory competition between fast-spiking interneurons and occurs within a single theta cycle. Therefore, the network activity can respond to fluctuations in a cycle-by-cycle manner, relegating distractors to a hyperpolarized phase in spite of variations

in instantaneous frequencies. Changes in instantaneous frequency that occur on a slower time scale than the switching time scale have little impact on perturbing the input driven dynamics of the network. Thus the slow local field fluctuations seen in bats may be sufficient to evoke a reliable response in stellate cells.

7.4 Role of neuromodulation in gating sequences

Our model demonstrated that theta oscillations can gate the transmission of information between different brain regions. One can selectively couple two regions by ensuring that the phase of theta is coherent across these regions and information is transmitted during a restricted phase window of theta. Inter-regional interactions via oscillatory phase coherence is not restricted to circuits including MEC, but widespread across many cortical and subcortical structures [Colgin, 2011, Colgin, 2013, Kay, 2005, Kim and Lee, 2011, Liebe et al., 2012, Fries, 2016]. A number of behaviors depend on recruiting a broad network of regions. For example, hippocampal and amygdalar circuits show theta coherence when animals are exposed to anxiety inducing situations [Adhikari et al., 2010]. Working memory in rodents [Jones and Wilson, 2005b] recruits hippocampal and medial prefrontal cortex via theta synchrony. Many adaptive behaviours coincide with an enhanced coherence in the phase of the local field oscillations between different brain regions [Reinhart et al., 2015, Tendler and Wagner, 2015]. Memories at various stages of encoding, consolidation and retrieval invoke different configurations of brain regions that are dynamically assembled by theta phase coherence across these regions. During the early phases of learning an association between a conditioned and an unconditioned stimulus, the hippocampal - LEC coupling is characterized by phase synchronized theta oscillations. As learning progresses, the phase synchrony between the hippocampus and LEC decreases with a concomitant increase in LEC-medial prefrontal cortex synchrony [Takehara-Nishiuchi et al., 2012]. Theta synchrony is a read-out of increased information transfer across brain regions. However, finer control over the input during each theta cycle is required to ensure that MEC networks selectively listen to or ignore incoming inputs. What are the mechanisms that ensure the right inputs arrive at the right phase of theta? Inhibitory interneurons that participate in

generating and maintaining hippocampal theta rhythms broadcast rhythmic inhibition that targets inhibitory interneurons in other areas [Gonzalez-Sulser et al., 2014]. These, in turn, synchronize principal neurons. The effectiveness of inhibition onto principal neurons can alter the degree of synchronization and the phase of principal neuron spikes. In the hippocampal-medial prefrontal cortex circuit, this is likely controlled by neuromodulators like dopamine [Benchenane et al., 2010]that can effectively shift the phase of principal neuron spikes with respect to a theta oscillation and selectively couple it to brain regions downstream. Modulatory control can therefore create transient functional networks that flexibly serve different behavioral contingencies.

7.5 Effects of synaptic plasticity on sequences

Our simulations operated in a regime where the system responded to a sequential external drive and moved the locus of activity from one neuron to another. Stellate cells spiked and registered the temporal location of this transition. In the MEC network, GABAergic connections onto the principal neurons show spike timing dependent plasticity that enhances the weights of inhibitory connections for those synapses where the postsynaptic stellate cell spikes after the inhibitory interneuron [Haas et al., 2006]. Repeated sequential activation of the same network will therefore lead to changes in synaptic weight that introduce asymmetries in the network architecture [Mehta et al., 1997]. These asymmetries can influence the autonomous activity of the network (Figure 2.3 b) to follow sequences that were reinforced by past inputs. These sequences may appear as episodes where the activity of the network is replayed [Ólafsdóttir et al., 2018]in the absence of any external inputs.

In sum, our study highlights the central role of theta oscillations in generating reliable sequences and forming transient functionally connected networks. This is possible due to the fortuitous similarity between the time scales of theta oscillations and conductances of stellate cells together with the architecture of the MEC network.

7.6 Reliability and Phase precession

Grid cells of MEC are shown to display phase precessing spikes in both linear as well as two-dimensional trajectories. In our model, one crucial mechanism by which theta rhythmic input to interneurons induced reliability is sequestering of stellate cell spiking to the least excitable phase of theta. Though we haven't explicitly modeled the emergence of phase precession, we have modeled the scenario where the stellate cells can inherit the phase precession from interneurons. If stellate cells generate spiked that progressively precess in phase, it may eventually disrupt the response of the network to external inputs. How to reconcile theta induced reliability, as we propose, with phase precession phenomenon.

The microcircuit that we modeled can be envisioned as a functional module that imparts reliability to the larger network of MEC in which it is embedded. With this perspective, the phase precession can be thought to be mediated by a different set of neurons in MEC that are not part of the reliability inducing subnetwork. In support of this hypothesis, Mizuseki et. al[2009], find that in the entorhinal cortex majority of neurons are phase-locked to theta than showing phase precession, and the steeper slope of phase precession of stellate cells among MEC notwithstanding, the phase precession in EC neurons is weaker and rarer compared to that of hippocampal neurons. Even when phase precession is observed, it never covers more than 360 degrees for a single traversal of the gid field. Indeed, the average range of phases for single traversals is 180 degrees [Schmidt et al., 2009]. Phase precession and reliability can coexist if the spikes are relegated to the least excitable half of a theta cycle.

The phase precession and reliability due to theta can also coexist, if additional mechanisms, not biologically unrealistic, are included. For example, the spikes of a stellate cell on successive cycles of theta can be made to have a lesser and lesser impact onto its postsynaptic inhibitory interneurons. This can be implemented if stellate cells are assumed to have limited resources of vesicles in their axon terminals: The later spikes occurring at more depolarized phases will be, with the depletion of presynaptic vesicles, unable to generate postsynaptic currents, and thus would fail to induce spikes in the interneurons; The initial spikes occurring at the most hyperpolarized phases would generate postsynaptic currents that would fail due to the

attenuating effect of the hyperpolarizing phase of theta.

Thus theta induces reliability as we propose can accommodate the phase coding of hippocampal formation as reflected in phase precessing spikes.

Appendix A

Methods

A.1 Neuron Models

Stellate cells and interneurons were modeled as conductance based, single compartment spiking neuron models. Stellate cells were endowed with voltage dependent ion channels that were active at subthreshold membrane potentials, apart from sodium, potassium and leak ion channels involved in spike generation. These ion channels enabled the stellate cell to produce sustained oscillations in response to a constant depolarization [Rotstein et al., 2006, Acker et al., 2003, Dickson et al., 2000]. The current balance equation for the equivalent circuit model of the membrane is given by,

Stellate cell

$$C\frac{dV}{dt} = I_{ext_s} - I_{Na} - I_K - I_L - I_h - I_{NaP} - I_{Syn} - I_{Noise} \tag{A.1}$$

Interneuron

$$C\frac{dV}{dt} = I_{ext_i} + I_{pulse} - I_{Na} - I_K - I_L - I_{Syn} - I_{Noise} - I_\theta \tag{A.2}$$

Ionic currents were modeled as follows,

$$I_x = g_x(v,t)(v - E_x) \tag{A.3}$$

where $g_x(v,t) =$ maximal conductance $\times f($state of gating variables$)$. The gating variables followed first order kinetics. For example, the gating variable, m was given by,

$$\frac{dm}{dt} = \frac{-(m - m_\infty)}{\tau_m} \tag{A.4}$$

where both m_∞ and τ_m are functions of voltage.
An equivalent representation is

$$\frac{dm}{dt} = \alpha_m(1 - m) - \beta_m m \tag{A.5}$$

with $m_\infty = \alpha_m/(\alpha_m + \beta_m)$; $\tau_m = 1/(\alpha_m + \beta_m)$

The functional form of each ionic current and the gating variables, maximal conductances and reversal potentials are provided in the tables below.

A.2 Synapse Model

Stellate cells were randomly connected to inhibitory interneurons with an excitatory synapse. Interneurons sent inhibitory connections to stellate cells as well as to other interneurons.The inhibitory population was modeled as an all-to-all connected network. The synapse was modeled as a conductance with a gating variable modulated by the presynaptic voltage.

$$I_{syn} = g_{syn} s (v_{post} - E_{syn}) \tag{A.6}$$

$$\frac{ds}{dt} = F(v_{pre})\alpha_s(1 - s) - \beta_s s \tag{A.7}$$

where, $F(v_{pre}) = (1 + \tanh(v_{pre}/4))/2$, models the opening of a synaptic ion channel in response to action potential generated by the presynaptic neuron. The reversal potential determined the nature of synapse to be excitatory (when set to 0mV), or inhibitory (when set to -80mV).

A.3 Connectivity

We modeled three network types - A small network motif comprised of two stellate cells and two interneurons (Figure 1b), and two larger networks with stellate cells and interneurons arranged on rings. In one of the larger networks (Figure 3b) with 40 stellate cells and 40 interneurons, the population of stellate cells and the population of interneurons were arranged on separate rings. Each interneuron sent projections to five adjacent stellate cells while each stellate cell sent projections to six randomly chosen inhibitory interneurons. In the network simulated in Figure 6, 80 interneurons were divided into two sub-populations 40 interneurons each. Each sub-population connected to the common pool of stellate cells. The neighboring interneurons on each ring connected to neighboring stellate cells on the stellate cell ring.

A.4 External input to the network

Theta rhythmic input to the network was provided by periodically modulating the excitability of interneurons using a sinusoidally varying conductance,

$$I_\theta = A\sin(2\pi\omega t + \phi)(V - V_{th}) \tag{A.8}$$

where, A is the amplitude of theta rhythm; ω its frequency in Hz. V_{th} is the threshold voltage for the theta drive.

In addition to a constant depolarizing input, a sequential pulse like input was used to drive the inhibitory interneurons. The temporal profile of the transient external pulse for an interneuron i is given by,

$$I^i_{pulse} = \begin{cases} p^i_\vee & \text{if } t < t^i_{s,min} \\ p^i_\wedge + (p^i_\vee - p^i_\wedge)e^{(t-t_{s,k})/\tau_r} & \text{if } t^i_{s,k} <= t < t^i_{e,k} \\ p^i_\wedge + (p^i_\vee - p^i_\wedge)e^{(t-t_{e,k})/\tau_f} & \text{if } t > t^i_{e,k} \end{cases} \tag{A.9}$$

The baseline value of the pulse was set to, $p^i_\vee$. At time, $t^i_{s,k}$, to rose to a maximum, $p^i_\wedge$, with a rise time of τ_r. At $t^i_{e,k}$ the pulse was switched off and fell to the

baseline value with a fall time, τ_f. During a simulation, if the neuron received multiple pulses, each was indexed by the variable k. Successive pulse-like inputs were then given to a neighbouring interneurons in successive theta cycles. The start time of a pulse to the i^{th} neuron was calculated using the following prescription,

$$t_s^i = \{t \mid t = iT + k\lambda,\ k = 0, 1, \dots\} \tag{A.10}$$

T, the time between pulses to successive interneurons, matched the period of the theta oscillation. The time between successive pulses to the same interneuron was given by λ. In the ring networks simulated here, the pulse visited all the interneurons before arriving back at the same neuron. Therefore we set $\lambda = NT$. The duration of the pulse was set to p_{width}. The end time,$t_{e,k}^i$, of a k^{th} pulse to neuron i is,

$$t_{e,k}^i = t_{s,k}^i + p_{width} \tag{A.11}$$

A similar sequence of pulses were given to the two rings of interneurons in Figure 6a. The top ring received inputs in a counter-clockwise direction while the order of inputs to the bottom ring followed a clockwise direction.

A.5 Measure of reliability

To compare the reliability of the responses of the network for a given sequence of inputs across noisy trials, we used a measure of similarity between spike trains termed SPIKE-distance [Kreuz et al., 2013]. This measure can be calculated for each neuron across all pairs of trials and averaged over time. This value was calculated for a sub-set of neurons ($N = 8$) that received input for all the theta frequencies that were simulated. The distribution of mean reliability across trial for each neuron is shown in Figure 5c. The analysis were implemented using a Python library, PySpike [Mulansky and Kreuz, 2016]. A brief summary of the way the method measures reliability is shown in figure .

All the simulations were performed using a home-grown C++ library, insilico, that uses odeint, a boost C++ library to solve ordinary differential equations. The differential equations were integrated using an Euler method with the time step of

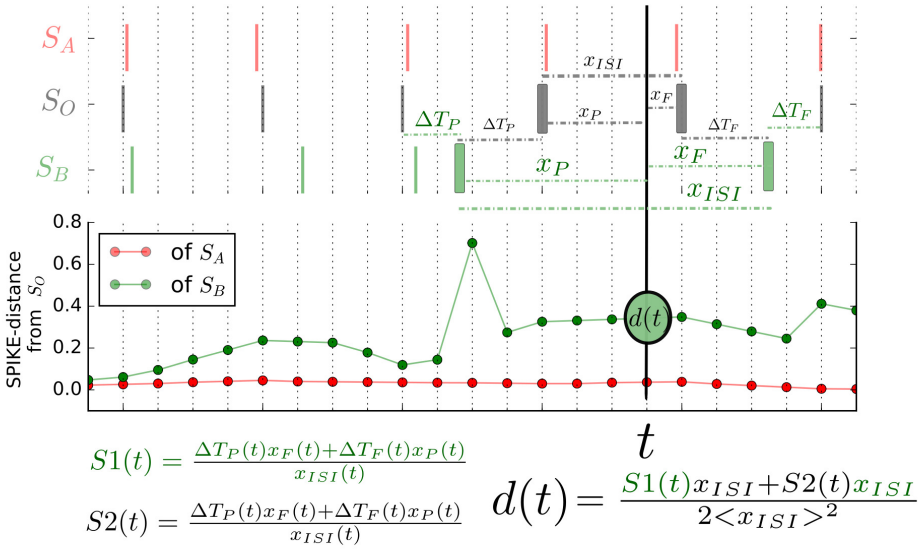

FIGURE A.1: *A brief description of reliability measure.* (a) upper panel - three spike trains (S_A, S_O, S_B) are shown. (b) Instantaneous pairwise spike distance between S_A and S_O is shown in red. Spike distance between S_B and S_O is shown in green. The estimation of spike distance, $d(t)$, between green (S_B) and black (S_O) spike trains (green circle) from four corner spike surrounding a point in time, t (where vertical black line spans the lower and upper panels), is illustrated using the step wise formulae used in arriving at it. As is clear from the figure, the similar spike trains S_O and S_A lead to smaller spike distance measure (red trace - lower panel) as opposed to more dissimilar spike trains S_B and S_O that maintain higher value of spike distance throughout (green trace -lower panel). The instantaneous spike distance also tracks changes in similarity of spike trains over time (green trace - lower panel)

.

0.01ms. The codes for running the simulations and analysing the outputs are available in the github repository
https://github.com/arunneru/theta_gates_reliable_sequences_mEC.

The odeint library can be found at the following website:
http://headmyshoulder.github.io/odeint-v2/.

A.6 Inheriting phase precession

Previous models explain how phase precession can be generated by interneurons. We have assumed that the interneurons are already phase precessing and connected them to a single stellate cell. Instead of explicitly modeling each interneuron we have generated artificial spike generators that simulate the phase precession. As neurons are successively recruited into the cycles of theta oscillations from line of interneurons, the temporal profile of inhibitory post synaptic currents onto a single stellate cell, within a cycle, changes dynamically. The inhibition onto the stellate cell as a function of the phase of theta in a cycle changes in a predictable manner as dictated by the connectivity profile of the inhibitory synapses from a line of interneurons. Thus the number of artificial simulators are further reduced to equal the fixed number of inhibitory neurons firing within a cycle of theta. The inhibition onto a single stellate cell is dynamically changed on every theta cycle to simulate the different connecctivity profile modeled.

Ion channel	*Current and Its kinetics*	*Maximal conductance and Reversal potential*
Stellate cell		
sodium	$I_{Na} = g_{Na} m^3 h (v - E_{Na})$ $\alpha_m = -0.1(v+23)/(e^{-0.1(v+23)} - 1)$ $\beta_m = 4e^{-(v+48)/18}$ $\alpha_h = 0.07e^{-(v+37.0)/20}$ $\beta_h = 1/(e^{-0.1(v+7)} + 1)$	$g_{Na} = 52$ $E_{Na} = 55$
potassium	$I_K = g_K n^4 (v - E_K)$ $\alpha_n = -0.01(v+27)/(e^{-0.1(v+27)} - 1)$ $\beta_n = 0.125e^{-(v+37)/80}$	$g_K = 11$ $E_K = -90$
persistent sodium	$I_{NaP} = g_{NaP} ms (v - E_{Na})$ $\tau_{ms} = 0.15$ $ms_\infty = 1/(1 + e^{-(v+38)/6.5})$	$g_{NaP} = 0.5$
HCN	$I_h = g_h (0.65mhf + 0.35mhs)(v - E_h)$ $mhs_\infty = 1/(1 + e^{(v+2.83)/15.9})^{58}$ $\tau_{mhs} = 5.6/(e^{(v-1.7)/14} + e^{-(v+260)/43}) + 1$ $mhf_\infty = 1/(1 + e^{(v+79.2)/9.78})$ $\tau_{mhf} = 0.51/(e^{(v-1.7)/10} + e^{-(v+340)/52}) + 1$	$g_h = 1.5$ $E_h = -20$
Interneuron		

sodium	$I_{Na} = g_{Na} m^3 h (v - E_{Na})$ $\alpha_m = 0.1(v+35)/(1-e^{-(v+35)/10})$ $\beta_m = 4e^{-(v+60)/18}$ $\alpha_h = 0.07e^{(v+58)/20}$ $\beta_h = 1/(e^{-0.1(v+28)}+1)$	$g_{Na} = 35$ $E_{Na} = 55$
potassium	$I_K = g_K n^4 (v - E_K)$ $\alpha_n = 0.01(v+34)/(1-e^{-0.1(v+34)})$ $\beta_n = 0.125e^{-(v+44)/80}$	$g_K = 9$ $E_K = -90$

TABLE A.1: Functional form of conductances and gating variables

Parameter	Symbol	Value
Synapse		
Maximal mutual inhibition conductance	g_{ii}	1.0 mS/cm^2
Maximal inhibitory conductance onto stellate cells	g_{ie}	0.6 mS/cm^2
Maximal excitatory conductance onto inhibitory interneurons	g_{ei}	0.03 mS/cm^2
Forward rate of inhibitory synapse	$\alpha_{s,inh}$	3.33 s^{-1}
Reverse rate of inhibitory synapse	$\beta_{s,inh}$	0.11 s^{-1}
Forward rate of excitatory synapse	$\alpha_{s,exc}$	100.0 s^{-1}
Reverse rate of excitatory synapse	$\beta_{s,exc}$	0.33 s^{-1}
Input		
External current to stellate cells	I_{ext_s}	-2.7 µA/cm^2
External current onto interneurons	I_{ext_i}	0.2 µA/cm^2
Baseline pulse current for interneuron	$p_{\vee,i}$	-0.05 µA/cm^2
Maximum pulse current for interneuron	$p_{\wedge,i}$	1.0 µA/cm^2
Amplitude of theta drive	A	0.04 mS/cm^2
Threshold voltage for theta drive	V_{th}	-80 mV

TABLE A.2: List of default network and input parameters

Appendix B

Permissions

SPRINGER NATURE LICENSE TERMS AND CONDITIONS

Jun 07, 2019

This Agreement between IISER Pune -- Arun Neru Balachandar ("You") and Springer Nature ("Springer Nature") consists of your license details and the terms and conditions provided by Springer Nature and Copyright Clearance Center.

License Number	4603440153034
License date	Jun 07, 2019
Licensed Content Publisher	Springer Nature
Licensed Content Publication	Nature
Licensed Content Title	Independent rate and temporal coding in hippocampal pyramidal cells
Licensed Content Author	John Huxter et al
Licensed Content Date	Oct 23, 2003
Type of Use	Thesis/Dissertation
Requestor type	academic/university or research institute
Format	print and electronic
Portion	figures/tables/illustrations
Number of figures/tables/illustrations	1
High-res required	no
Will you be translating?	no
Circulation/distribution	<501
Author of this Springer Nature content	no
Title	Graduate student
Institution name	IISER PUNE
Expected presentation date	Aug 2019
Portions	Figure 1 a
Requestor Location	IISER Pune Biology Division, Main building, IISER Pune, Dr.Homi Bhabha Road, Pashan Pune, MAHARASHTRA 411008 India Attn: IISER Pune
Total	0.00 USD

Terms and Conditions

Springer Nature Terms and Conditions for RightsLink Permissions

Springer Nature Customer Service Centre GmbH (the Licensor) hereby grants you a non-exclusive, world-wide licence to reproduce the material and for the purpose and requirements specified in the attached copy of your order form, and for no other use, subject to the conditions below:

1. The Licensor warrants that it has, to the best of its knowledge, the rights to license reuse of this material. However, you should ensure that the material you are requesting is original to the Licensor and does not carry the copyright of another entity (as credited in the published version).

If the credit line on any part of the material you have requested indicates that it was reprinted or adapted with permission from another source, then you should also seek permission from that source to reuse the material.

2. Where **print only** permission has been granted for a fee, separate permission must be obtained for any additional electronic re-use.

3. Permission granted **free of charge** for material in print is also usually granted for any electronic version of that work, provided that the material is incidental to your work as a whole and that the electronic version is essentially equivalent to, or substitutes for, the print version.

4. A licence for 'post on a website' is valid for 12 months from the licence date. This licence does not cover use of full text articles on websites.

5. Where **'reuse in a dissertation/thesis'** has been selected the following terms apply: Print rights of the final author's accepted manuscript (for clarity, NOT the published version) for up to 100 copies, electronic rights for use only on a personal website or institutional repository as defined by the Sherpa guideline (www.sherpa.ac.uk/romeo/).

6. Permission granted for books and journals is granted for the lifetime of the first edition and does not apply to second and subsequent editions (except where the first edition permission was granted free of charge or for signatories to the STM Permissions Guidelines http://www.stm-assoc.org/copyright-legal-affairs/permissions/permissions-guidelines/), and does not apply for editions in other languages unless additional translation rights have been granted separately in the licence.

7. Rights for additional components such as custom editions and derivatives require additional permission and may be subject to an additional fee. Please apply to Journalpermissions@springernature.com/bookpermissions@springernature.com for these rights.

8. The Licensor's permission must be acknowledged next to the licensed material in print. In electronic form, this acknowledgement must be visible at the same time as the figures/tables/illustrations or abstract, and must be hyperlinked to the journal/book's homepage. Our required acknowledgement format is in the Appendix below.

9. Use of the material for incidental promotional use, minor editing privileges (this does not include cropping, adapting, omitting material or any other changes that affect the meaning, intention or moral rights of the author) and copies for the disabled are permitted under this licence.

10. Minor adaptations of single figures (changes of format, colour and style) do not require the Licensor's approval. However, the adaptation should be credited as shown in Appendix below.

Appendix — Acknowledgements:

For Journal Content:
Reprinted by permission from [**the Licensor**]: [**Journal Publisher** (e.g. Nature/Springer/Palgrave)] [**JOURNAL NAME**] [**REFERENCE CITATION** (Article name, Author(s) Name), [**COPYRIGHT**] (year of publication)

For **Advance Online Publication papers:**
Reprinted by permission from [**the Licensor**]: [**Journal Publisher** (e.g. Nature/Springer/Palgrave)] [**JOURNAL NAME**] [**REFERENCE CITATION** (Article name, Author(s) Name), [**COPYRIGHT**] (year of publication), advance online publication, day month year (doi: 10.1038/sj.[JOURNAL ACRONYM].)

For Adaptations/Translations:
Adapted/Translated by permission from [**the Licensor**]: [**Journal Publisher** (e.g. Nature/Springer/Palgrave)] [**JOURNAL NAME**] [**REFERENCE CITATION** (Article name, Author(s) Name), [**COPYRIGHT**] (year of publication)

Note: For any republication from the British Journal of Cancer, the following credit line style applies:

Reprinted/adapted/translated by permission from [**the Licensor**]: on behalf of Cancer Research UK: : [**Journal Publisher** (e.g. Nature/Springer/Palgrave)] [**JOURNAL NAME**] [**REFERENCE CITATION** (Article name, Author(s) Name), [**COPYRIGHT]** (year of publication)

For **Advance Online Publication** papers:
Reprinted by permission from The [**the Licensor**]: on behalf of Cancer Research UK: [**Journal Publisher** (e.g. Nature/Springer/Palgrave)] [**JOURNAL NAME**] [**REFERENCE CITATION** (Article name, Author(s) Name), [**COPYRIGHT**] (year of publication), advance online publication, day month year (doi: 10.1038/sj. [JOURNAL ACRONYM])

For Book content:
Reprinted/adapted by permission from [**the Licensor**]: [**Book Publisher** (e.g. Palgrave Macmillan, Springer etc) [**Book Title**] by [**Book author**(s)] [**COPYRIGHT**] (year of publication)

Other Conditions:

Version 1.1

SPRINGER NATURE LICENSE TERMS AND CONDITIONS

Jun 07, 2019

This Agreement between IISER Pune -- Arun Neru Balachandar ("You") and Springer Nature ("Springer Nature") consists of your license details and the terms and conditions provided by Springer Nature and Copyright Clearance Center.

License Number	4603480334714
License date	Jun 07, 2019
Licensed Content Publisher	Springer Nature
Licensed Content Publication	Nature Neuroscience
Licensed Content Title	Theta phase–specific codes for two-dimensional position, trajectory and heading in the hippocampus
Licensed Content Author	John R Huxter, Timothy J Senior, Kevin Allen, Jozsef Csicsvari
Licensed Content Date	Apr 20, 2008
Licensed Content Volume	11
Licensed Content Issue	5
Type of Use	Thesis/Dissertation
Requestor type	academic/university or research institute
Format	print and electronic
Portion	figures/tables/illustrations
Number of figures/tables/illustrations	1
High-res required	no
Will you be translating?	no
Circulation/distribution	<501
Author of this Springer Nature content	no
Title	Graduate student
Institution name	IISER PUNE
Expected presentation date	Aug 2019
Portions	Supplementary Figure S5 a
Requestor Location	IISER Pune Biology Division, Main building, IISER Pune, Dr.Homi Bhabha Road, Pashan Pune, MAHARASHTRA 411008 India Attn: IISER Pune
Total	0.00 USD
Terms and Conditions	

Springer Nature Terms and Conditions for RightsLink Permissions

Springer Nature Customer Service Centre GmbH (the Licensor) hereby grants you a non-exclusive, world-wide licence to reproduce the material and for the purpose and requirements specified in the attached copy of your order form, and for no other use, subject to the conditions below:

1. The Licensor warrants that it has, to the best of its knowledge, the rights to license reuse of this material. However, you should ensure that the material you are requesting is original to the Licensor and does not carry the copyright of another entity (as credited in the published version).

   If the credit line on any part of the material you have requested indicates that it was reprinted or adapted with permission from another source, then you should also seek permission from that source to reuse the material.

2. Where **print only** permission has been granted for a fee, separate permission must be obtained for any additional electronic re-use.

3. Permission granted **free of charge** for material in print is also usually granted for any electronic version of that work, provided that the material is incidental to your work as a whole and that the electronic version is essentially equivalent to, or substitutes for, the print version.

4. A licence for 'post on a website' is valid for 12 months from the licence date. This licence does not cover use of full text articles on websites.

5. Where **'reuse in a dissertation/thesis'** has been selected the following terms apply: Print rights of the final author's accepted manuscript (for clarity, NOT the published version) for up to 100 copies, electronic rights for use only on a personal website or institutional repository as defined by the Sherpa guideline (www.sherpa.ac.uk/romeo/).

6. Permission granted for books and journals is granted for the lifetime of the first edition and does not apply to second and subsequent editions (except where the first edition permission was granted free of charge or for signatories to the STM Permissions Guidelines http://www.stm-assoc.org/copyright-legal-affairs/permissions/permissions-guidelines/), and does not apply for editions in other languages unless additional translation rights have been granted separately in the licence.

7. Rights for additional components such as custom editions and derivatives require additional permission and may be subject to an additional fee. Please apply to Journalpermissions@springernature.com/bookpermissions@springernature.com for these rights.

8. The Licensor's permission must be acknowledged next to the licensed material in print. In electronic form, this acknowledgement must be visible at the same time as the figures/tables/illustrations or abstract, and must be hyperlinked to the journal/book's homepage. Our required acknowledgement format is in the Appendix below.

9. Use of the material for incidental promotional use, minor editing privileges (this does not include cropping, adapting, omitting material or any other changes that affect the meaning, intention or moral rights of the author) and copies for the disabled are permitted under this licence.

10. Minor adaptations of single figures (changes of format, colour and style) do not require the Licensor's approval. However, the adaptation should be credited as shown in Appendix below.

Appendix — Acknowledgements:

For Journal Content:
Reprinted by permission from [**the Licensor**]: [**Journal Publisher** (e.g. Nature/Springer/Palgrave)] [**JOURNAL NAME**] [**REFERENCE CITATION** (Article name, Author(s) Name), [**COPYRIGHT**] (year of publication)

For **Advance Online Publication papers:**
Reprinted by permission from [**the Licensor**]: [**Journal Publisher** (e.g. Nature/Springer/Palgrave)] [**JOURNAL NAME**] [**REFERENCE CITATION** (Article name, Author(s) Name), [**COPYRIGHT**] (year of publication), advance online publication, day month year (doi: 10.1038/sj.[JOURNAL ACRONYM].)

For Adaptations/Translations:
Adapted/Translated by permission from [**the Licensor**]: [**Journal Publisher** (e.g. Nature/Springer/Palgrave)] [**JOURNAL NAME**] [**REFERENCE CITATION** (Article name, Author(s) Name), [**COPYRIGHT**] (year of publication)

Note: For any republication from the British Journal of Cancer, the following credit line style applies:

Reprinted/adapted/translated by permission from [**the Licensor**]: on behalf of Cancer Research UK: : [**Journal Publisher** (e.g. Nature/Springer/Palgrave)] [**JOURNAL NAME**] [**REFERENCE CITATION** (Article name, Author(s) Name), [**COPYRIGHT]** (year of publication)

For **Advance Online Publication** papers:
Reprinted by permission from The [**the Licensor**]: on behalf of Cancer Research UK: [**Journal Publisher** (e.g. Nature/Springer/Palgrave)] [**JOURNAL NAME**] [**REFERENCE CITATION** (Article name, Author(s) Name), [**COPYRIGHT**] (year of publication), advance online publication, day month year (doi: 10.1038/sj. [JOURNAL ACRONYM])

For Book content:
Reprinted/adapted by permission from [**the Licensor**]: [**Book Publisher** (e.g. Palgrave Macmillan, Springer etc) [**Book Title**] by [**Book author**(s)] [**COPYRIGHT**] (year of publication)

Other Conditions:

Version 1.1

SPRINGER NATURE LICENSE TERMS AND CONDITIONS

Jun 07, 2019

This Agreement between IISER Pune -- Arun Neru Balachandar ("You") and Springer Nature ("Springer Nature") consists of your license details and the terms and conditions provided by Springer Nature and Copyright Clearance Center.

License Number	4603460619130
License date	Jun 07, 2019
Licensed Content Publisher	Springer Nature
Licensed Content Publication	Nature
Licensed Content Title	Microstructure of a spatial map in the entorhinal cortex
Licensed Content Author	Torkel Hafting et al
Licensed Content Date	Jun 19, 2005
Type of Use	Thesis/Dissertation
Requestor type	academic/university or research institute
Format	print and electronic
Portion	figures/tables/illustrations
Number of figures/tables/illustrations	1
High-res required	no
Will you be translating?	no
Circulation/distribution	<501
Author of this Springer Nature content	no
Title	Graduate student
Institution name	IISER PUNE
Expected presentation date	Aug 2019
Portions	Figure 3 a
Requestor Location	IISER Pune Biology Division, Main building, IISER Pune, Dr.Homi Bhabha Road, Pashan Pune, MAHARASHTRA 411008 India Attn: IISER Pune
Total	0.00 USD

Terms and Conditions

Springer Nature Terms and Conditions for RightsLink Permissions

Springer Nature Customer Service Centre GmbH (the Licensor) hereby grants you a non-exclusive, world-wide licence to reproduce the material and for the purpose and requirements specified in the attached copy of your order form, and for no other use, subject to the conditions below:

1. The Licensor warrants that it has, to the best of its knowledge, the rights to license reuse of this material. However, you should ensure that the material you are requesting is original to the Licensor and does not carry the copyright of another entity (as credited in the published version).

   If the credit line on any part of the material you have requested indicates that it was

reprinted or adapted with permission from another source, then you should also seek permission from that source to reuse the material.

2. Where **print only** permission has been granted for a fee, separate permission must be obtained for any additional electronic re-use.

3. Permission granted **free of charge** for material in print is also usually granted for any electronic version of that work, provided that the material is incidental to your work as a whole and that the electronic version is essentially equivalent to, or substitutes for, the print version.

4. A licence for 'post on a website' is valid for 12 months from the licence date. This licence does not cover use of full text articles on websites.

5. Where **'reuse in a dissertation/thesis'** has been selected the following terms apply: Print rights of the final author's accepted manuscript (for clarity, NOT the published version) for up to 100 copies, electronic rights for use only on a personal website or institutional repository as defined by the Sherpa guideline (www.sherpa.ac.uk/romeo/).

6. Permission granted for books and journals is granted for the lifetime of the first edition and does not apply to second and subsequent editions (except where the first edition permission was granted free of charge or for signatories to the STM Permissions Guidelines http://www.stm-assoc.org/copyright-legal-affairs/permissions/permissions-guidelines/), and does not apply for editions in other languages unless additional translation rights have been granted separately in the licence.

7. Rights for additional components such as custom editions and derivatives require additional permission and may be subject to an additional fee. Please apply to Journalpermissions@springernature.com/bookpermissions@springernature.com for these rights.

8. The Licensor's permission must be acknowledged next to the licensed material in print. In electronic form, this acknowledgement must be visible at the same time as the figures/tables/illustrations or abstract, and must be hyperlinked to the journal/book's homepage. Our required acknowledgement format is in the Appendix below.

9. Use of the material for incidental promotional use, minor editing privileges (this does not include cropping, adapting, omitting material or any other changes that affect the meaning, intention or moral rights of the author) and copies for the disabled are permitted under this licence.

10. Minor adaptations of single figures (changes of format, colour and style) do not require the Licensor's approval. However, the adaptation should be credited as shown in Appendix below.

Appendix — Acknowledgements:

For Journal Content:
Reprinted by permission from [**the Licensor**]: [**Journal Publisher** (e.g. Nature/Springer/Palgrave)] [**JOURNAL NAME**] [**REFERENCE CITATION** (Article name, Author(s) Name), [**COPYRIGHT**] (year of publication)

For **Advance Online Publication papers:**
Reprinted by permission from [**the Licensor**]: [**Journal Publisher** (e.g. Nature/Springer/Palgrave)] [**JOURNAL NAME**] [**REFERENCE CITATION** (Article name, Author(s) Name), [**COPYRIGHT**] (year of publication), advance online publication, day month year (doi: 10.1038/sj.[JOURNAL ACRONYM].)

For Adaptations/Translations:
Adapted/Translated by permission from [**the Licensor**]: [**Journal Publisher** (e.g. Nature/Springer/Palgrave)] [**JOURNAL NAME**] [**REFERENCE CITATION** (Article name, Author(s) Name), [**COPYRIGHT**] (year of publication)

Note: For any republication from the British Journal of Cancer, the following credit line style applies:

Reprinted/adapted/translated by permission from [**the Licensor**]: on behalf of Cancer Research UK: : [**Journal Publisher** (e.g. Nature/Springer/Palgrave)] [**JOURNAL NAME**] [**REFERENCE CITATION** (Article name, Author(s) Name), [**COPYRIGHT]** (year of publication)

For **Advance Online Publication** papers:
Reprinted by permission from The [**the Licensor**]: on behalf of Cancer Research UK: [**Journal Publisher** (e.g. Nature/Springer/Palgrave)] [**JOURNAL NAME**] [**REFERENCE CITATION** (Article name, Author(s) Name), [**COPYRIGHT**] (year of publication), advance online publication, day month year (doi: 10.1038/sj. [JOURNAL ACRONYM])

For Book content:
Reprinted/adapted by permission from [**the Licensor**]: [**Book Publisher** (e.g. Palgrave Macmillan, Springer etc) [**Book Title**] by [**Book author**(s)] [**COPYRIGHT**] (year of publication)

Other Conditions:

Version 1.1

THE AMERICAN ASSOCIATION FOR THE ADVANCEMENT OF SCIENCE LICENSE TERMS AND CONDITIONS

May 20, 2019

This Agreement between IISER Pune -- Arun Neru Balachandar ("You") and The American Association for the Advancement of Science ("The American Association for the Advancement of Science") consists of your license details and the terms and conditions provided by The American Association for the Advancement of Science and Copyright Clearance Center.

License Number	4593081334500
License date	May 20, 2019
Licensed Content Publisher	The American Association for the Advancement of Science
Licensed Content Publication	Science
Licensed Content Title	Internally Generated Cell Assembly Sequences in the Rat Hippocampus
Licensed Content Author	Eva Pastalkova,Vladimir Itskov,Asohan Amarasingham,György Buzsáki
Licensed Content Date	Sep 5, 2008
Licensed Content Volume	321
Licensed Content Issue	5894
Volume number	321
Issue number	5894
Type of Use	Thesis / Dissertation
Requestor type	Scientist/individual at a research institution
Format	Print and electronic
Portion	Figure
Number of figures/tables	1
Order reference number	
Title of your thesis / dissertation	Graduate student
Expected completion date	Aug 2019
Estimated size(pages)	1
Requestor Location	IISER Pune Biology Division, Main building, IISER Pune, Dr.Homi Bhabha Road, Pashan Pune, MAHARASHTRA 411008 India Attn: IISER Pune
Total	0.00 USD
Terms and Conditions	

American Association for the Advancement of Science TERMS AND CONDITIONS
Regarding your request, we are pleased to grant you non-exclusive, non-transferable permission, to republish the AAAS material identified above in your work identified above, subject to the terms and conditions herein. We must be contacted for permission for any uses other than those specifically identified in your request above.
The following credit line must be printed along with the AAAS material: "From [Full Reference Citation]. Reprinted with permission from AAAS."

All required credit lines and notices must be visible any time a user accesses any part of the AAAS material and must appear on any printed copies and authorized user might make.

This permission does not apply to figures / photos / artwork or any other content or materials included in your work that are credited to non-AAAS sources. If the requested material is sourced to or references non-AAAS sources, you must obtain authorization from that source as well before using that material. You agree to hold harmless and indemnify AAAS against any claims arising from your use of any content in your work that is credited to non-AAAS sources.

If the AAAS material covered by this permission was published in Science during the years 1974 - 1994, you must also obtain permission from the author, who may grant or withhold permission, and who may or may not charge a fee if permission is granted. See original article for author's address. This condition does not apply to news articles.

The AAAS material may not be modified or altered except that figures and tables may be modified with permission from the author. Author permission for any such changes must be secured prior to your use.

Whenever possible, we ask that electronic uses of the AAAS material permitted herein include a hyperlink to the original work on AAAS's website (hyperlink may be embedded in the reference citation).

AAAS material reproduced in your work identified herein must not account for more than 30% of the total contents of that work.

AAAS must publish the full paper prior to use of any text.

AAAS material must not imply any endorsement by the American Association for the Advancement of Science.

This permission is not valid for the use of the AAAS and/or Science logos.

AAAS makes no representations or warranties as to the accuracy of any information contained in the AAAS material covered by this permission, including any warranties of merchantability or fitness for a particular purpose.

If permission fees for this use are waived, please note that AAAS reserves the right to charge for reproduction of this material in the future.

Permission is not valid unless payment is received within sixty (60) days of the issuance of this permission. If payment is not received within this time period then all rights granted herein shall be revoked and this permission will be considered null and void.

In the event of breach of any of the terms and conditions herein or any of CCC's Billing and Payment terms and conditions, all rights granted herein shall be revoked and this permission will be considered null and void.

AAAS reserves the right to terminate this permission and all rights granted herein at its discretion, for any purpose, at any time. In the event that AAAS elects to terminate this permission, you will have no further right to publish, publicly perform, publicly display, distribute or otherwise use any matter in which the AAAS content had been included, and all fees paid hereunder shall be fully refunded to you. Notification of termination will be sent to the contact information as supplied by you during the request process and termination shall be immediate upon sending the notice. Neither AAAS nor CCC shall be liable for any costs, expenses, or damages you may incur as a result of the termination of this permission, beyond the refund noted above.

This Permission may not be amended except by written document signed by both parties.

The terms above are applicable to all permissions granted for the use of AAAS material. Below you will find additional conditions that apply to your particular type of use.

FOR A THESIS OR DISSERTATION

If you are using figure(s)/table(s), permission is granted for use in print and electronic versions of your dissertation or thesis. A full text article may be used in print versions only of a dissertation or thesis.

Permission covers the distribution of your dissertation or thesis on demand by ProQuest / UMI, provided the AAAS material covered by this permission remains in situ.

If you are an Original Author on the AAAS article being reproduced, please refer to your License to Publish for rules on reproducing your paper in a dissertation or thesis.

FOR JOURNALS:

Permission covers both print and electronic versions of your journal article, however the AAAS material may not be used in any manner other than within the context of your article.

FOR BOOKS/TEXTBOOKS:

If this license is to reuse figures/tables, then permission is granted for non-exclusive world rights in all languages in both print and electronic formats (electronic formats are defined below).

If this license is to reuse a text excerpt or a full text article, then permission is granted for non-exclusive world rights in English only. You have the option of securing either print or electronic rights or both, but electronic rights are not automatically granted and do garner additional fees. Permission for translations of text excerpts or full text articles into other languages must be obtained separately.

Licenses granted for use of AAAS material in electronic format books/textbooks are valid only in cases where the electronic version is equivalent to or substitutes for the print version of the book/textbook. The AAAS material reproduced as permitted herein must remain in situ and must not be exploited separately (for example, if permission covers the use of a full text article, the article may not be offered for access or for purchase as a stand-alone unit), except in the case of permitted textbook companions as noted below.

You must include the following notice in any electronic versions, either adjacent to the reprinted AAAS material or in the terms and conditions for use of your electronic products: "Readers may view, browse, and/or download material for temporary copying purposes only, provided these uses are for noncommercial personal purposes. Except as provided by law, this material may not be further reproduced, distributed, transmitted, modified, adapted, performed, displayed, published, or sold in whole or in part, without prior written permission from the publisher."

If your book is an academic textbook, permission covers the following companions to your textbook, provided such companions are distributed only in conjunction with your textbook at no additional cost to the user:

- Password-protected website
- Instructor's image CD/DVD and/or PowerPoint resource
- Student CD/DVD

All companions must contain instructions to users that the AAAS material may be used for non-commercial, classroom purposes only. Any other uses require the prior written permission from AAAS.

If your license is for the use of AAAS Figures/Tables, then the electronic rights granted herein permit use of the Licensed Material in any Custom Databases that you distribute the electronic versions of your textbook through, so long as the Licensed Material remains within the context of a chapter of the title identified in your request and cannot be downloaded by a user as an independent image file.

Rights also extend to copies/files of your Work (as described above) that you are required to provide for use by the visually and/or print disabled in compliance with state and federal laws.

This permission only covers a single edition of your work as identified in your request.

FOR NEWSLETTERS:

Permission covers print and/or electronic versions, provided the AAAS material reproduced as permitted herein remains in situ and is not exploited separately (for example, if permission covers the use of a full text article, the article may not be offered for access or for purchase as a stand-alone unit)

FOR ANNUAL REPORTS:

Permission covers print and electronic versions provided the AAAS material reproduced as permitted herein remains in situ and is not exploited separately (for example, if permission covers the use of a full text article, the article may not be offered for access or for purchase as a stand-alone unit)

FOR PROMOTIONAL/MARKETING USES:

Permission covers the use of AAAS material in promotional or marketing pieces such as information packets, media kits, product slide kits, brochures, or flyers limited to a single print run. The AAAS Material may not be used in any manner which implies endorsement or promotion by the American Association for the Advancement of Science (AAAS) or Science of any product or service. AAAS does not permit the reproduction of its name, logo or text on promotional literature.

SPRINGER NATURE LICENSE TERMS AND CONDITIONS

May 20, 2019

This Agreement between IISER Pune -- Arun Neru Balachandar ("You") and Springer Nature ("Springer Nature") consists of your license details and the terms and conditions provided by Springer Nature and Copyright Clearance Center.

License Number	4593150304814
License date	May 20, 2019
Licensed Content Publisher	Springer Nature
Licensed Content Publication	Nature
Licensed Content Title	Mapping of a non-spatial dimension by the hippocampal–entorhinal circuit
Licensed Content Author	Dmitriy Aronov, Rhino Nevers, David W. Tank
Licensed Content Date	Mar 29, 2017
Licensed Content Volume	543
Licensed Content Issue	7647
Type of Use	Thesis/Dissertation
Requestor type	academic/university or research institute
Format	print and electronic
Portion	figures/tables/illustrations
Number of figures/tables/illustrations	2
High-res required	no
Will you be translating?	no
Circulation/distribution	<501
Author of this Springer Nature content	no
Title	Graduate student
Institution name	IISER PUNE
Expected presentation date	Aug 2019
Portions	Figure 1 and Figure 2
Requestor Location	IISER Pune Biology Division, Main building, IISER Pune, Dr.Homi Bhabha Road, Pashan Pune, MAHARASHTRA 411008 India Attn: IISER Pune
Total	0.00 USD
Terms and Conditions	

Springer Nature Terms and Conditions for RightsLink Permissions

Springer Nature Customer Service Centre GmbH (the Licensor) hereby grants you a non-exclusive, world-wide licence to reproduce the material and for the purpose and requirements specified in the attached copy of your order form, and for no other use, subject to the conditions below:

1. The Licensor warrants that it has, to the best of its knowledge, the rights to license reuse of this material. However, you should ensure that the material you are requesting is original to the Licensor and does not carry the copyright of another entity (as credited in the published version).

   If the credit line on any part of the material you have requested indicates that it was reprinted or adapted with permission from another source, then you should also seek permission from that source to reuse the material.

2. Where **print only** permission has been granted for a fee, separate permission must be obtained for any additional electronic re-use.

3. Permission granted **free of charge** for material in print is also usually granted for any electronic version of that work, provided that the material is incidental to your work as a whole and that the electronic version is essentially equivalent to, or substitutes for, the print version.

4. A licence for 'post on a website' is valid for 12 months from the licence date. This licence does not cover use of full text articles on websites.

5. Where **'reuse in a dissertation/thesis'** has been selected the following terms apply: Print rights of the final author's accepted manuscript (for clarity, NOT the published version) for up to 100 copies, electronic rights for use only on a personal website or institutional repository as defined by the Sherpa guideline (www.sherpa.ac.uk/romeo/).

6. Permission granted for books and journals is granted for the lifetime of the first edition and does not apply to second and subsequent editions (except where the first edition permission was granted free of charge or for signatories to the STM Permissions Guidelines http://www.stm-assoc.org/copyright-legal-affairs/permissions/permissions-guidelines/), and does not apply for editions in other languages unless additional translation rights have been granted separately in the licence.

7. Rights for additional components such as custom editions and derivatives require additional permission and may be subject to an additional fee. Please apply to Journalpermissions@springernature.com/bookpermissions@springernature.com for these rights.

8. The Licensor's permission must be acknowledged next to the licensed material in print. In electronic form, this acknowledgement must be visible at the same time as the figures/tables/illustrations or abstract, and must be hyperlinked to the journal/book's homepage. Our required acknowledgement format is in the Appendix below.

9. Use of the material for incidental promotional use, minor editing privileges (this does not include cropping, adapting, omitting material or any other changes that affect the meaning, intention or moral rights of the author) and copies for the disabled are permitted under this licence.

10. Minor adaptations of single figures (changes of format, colour and style) do not require the Licensor's approval. However, the adaptation should be credited as shown in Appendix below.

Appendix — Acknowledgements:

For Journal Content:
Reprinted by permission from [**the Licensor**]: [**Journal Publisher** (e.g. Nature/Springer/Palgrave)] [**JOURNAL NAME**] [**REFERENCE CITATION** (Article name, Author(s) Name), [**COPYRIGHT**] (year of publication)

For **Advance Online Publication papers:**
Reprinted by permission from [**the Licensor**]: [**Journal Publisher** (e.g. Nature/Springer/Palgrave)] [**JOURNAL NAME**] [**REFERENCE CITATION** (Article name, Author(s) Name), [**COPYRIGHT**] (year of publication), advance online publication, day month year (doi: 10.1038/sj.[JOURNAL ACRONYM].)

For Adaptations/Translations:
Adapted/Translated by permission from [**the Licensor**]: [**Journal Publisher** (e.g. Nature/Springer/Palgrave)] [**JOURNAL NAME**] [**REFERENCE CITATION** (Article name, Author(s) Name), [**COPYRIGHT**] (year of publication)

Note: For any republication from the British Journal of Cancer, the following credit line style applies:

Reprinted/adapted/translated by permission from [**the Licensor**]: on behalf of Cancer Research UK: : [**Journal Publisher** (e.g. Nature/Springer/Palgrave)] [**JOURNAL NAME**] [**REFERENCE CITATION** (Article name, Author(s) Name), [**COPYRIGHT]** (year of publication)

For **Advance Online Publication** papers:
Reprinted by permission from The [**the Licensor**]: on behalf of Cancer Research UK: [**Journal Publisher** (e.g. Nature/Springer/Palgrave)] [**JOURNAL NAME**] [**REFERENCE CITATION** (Article name, Author(s) Name), [**COPYRIGHT**] (year of publication), advance online publication, day month year (doi: 10.1038/sj. [JOURNAL ACRONYM])

For Book content:
Reprinted/adapted by permission from [**the Licensor**]: [**Book Publisher** (e.g. Palgrave Macmillan, Springer etc) [**Book Title**] by [**Book author**(s)] [**COPYRIGHT**] (year of publication)

Other Conditions:

Version 1.1

Questions? customercare@copyright.com or +1-855-239-3415 (toll free in the US) or +1-978-646-2777.

SPRINGER NATURE LICENSE TERMS AND CONDITIONS

May 21, 2019

This Agreement between IISER Pune -- Arun Neru Balachandar ("You") and Springer Nature ("Springer Nature") consists of your license details and the terms and conditions provided by Springer Nature and Copyright Clearance Center.

License Number	4593441039021
License date	May 21, 2019
Licensed Content Publisher	Springer Nature
Licensed Content Publication	Nature
Licensed Content Title	Hippocampus-independent phase precession in entorhinal grid cells
Licensed Content Author	Torkel Hafting, Marianne Fyhn, Tora Bonnevie, May-Britt Moser, Edvard I. Moser
Licensed Content Date	May 14, 2008
Licensed Content Volume	453
Licensed Content Issue	7199
Type of Use	Thesis/Dissertation
Requestor type	academic/university or research institute
Format	print and electronic
Portion	figures/tables/illustrations
Number of figures/tables/illustrations	1
High-res required	no
Will you be translating?	no
Circulation/distribution	<501
Author of this Springer Nature content	no
Title	Graduate student
Institution name	IISER PUNE
Expected presentation date	Aug 2019
Portions	figure 1c,1d,1g
Requestor Location	IISER Pune Biology Division, Main building, IISER Pune, Dr.Homi Bhabha Road, Pashan Pune, MAHARASHTRA 411008 India Attn: IISER Pune
Total	0.00 USD
Terms and Conditions	

Springer Nature Terms and Conditions for RightsLink Permissions

Springer Nature Customer Service Centre GmbH (the Licensor) hereby grants you a non-exclusive, world-wide licence to reproduce the material and for the purpose and requirements specified in the attached copy of your order form, and for no other use, subject to the conditions below:

1. The Licensor warrants that it has, to the best of its knowledge, the rights to license reuse of this material. However, you should ensure that the material you are requesting is original to the Licensor and does not carry the copyright of another entity (as credited in the published version).

   If the credit line on any part of the material you have requested indicates that it was reprinted or adapted with permission from another source, then you should also seek permission from that source to reuse the material.

2. Where **print only** permission has been granted for a fee, separate permission must be obtained for any additional electronic re-use.

3. Permission granted **free of charge** for material in print is also usually granted for any electronic version of that work, provided that the material is incidental to your work as a whole and that the electronic version is essentially equivalent to, or substitutes for, the print version.

4. A licence for 'post on a website' is valid for 12 months from the licence date. This licence does not cover use of full text articles on websites.

5. Where **'reuse in a dissertation/thesis'** has been selected the following terms apply: Print rights of the final author's accepted manuscript (for clarity, NOT the published version) for up to 100 copies, electronic rights for use only on a personal website or institutional repository as defined by the Sherpa guideline (www.sherpa.ac.uk/romeo/).

6. Permission granted for books and journals is granted for the lifetime of the first edition and does not apply to second and subsequent editions (except where the first edition permission was granted free of charge or for signatories to the STM Permissions Guidelines http://www.stm-assoc.org/copyright-legal-affairs/permissions/permissions-guidelines/), and does not apply for editions in other languages unless additional translation rights have been granted separately in the licence.

7. Rights for additional components such as custom editions and derivatives require additional permission and may be subject to an additional fee. Please apply to Journalpermissions@springernature.com/bookpermissions@springernature.com for these rights.

8. The Licensor's permission must be acknowledged next to the licensed material in print. In electronic form, this acknowledgement must be visible at the same time as the figures/tables/illustrations or abstract, and must be hyperlinked to the journal/book's homepage. Our required acknowledgement format is in the Appendix below.

9. Use of the material for incidental promotional use, minor editing privileges (this does not include cropping, adapting, omitting material or any other changes that affect the meaning, intention or moral rights of the author) and copies for the disabled are permitted under this licence.

10. Minor adaptations of single figures (changes of format, colour and style) do not require the Licensor's approval. However, the adaptation should be credited as shown in Appendix below.

Appendix — Acknowledgements:

For Journal Content:
Reprinted by permission from [**the Licensor**]: [**Journal Publisher** (e.g. Nature/Springer/Palgrave)] [**JOURNAL NAME**] [**REFERENCE CITATION** (Article name, Author(s) Name), [**COPYRIGHT**] (year of publication)

For **Advance Online Publication papers:**
Reprinted by permission from [**the Licensor**]: [**Journal Publisher** (e.g. Nature/Springer/Palgrave)] [**JOURNAL NAME**] [**REFERENCE CITATION** (Article name, Author(s) Name), [**COPYRIGHT**] (year of publication), advance online publication, day month year (doi: 10.1038/sj.[JOURNAL ACRONYM].)

For Adaptations/Translations:
Adapted/Translated by permission from [**the Licensor**]: [**Journal Publisher** (e.g. Nature/Springer/Palgrave)] [**JOURNAL NAME**] [**REFERENCE CITATION** (Article name, Author(s) Name), [**COPYRIGHT**] (year of publication)

Note: For any republication from the British Journal of Cancer, the following credit line style applies:

Reprinted/adapted/translated by permission from [**the Licensor**]: on behalf of Cancer Research UK: : [**Journal Publisher** (e.g. Nature/Springer/Palgrave)] [**JOURNAL NAME**] [**REFERENCE CITATION** (Article name, Author(s) Name), [**COPYRIGHT**] (year of publication)

For **Advance Online Publication** papers:
Reprinted by permission from The [**the Licensor**]: on behalf of Cancer Research UK: [**Journal Publisher** (e.g. Nature/Springer/Palgrave)] [**JOURNAL NAME**] [**REFERENCE CITATION** (Article name, Author(s) Name), [**COPYRIGHT**] (year of publication), advance online publication, day month year (doi: 10.1038/sj. [JOURNAL ACRONYM])

For Book content:
Reprinted/adapted by permission from [**the Licensor**]: [**Book Publisher** (e.g. Palgrave Macmillan, Springer etc) [**Book Title**] by [**Book author**(s)] [**COPYRIGHT**] (year of publication)

Other Conditions:

Version 1.1

References

[Acker et al., 2003] Acker, C. D., Kopell, N., and White, J. A. (2003). Synchronization of strongly coupled excitatory neurons: Relating network behavior to biophysics. *Journal of Computational Neuroscience*, 15(1):71–90.

[Adams and Benson, 1985] Adams, W. B. and Benson, J. A. (1985). The generation and modulation of endogenous rhythmicity in the aplysia bursting pacemaker neurone r15. *Progress in Biophysics and Molecular Biology*, 46(1):1–49.

[Adey, 1960] Adey, W. R. (1960). Hippocampal slow waves. *Archives of Neurology*, 3(1):74.

[Adhikari et al., 2010] Adhikari, A., Topiwala, M. A., and Gordon, J. A. (2010). Synchronized activity between the ventral hippocampus and the medial prefrontal cortex during anxiety. *Neuron*, 65(2):257–269.

[Aghajan et al., 2017] Aghajan, Z. M., Schuette, P., Fields, T. A., Tran, M. E., Siddiqui, S. M., Hasulak, N. R., Tcheng, T. K., Eliashiv, D., Mankin, E. A., Stern, J., Fried, I., and Suthana, N. (2017). Theta oscillations in the human medial temporal lobe during real-world ambulatory movement. *Current Biology*, 27(24):3743 – 3751.e3.

[Akam and Kullmann, 2010] Akam, T. and Kullmann, D. M. (2010). Oscillations and filtering networks support flexible routing of information. *Neuron*, 67(2):308–320.

[Akam and Kullmann, 2014] Akam, T. and Kullmann, D. M. (2014). Oscillatory multiplexing of population codes for selective communication in the mammalian brain. *Nature Reviews Neuroscience*, 15(2):111–122.

[Alonso and Klink, 1993] Alonso, A. and Klink, R. (1993). Differential electroresponsiveness of stellate and pyramidal-like cells of medial entorhinal cortex layer II. *Journal of Neurophysiology*, 70(1):128–143.

[Arai et al., 2014] Arai, M., Brandt, V., and Dabaghian, Y. (2014). The effects of theta precession on spatial learning and simplicial complex dynamics in a topological model of the hippocampal spatial map. *PLoS Computational Biology*, 10(6):e1003651.

[Arnolds et al., 1980] Arnolds, D., Silva, F. L. D., Aitink, J., Kamp, A., and Boeijinga, P. (1980). The spectral properties of hippocampal eeg related to behaviour in man. *Electroencephalography and Clinical Neurophysiology*, 50(3):324 – 328.

[Aronov et al., 2017] Aronov, D., Nevers, R., and Tank, D. W. (2017). Mapping of a non-spatial dimension by the hippocampal–entorhinal circuit. *Nature*, 543(7647):719–722.

[Arshavsky et al., 1985] Arshavsky, Y., Beloozerova, I., Orlovsky, G., Panchin, Y., and Pavlova, G. (1985). Control of locomotion in marine mollusc clione limacina IV. role of type 12 interneurons. *Experimental Brain Research*, 58(2).

[Assisi et al., 2011] Assisi, C., Stopfer, M., and Bazhenov, M. (2011). Using the structure of inhibitory networks to unravel mechanisms of spatiotemporal patterning. *Neuron*, 69(2):373–386.

[Barnes et al., 2005] Barnes, T. D., Kubota, Y., Hu, D., Jin, D. Z., and Graybiel, A. M. (2005). Activity of striatal neurons reflects dynamic encoding and recoding of procedural memories. *Nature*, 437(7062):1158–1161.

[Barry et al., 2012] Barry, C., Ginzberg, L. L., O'Keefe, J., and Burgess, N. (2012). Grid cell firing patterns signal environmental novelty by expansion. *Proceedings of the National Academy of Sciences*, 109(43):17687–17692.

[Benchenane et al., 2010] Benchenane, K., Peyrache, A., Khamassi, M., Tierney, P. L., Gioanni, Y., Battaglia, F. P., and Wiener, S. I. (2010). Coherent theta oscillations and reorganization of spike timing in the hippocampal- prefrontal network upon learning. *Neuron*, 66(6):921–936.

[Berggaard et al., 2018] Berggaard, N., Bjerke, I. E., Paulsen, A. E. B., Hoang, L., Skogaker, N. E. T., Witter, M. P., and van der Want, J. J. L. (2018). Development of

parvalbumin-expressing basket terminals in layer II of the rat medial entorhinal cortex. *eneuro*, 5(3):ENEURO.0438–17.2018.

[Boccara et al., 2010] Boccara, C. N., Sargolini, F., Thoresen, V. H., Solstad, T., Witter, M. P., Moser, E. I., and Moser, M.-B. (2010). Grid cells in pre- and parasubiculum. *Nature Neuroscience*, 13(8):987–994.

[Bohbot et al., 2017] Bohbot, V. D., Copara, M. S., Gotman, J., and Ekstrom, A. D. (2017). Low-frequency theta oscillations in the human hippocampus during real-world and virtual navigation. *Nature Communications*, 8(1).

[Bonnevie et al., 2013] Bonnevie, T., Dunn, B., Fyhn, M., Hafting, T., Derdikman, D., Kubie, J. L., Roudi, Y., Moser, E. I., and Moser, M.-B. (2013). Grid cells require excitatory drive from the hippocampus. *Nature Neuroscience*, 16:309–317.

[Bose et al., 2000] Bose, A., Booth, V., and Recce, M. (2000). A temporal mechanism for generating the phase precession of hippocampal place cells. *Journal of Computational Neuroscience*, 9(1):5–30.

[Bose and Recce, 2001] Bose, A. and Recce, M. (2001). Phase precession and phase-locking of hippocampal pyramidal cells. *Hippocampus*, 11(3):204–215.

[Brandon et al., 2011] Brandon, M. P., Bogaard, A. R., Libby, C. P., Connerney, M. A., Gupta, K., and Hasselmo, M. E. (2011). Reduction of Theta Rhythm Dissociates Grid Cell Spatial Periodicity from Directional Tuning. *Science*, 332(6029):595–599.

[Buetfering et al., 2014] Buetfering, C., Allen, K., and Monyer, H. (2014). Parvalbumin interneurons provide grid cell–driven recurrent inhibition in the medial entorhinal cortex. *Nature Neuroscience*, 17(5):710–718.

[Buonomano and Merzenich, 1998] Buonomano, D. V. and Merzenich, M. M. (1998). Cortical plasticity: From synapses to maps. *Annual Review of Neuroscience*, 21(1):149–186. PMID: 9530495.

[Burak and Fiete, 2009] Burak, Y. and Fiete, I. R. (2009). Accurate path integration in continuous attractor network models of grid cells. *PLoS Computational Biology*, 5(2):e1000291.

[Burgess et al., 2007] Burgess, N., Barry, C., and O'Keefe, J. (2007). An oscillatory interference model of grid cell firing. *Hippocampus*, 17(9):801–812.

[Burwell and Amaral, 1998] Burwell, R. D. and Amaral, D. G. (1998). Cortical afferents of the perirhinal, postrhinal, and entorhinal cortices of the rat. *The Journal of Comparative Neurology*, 398(2):179–205.

[Buzsáki, 2002] Buzsáki, G. (2002). Theta Oscillations in the Hippocampus. *Neuron*, 33(3):325–340.

[Buzsáki, 2006] Buzsáki, G. (2006). *Rhythms of the Brain*. Oxford University Press.

[Buzsáki and Draguhn, 2004] Buzsáki, G. and Draguhn, A. (2004). Neuronal oscillations in cortical networks. *Science*, 304(5679):1926.

[Buzsáki et al., 2013] Buzsáki, G., Logothetis, N., and Singer, W. (2013). Scaling brain size, keeping timing: Evolutionary preservation of brain rhythms. *Neuron*, 80(3):751–764.

[Buzsáki and Tingley, 2018] Buzsáki, G. and Tingley, D. (2018). Space and time: the hippocampus as a sequence generator. *Trends in Cognitive Sciences*, 22(10):853–869.

[Cappaert et al., 2015] Cappaert, N. L., Strien, N. M. V., and Witter, M. P. (2015). Chapter 20 - hippocampal formation. In Paxinos, G., editor, *The Rat Nervous System (Fourth Edition)*, pages 511 – 573. Academic Press, San Diego, fourth edition edition.

[Carpenter et al., 2017] Carpenter, F., Burgess, N., and Barry, C. (2017). Modulating medial septal cholinergic activity reduces medial entorhinal theta frequency without affecting speed or grid coding. *Scientific Reports*, 7(1).

[Cauter et al., 2012] Cauter, T. V., Camon, J., Alvernhe, A., Elduayen, C., Sargolini, F., and Save, E. (2012). Distinct roles of medial and lateral entorhinal cortex in spatial cognition. *Cerebral Cortex*, 23(2):451–459.

[Chadwick et al., 2016] Chadwick, A., van Rossum, M. C., and Nolan, M. F. (2016). Flexible theta sequence compression mediated via phase precessing interneurons. *eLife*, 5:e20349.

[Clouter et al., 2017] Clouter, A., Shapiro, K. L., and Hanslmayr, S. (2017). Theta phase synchronization is the glue that binds human associative memory. *Current Biology*, 27(20):3143–3148.e6.

[Colgin, 2011] Colgin, L. L. (2011). Oscillations and hippocampal–prefrontal synchrony. *Current Opinion in Neurobiology*, 21(3):467 – 474. Behavioural and cognitive neuroscience.

[Colgin, 2013] Colgin, L. L. (2013). Mechanisms and functions of theta rhythms. *Annual Review of Neuroscience*, pages 295–314.

[Couey et al., 2013] Couey, J. J., Witoelar, A., Zhang, S.-j., Zheng, K., Ye, J., Dunn, B., Czajkowski, R., Moser, M.-B., Moser, E. I., Roudi, Y., and Witter, M. P. (2013). Recurrent inhibitory circuitry as a mechanism for grid formation. *Nature Neuroscience*, 16(3):318–324.

[D'Albis and Kempter, 2017] D'Albis, T. and Kempter, R. (2017). A single-cell spiking model for the origin of grid-cell patterns. *PLOS Computational Biology*, 13(10):e1005782.

[DeCoteau et al., 2007] DeCoteau, W. E., Thorn, C., Gibson, D. J., Courtemanche, R., Mitra, P., Kubota, Y., and Graybiel, A. M. (2007). Learning-related coordination of striatal and hippocampal theta rhythms during acquisition of a procedural maze task. *Proceedings of the National Academy of Sciences*, 104(13):5644–5649.

[Dickinson et al., 1990] Dickinson, P. S., Mecsas, C., and Marder, E. (1990). Neuropeptide fusion of two motor-pattern generator circuits. *Nature*, 344(6262):155–158.

[Dickson et al., 2000] Dickson, C. T., Magistretti, J., Shalinsky, M. H., Fransén, E., Hasselmo, M. E., and Alonso, A. (2000). Properties and role of I(h) in the pacing of subthreshold oscillations in entorhinal cortex layer II neurons. *Journal of Neurophysiology*, 83(5):2562–2579.

[Diehl et al., 2017] Diehl, G. W., Hon, O. J., Leutgeb, S., and Leutgeb, J. K. (2017). Grid and nongrid cells in medial entorhinal cortex represent spatial location and

environmental features with complementary coding schemes. *Neuron*, 94(1):83–92.e6.

[Domnisoru et al., 2013] Domnisoru, C., Kinkhabwala, A. A., and Tank, D. W. (2013). Membrane potential dynamics of grid cells. *Nature*, 495(7440):199–204.

[Doppelmayr et al., 1998] Doppelmayr, M., Klimesch, W., Schwaiger, J., Auinger, P., and Winkler, T. (1998). Theta synchronization in the human eeg and episodic retrieval. *Neuroscience Letters*, 257(1):41 – 44.

[Dordek et al., 2016] Dordek, Y., Soudry, D., Meir, R., and Derdikman, D. (2016). Extracting grid cell characteristics from place cell inputs using non-negative principal component analysis. *eLife*, 5:e10094.

[Dragoi and Buzsáki, 2006] Dragoi, G. and Buzsáki, G. (2006). Temporal encoding of place sequences by hippocampal cell assemblies. *Neuron*, 50(1):145–157.

[Duffy et al., 2019] Duffy, A., Abe, E., Perkel, D. J., and Fairhall, A. L. (2019). Variation in sequence dynamics improves maintenance of stereotyped behavior in an example from bird song. *Proceedings of the National Academy of Sciences*, page 201815910.

[Ego-Stengel and Wilson, 2007] Ego-Stengel, V. and Wilson, M. A. (2007). Spatial selectivity and theta phase precession in CA1 interneurons. *Hippocampus*, 17(2):161–174.

[Eichenbaum, 2014] Eichenbaum, H. (2014). Time cells in the hippocampus: a new dimension for mapping memories. *Nature Reviews Neuroscience*, 15(11):732–744.

[Eichenbaum et al., 1999] Eichenbaum, H., Dudchenko, P., Wood, E., Shapiro, M., and Tanila, H. (1999). The hippocampus, memory, and place cells. *Neuron*, 23(2):209–226.

[Eliav et al., 2018] Eliav, T., Geva-Sagiv, M., Yartsev, M. M., Finkelstein, A., Rubin, A., Las, L., and Ulanovsky, N. (2018). Nonoscillatory phase coding and synchronization in the bat hippocampal formation. *Cell*, 175(4):1119–1130.

[Ermentrout et al., 2008] Ermentrout, G. B., Galán, R. F., and Urban, N. N. (2008). Reliability, synchrony and noise. *Trends in Neurosciences*, 31(8):428–434.

[Fell and Axmacher, 2011] Fell, J. and Axmacher, N. (2011). The role of phase synchronization in memory processes. *Nature Reviews Neuroscience*, 12(2):105–118.

[Fell et al., 2001] Fell, J., Klaver, P., Lehnertz, K., Grunwald, T., Schaller, C., Elger, C. E., and Fernández, G. (2001). Human memory formation is accompanied by rhinal-hippocampal coupling and decoupling. *Nature Neuroscience*, 4(12):1259–1264.

[Feng et al., 2015] Feng, T., Silva, D., and Foster, D. J. (2015). Dissociation between the experience-dependent development of hippocampal theta sequences and single-trial phase precession. *Journal of Neuroscience*, 35(12):4890–4902.

[Foster and Wilson, 2007] Foster, D. J. and Wilson, M. A. (2007). Hippocampal theta sequences. *Hippocampus*, 17(11):1093–1099.

[Frank et al., 2000] Frank, L. M., Brown, E. N., and Wilson, M. (2000). Trajectory encoding in the hippocampus and entorhinal cortex. *Neuron*, 27(1):169–178.

[Frank et al., 2001] Frank, L. M., Brown, E. N., and Wilson, M. A. (2001). A comparison of the firing properties of putative excitatory and inhibitory neurons from CA1 and the entorhinal cortex. *Journal of Neurophysiology*, 86(4):2029–2040.

[Fransén et al., 2004] Fransén, E., Alonso, A. A., Dickson, C. T., Magistretti, J., and Hasselmo, M. E. (2004). Ionic mechanisms in the generation of subthreshold oscillations and action potential clustering in entorhinal layer II stellate neurons. *Hippocampus*, 14(3):368–384.

[Fries, 2016] Fries, P. (2016). Rhythms for cognition: communication through coherence. *Neuron*, 88(1):220–235.

[Friesen, 1994] Friesen, W. O. (1994). Reciprocal inhibition: A mechanism underlying oscillatory animal movements. *Neuroscience & Biobehavioral Reviews*, 18(4):547–553.

[Fuchs et al., 2016] Fuchs, E. C., Neitz, A., Pinna, R., Melzer, S., Caputi, A., and Monyer, H. (2016). Local and distant input controlling excitation in layer II of the medial entorhinal cortex. *Neuron*, 89(1):194–208.

[Fuhrmann et al., 2015] Fuhrmann, F., Justus, D., Sosulina, L., Kaneko, H., Beutel, T., Friedrichs, D., Schoch, S., Schwarz, M. K., Fuhrmann, M., and Remy, S. (2015). Locomotion, theta oscillations, and the speed-correlated firing of hippocampal neurons are controlled by a medial septal glutamatergic circuit. *Neuron*, 86(5):1253–1264.

[Fujisawa and Buzsáki, 2011] Fujisawa, S. and Buzsáki, G. (2011). A 4 hz oscillation adaptively synchronizes prefrontal, VTA, and hippocampal activities. *Neuron*, 72(1):153–165.

[Fyhn et al., 2004] Fyhn, M., Molden, S., Witter, M. P., Moser, E. I., and Moser, M.-B. (2004). Spatial representation in the entorhinal cortex. *Science*, 305(5688):1258 LP – 1264.

[Getting, 1989] Getting, P. A. (1989). Emerging principles governing the operation of neural networks. *Annual Review of Neuroscience*, 12(1):185–204.

[Giocomo et al., 2011] Giocomo, L. M., Moser, M.-B., and Moser, E. I. (2011). Computational models of grid cells. *Neuron*, 71(4):589–603.

[Gonzalez-Sulser et al., 2014] Gonzalez-Sulser, A., Parthier, D., Candela, A., McClure, C., Pastoll, H., Garden, D., Sürmeli, G., and Nolan, M. F. (2014). GABAergic projections from the medial septum selectively inhibit interneurons in the medial entorhinal cortex. *The Journal of Neuroscience*, 34(50):16739 LP – 16743.

[Graubard et al., 1983] Graubard, K., Raper, J. A., and Hartline, D. K. (1983). Graded synaptic transmission between identified spiking neurons. *Journal of Neurophysiology*, 50(2):508–521.

[Gu et al., 2018] Gu, Y., Lewallen, S., Kinkhabwala, A. A., Domnisoru, C., Yoon, K., Gauthier, J. L., Fiete, I. R., and Tank, D. W. (2018). A map-like micro-organization of grid cells in the medial entorhinal cortex. *Cell*, 175(3):736–750.e30.

[Guanella et al., 2007] Guanella, A., Kiper, D., and Verschure, P. (2007). A model of grid cells based on a twisted torus topology. *International Journal of Neural Systems*, 17(04):231–240.

[Haas et al., 2006] Haas, J. S., Nowotny, T., and Abarbanel, H. (2006). Spike-timing-dependent plasticity of inhibitory synapses in the entorhinal cortex. *Journal of Neurophysiology*, 96(6):3305–3313.

[Hafting et al., 2008] Hafting, T., Fyhn, M., Bonnevie, T., Moser, M.-B., and Moser, E. I. (2008). Hippocampus-independent phase precession in entorhinal grid cells. *Nature*, 453(7199):1248–1252.

[Hafting et al., 2005] Hafting, T., Fyhn, M., Molden, S., Moser, M.-B., and Moser, E. I. (2005). Microstructure of a spatial map in the entorhinal cortex. *Nature*, 436(7052):801–6.

[Haken, 2008] Haken, H. (2008). *Brain Dynamics*. Springer Berlin Heidelberg.

[Hargreaves et al., 2007] Hargreaves, E. L., Yoganarasimha, D., and Knierim, J. J. (2007). Cohesiveness of spatial and directional representations recorded from neural ensembles in the anterior thalamus, parasubiculum, medial entorhinal cortex, and hippocampus. *Hippocampus*, 17(9):826–841.

[Harris-Warrick and Marder, 1991] Harris-Warrick, R. M. and Marder, E. (1991). Modulation of neural networks for behavior. *Annual Review of Neuroscience*, 14(1):39–57.

[Heggland et al., 2019] Heggland, I., Kvello, P., and Witter, M. P. (2019). Electrophysiological characterization of networks and single cells in the hippocampal region of a transgenic rat model of alzheimer's disease. *eNeuro*, 6(1).

[Heys and Hasselmo, 2012] Heys, J. G. and Hasselmo, M. E. (2012). Neuromodulation of ih in layer II medial entorhinal cortex stellate cells: A voltage-clamp study. *Journal of Neuroscience*, 32(26):9066–9072.

[Hinman et al., 2016] Hinman, J. R., Brandon, M. P., Climer, J. R., Chapman, G. W., and Hasselmo, M. E. (2016). Multiple running speed signals in medial entorhinal cortex. *Neuron*, 91(3):666–679. 27427460[pmid].

[Hinman et al., 2011] Hinman, J. R., Penley, S. C., Long, L. L., Escabí, M. A., and Chrobak, J. J. (2011). Septotemporal variation in dynamics of theta: speed and habituation. *Journal of Neurophysiology*, 105(6):2675–2686.

[Hölscher et al., 1997] Hölscher, C., Anwyl, R., and Rowan, M. J. (1997). Stimulation on the positive phase of hippocampal theta rhythm induces long-term potentiation that can be depotentiated by stimulation on the negative phase in area CA1in vivo. *The Journal of Neuroscience*, 17(16):6470–6477.

[Høydal et al., 2019] Høydal, Ø. A., Skytøen, E. R., Andersson, S. O., Moser, M.-B., and Moser, E. I. (2019). Object-vector coding in the medial entorhinal cortex. *Nature*, 568(7752):400–404.

[Huxter et al., 2003] Huxter, J., Burgess, N., and OKeefe, J. (2003). Independent rate and temporal coding in hippocampal pyramidal cells. *Nature*, 425(6960):828–832.

[Huxter et al., 2008] Huxter, J. R., Senior, T. J., Allen, K., and Csicsvari, J. (2008). Theta phase–specific codes for two-dimensional position, trajectory and heading in the hippocampus. *Nature Neuroscience*, 11(5):587–594.

[Igarashi, 2015] Igarashi, K. M. (2015). Plasticity in oscillatory coupling between hippocampus and cortex. *Current Opinion in Neurobiology*, 35:163–168.

[Jeewajee et al., 2008] Jeewajee, A., Barry, C., O'Keefe, J., and Burgess, N. (2008). Grid cells and theta as oscillatory interference: Electrophysiological data from freely moving rats. *Hippocampus*, 18(12):1175–1185.

[Jensen and Lisman, 2000] Jensen, O. and Lisman, J. E. (2000). Position reconstruction from an ensemble of hippocampal place cells: Contribution of theta phase coding. *Journal of Neurophysiology*, 83(5):2602–2609. PMID: 10805660.

[Jones and Wilson, 2005a] Jones, M. W. and Wilson, M. A. (2005a). Phase precession of medial prefrontal cortical activity relative to the hippocampal theta rhythm. *Hippocampus*, 15(7):867–873.

[Jones and Wilson, 2005b] Jones, M. W. and Wilson, M. A. (2005b). Theta rhythms coordinate hippocampal–prefrontal interactions in a spatial memory task. *PLOS Biology*, 3(12).

[Justus et al., 2016] Justus, D., Dalügge, D., Bothe, S., Fuhrmann, F., Hannes, C., Kaneko, H., Friedrichs, D., Sosulina, L., Schwarz, I., Elliott, D. A., Schoch, S., Bradke, F., Schwarz, M. K., and Remy, S. (2016). Glutamatergic synaptic integration of locomotion speed via septoentorhinal projections. *Nature Neuroscience*, 20(1):16–19.

[Kay, 2005] Kay, L. M. (2005). Theta oscillations and sensorimotor performance. *Proceedings of the National Academy of Sciences*, 102(10):3863–3868.

[Kayser et al., 2009] Kayser, C., Montemurro, M. A., Logothetis, N. K., and Panzeri, S. (2009). Spike-phase coding boosts and stabilizes information carried by spatial and temporal spike patterns. *Neuron*, 61(4):597–608.

[Keene et al., 2016] Keene, C. S., Bladon, J., McKenzie, S., Liu, C. D., OKeefe, J., and Eichenbaum, H. (2016). Complementary functional organization of neuronal activity patterns in the perirhinal, lateral entorhinal, and medial entorhinal cortices. *The Journal of Neuroscience*, 36(13):3660–3675.

[Kenet et al., 2003] Kenet, T., Bibitchkov, D., Tsodyks, M., Grinvald, A., and Arieli, A. (2003). Spontaneously emerging cortical representations of visual attributes. *Nature*, 425(6961):954–956.

[Kerr et al., 2007] Kerr, K. M., Agster, K. L., Furtak, S. C., and Burwell, R. D. (2007). Functional neuroanatomy of the parahippocampal region: The lateral and medial entorhinal areas. *Hippocampus*, 17(9):697–708.

[Kim and Lee, 2011] Kim, J. and Lee, I. (2011). Neural Correlates of Object-in-Place Learning in Hippocampus and Prefrontal Cortex. *Journal of Neuroscience*, 31(47):16991–17006.

[Kim and Linden, 2007] Kim, S. J. and Linden, D. J. (2007). Ubiquitous plasticity and memory storage. *Neuron*, 56(4):582–592.

[Klimesch, 1999] Klimesch, W. (1999). EEG alpha and theta oscillations reflect cognitive and memory performance: a review and analysis. *Brain Research Reviews*, 29(2-3):169–195.

[Klink and Alonso, 1993] Klink, R. and Alonso, A. (1993). Ionic mechanisms for the subthreshold oscillations and differential electroresponsiveness of medial entorhinal cortex layer ii neurons. *Journal of Neurophysiology*, 70(1):144–157.

[Koenig et al., 2011] Koenig, J., Linder, A. N., Leutgeb, J. K., and Leutgeb, S. (2011). The spatial periodicity of grid cells. *Science*, 592(Issue: 6029):592–595.

[Kornienko et al., 2018] Kornienko, O., Latuske, P., Bassler, M., Kohler, L., and Allen, K. (2018). Non-rhythmic head-direction cells in the parahippocampal region are not constrained by attractor network dynamics. *eLife*, 7.

[Korotkova et al., 2018] Korotkova, T., Ponomarenko, A., Monaghan, C. K., Poulter, S. L., Cacucci, F., Wills, T., Hasselmo, M. E., and Lever, C. (2018). Reconciling the different faces of hippocampal theta: The role of theta oscillations in cognitive, emotional and innate behaviors. *Neuroscience Biobehavioral Reviews*, 85:65 – 80. SI: 2016 IBNS Meeting.

[Kreuz et al., 2013] Kreuz, T., Chicharro, D., Houghton, C., Andrzejak, R. G., and Mormann, F. (2013). Monitoring spike train synchrony. *Journal of Neurophysiology*, 109(5):1457–1472.

[Kropff et al., 2015] Kropff, E., Carmichael, J. E., Moser, M.-B., and Moser, E. I. (2015). Speed cells in the medial entorhinal cortex. *Nature*, 523(7561):419–424.

[Kropff and Treves, 2008] Kropff, E. and Treves, A. (2008). The emergence of grid cells: Intelligent design or just adaptation? *Hippocampus*, 18(12):1256–1269.

[Krupic et al., 2015] Krupic, J., Bauza, M., Burton, S., Barry, C., and O'Keefe, J. (2015). Grid cell symmetry is shaped by environmental geometry. *Nature*, 518(7538):232–235.

[Landau et al., 2015] Landau, A., Schreyer, H., van Pelt, S., and Fries, P. (2015). Distributed attention is implemented through theta-rhythmic gamma modulation. *Current Biology*, 25(17):2332 – 2337.

[Larson et al., 1986] Larson, J., Wong, D., and Lynch, G. (1986). Patterned stimulation at the theta frequency is optimal for the induction of hippocampal long-term potentiation. *Brain Research*, 368(2):347–350.

[Lengyel et al., 2003] Lengyel, M., Szatmáry, Z., and Érdi, P. (2003). Dynamically detuned oscillations account for the coupled rate and temporal code of place cell firing. *Hippocampus*, 13(6):700–714.

[Liebe et al., 2012] Liebe, S., Hoerzer, G. M., Logothetis, N. K., and Rainer, G. (2012). Theta coupling between V4 and prefrontal cortex predicts visual short-term memory performance. *Nature Neuroscience*, 15(3):456–462.

[Lisman and Redish, 2009] Lisman, J. and Redish, A. (2009). Prediction, sequences and the hippocampus. *Philosophical Transactions of the Royal Society B: Biological Sciences*, 364(1521):1193–1201.

[Lu et al., 2006] Lu, J., Sherman, D., Devor, M., and Saper, C. B. (2006). A putative flip–flop switch for control of REM sleep. *Nature*, 441(7093):589–594.

[Magistretti and Alonso, 1999] Magistretti, J. and Alonso, A. (1999). Biophysical properties and slow voltage-dependent inactivation of a sustained sodium current in entorhinal cortex layer-II principal neurons. *The Journal of General Physiology*, 114(4):491–509.

[Magistretti and Alonso, 2002] Magistretti, J. and Alonso, A. (2002). Fine gating properties of channels responsible for persistent sodium current generation in entorhinal cortex neurons. *The Journal of General Physiology*, 120(6):855–873.

[Magistretti et al., 1999] Magistretti, J., Ragsdale, D. S., and Alonso, A. (1999). High conductance sustained single-channel activity responsible for the low-threshold persistent nacurrent in entorhinal cortex neurons. *The Journal of Neuroscience*, 19(17):7334–7341.

[Maurer and McNaughton, 2007] Maurer, A. P. and McNaughton, B. L. (2007). Network and intrinsic cellular mechanisms underlying theta phase precession of hippocampal neurons. *Trends in Neurosciences*, 30(7):325–333.

[McNaughton et al., 1996] McNaughton, B. L., Barnes, C. A., Gerrard, J. L., Gothard, K., Jung, M. W., Knierim, J. J., Kudrimoti, H., Qin, Y., Skaggs, W. E., Suster, M., and Weaver, K. L. (1996). Deciphering the hippocampal polyglot: the hippocampus as a path integration system. *Journal of Experimental Biology*, 199(1):173–185.

[McNaughton et al., 2006] McNaughton, B. L., Battaglia, F. P., Jensen, O., Moser, E. I., and Moser, M.-B. (2006). Path integration and the neural basis of the cognitive map. *Nature Reviews Neuroscience*, 7(8):663–678.

[Mehta et al., 1997] Mehta, M. R., Barnes, C. A., and McNaughton, B. L. (1997). Experience-dependent, asymmetric expansion of hippocampal place fields. *Proceedings of the National Academy of Sciences*, 94(16):8918–8921.

[Mehta et al., 2002] Mehta, M. R., Lee, A. K., and Wilson, M. A. (2002). Role of experience and oscillations in transforming a rate code into a temporal code. *Nature*, 417(6890):741–746.

[Miao et al., 2017] Miao, C., Cao, Q., Moser, M.-B., and Moser, E. I. (2017). Parvalbumin and somatostatin interneurons control different space-coding networks in the medial entorhinal cortex. *Cell*, 171(3):507–521.e17.

[Mitchell et al., 1982] Mitchell, S. J., Rawlins, J. N., Steward, O., and Olton, D. S. (1982). Medial septal area lesions disrupt theta rhythm and cholinergic staining in medial entorhinal cortex and produce impaired radial arm maze behavior in rats. *Journal of Neuroscience*, 2(3):292–302.

[Mittal and Narayanan, 2018] Mittal, D. and Narayanan, R. (2018). Degeneracy in the robust expression of spectral selectivity, subthreshold oscillations, and intrinsic excitability of entorhinal stellate cells. *Journal of Neurophysiology*, 120(2):576–600. PMID: 29718802.

[Mizuseki et al., 2009] Mizuseki, K., Sirota, A., Pastalkova, E., and Buzsáki, G. (2009). Theta oscillations provide temporal windows for local circuit computation in the entorhinal-hippocampal loop. *Neuron*, 64(2):267–280. 19874793[pmid].

[Modi et al., 2014] Modi, M. N., Dhawale, A. K., and Bhalla, U. S. (2014). CA1 cell activity sequences emerge after reorganization of network correlation structure during associative learning. *eLife*, 3.

[Moser et al., 2017] Moser, E. I., Moser, M.-B., and McNaughton, B. L. (2017). Spatial representation in the hippocampal formation: a history. *Nature Neuroscience*, 20:1448 EP –.

[Moser et al., 2014] Moser, E. I., Roudi, Y., Witter, M. P., Kentros, C., Bonhoeffer, T., and Moser, M.-B. (2014). Grid cells and cortical representation. *Nature Reviews Neuroscience*, 15:466 EP –. Review Article.

[Mulansky and Kreuz, 2016] Mulansky, M. and Kreuz, T. (2016). PySpike—A Python library for analyzing spike train synchrony. *SoftwareX*, 5:183–189.

[N et al., 1979] N, R. J., J, F., and A, G. J. (1979). Septo-hippocampal connections and the hippocampal theta rhythm. *Experimental brain research*, 37(1):49–63.

[Najafi et al., 2018] Najafi, F., Elsayed, G. F., Cao, R., Pnevmatikakis, E., Latham, P. E., Cunningham, J. P., and Churchland, A. K. (2018). Excitatory and inhibitory subnetworks are equally selective during decision-making and emerge simultaneously during learning. *bioRxiv*.

[Narayanan and Johnston, 2010] Narayanan, R. and Johnston, D. (2010). ThehCurrent is a candidate mechanism for regulating the sliding modification threshold in a BCM-like synaptic learning rule. *Journal of Neurophysiology*, 104(2):1020–1033.

[Navratilova et al., 2011] Navratilova, Z., Giocomo, L. M., Fellous, J.-M., Hasselmo, M. E., and McNaughton, B. L. (2011). Phase precession and variable spatial scaling in a periodic attractor map model of medial entorhinal grid cells with realistic after-spike dynamics. *Hippocampus*, 22(4):772–789.

[Naya, 2001] Naya, Y. (2001). Backward spreading of memory-retrieval signal in the primate temporal cortex. *Science*, 291(5504):661–664.

[Nilssen et al., 2018] Nilssen, X. E. S., Jacobsen, X. B., Fjeld, G., Nair, R. R., Blankvoort, X. S., Kentros, X. C., and Witter, X. M. P. (2018). Inhibitory connectivity dominates the fan cell network in layer II of lateral entorhinal cortex. *Journal of Neuroscience*, 38(45):9712–9727.

[Ohara et al., 2018] Ohara, S., Onodera, M., Simonsen, Ø. W., Yoshino, R., Hioki, H., Iijima, T., Tsutsui, K.-I., and Witter, M. P. (2018). Intrinsic projections of layer vb neurons to layers va, III, and II in the lateral and medial entorhinal cortex of the rat. *Cell Reports*, 24(1):107–116.

[O'Keefe, 1976] O'Keefe, J. (1976). Place units in the hippocampus of the freely moving rat. *Experimental Neurology*, 51(1):78–109.

[OKeefe and Burgess, 2005] OKeefe, J. and Burgess, N. (2005). Dual phase and rate coding in hippocampal place cells: Theoretical significance and relationship to entorhinal grid cells. *Hippocampus*, 15(7):853–866.

[OKeefe and Recce, 1993] OKeefe, J. and Recce, M. L. (1993). Phase relationship between hippocampal place units and the EEG theta rhythm. *Hippocampus*, 3(3):317–330.

[Panzeri et al., 2010] Panzeri, S., Brunel, N., Logothetis, N. K., and Kayser, C. (2010). Sensory neural codes using multiplexed temporal scales. *Trends in Neurosciences*, 33(3):111–120.

[Pastalkova et al., 2008] Pastalkova, E., Itskov, V., Amarasingham, A., and Buzsaki, G. (2008). Internally generated cell assembly sequences in the rat hippocampus. *Science*, 321(5894):1322–1327.

[Pastoll et al., 2019] Pastoll, H., Garden, D., Papastathopoulos, I., Sürmeli, G., and Nolan, M. F. (2019). Inter- and intra-animal variation of integrative properties of stellate cells in the medial entorhinal cortex. *bioRxiv*.

[Pastoll et al., 2012] Pastoll, H., Ramsden, H., and Nolan, M. (2012). Intrinsic electrophysiological properties of entorhinal cortex stellate cells and their contribution to grid cell firing fields. *Frontiers in Neural Circuits*, 6:17.

[qiang Bi and ming Poo, 1998] qiang Bi, G. and ming Poo, M. (1998). Synaptic modifications in cultured hippocampal neurons: Dependence on spike timing, synaptic strength, and postsynaptic cell type. *The Journal of Neuroscience*, 18(24):10464–10472.

[Rabinovich et al., 2006] Rabinovich, M. I., Varona, P., Selverston, A. I., and Abarbanel, H. D. I. (2006). Dynamical principles in neuroscience. *Reviews of Modern Physics*, 78(4):1213–1265.

[Ray et al., 2014] Ray, S., Naumann, R., Burgalossi, A., Tang, Q., Schmidt, H., and Brecht, M. (2014). Grid-layout and theta-modulation of layer 2 pyramidal neurons in medial entorhinal cortex. *Science*, page 1243028.

[Reifenstein et al., 2012] Reifenstein, E. T., Kempter, R., Schreiber, S., Stemmler, M. B., and Herz, A. V. M. (2012). Grid cells in rat entorhinal cortex encode physical space with independent firing fields and phase precession at the single-trial level. *Proceedings of the National Academy of Sciences*, 109(16):6301–6306.

[Reinhart et al., 2015] Reinhart, R. M. G., Zhu, J., Park, S., and Woodman, G. F. (2015). Synchronizing theta oscillations with direct-current stimulation strengthens adaptive control in the human brain. *Proceedings of the National Academy of Sciences*, 112(30).

[Remme et al., 2010] Remme, M. W., Lengyel, M., and Gutkin, B. S. (2010). Democracy-independence trade-off in oscillating dendrites and its implications for grid cells. *Neuron*, 66(3):429–437.

[Remondes and Wilson, 2013] Remondes, M. and Wilson, M. A. (2013). Cingulate-hippocampus coherence and trajectory coding in a sequential choice task. *Neuron*, 80(5):1277–1289.

[Rizzuto et al., 2003] Rizzuto, D. S., Madsen, J. R., Bromfield, E. B., Schulze-Bonhage, A., Seelig, D., Aschenbrenner-Scheibe, R., and Kahana, M. J. (2003). Reset of human neocortical oscillations during a working memory task. *Proceedings of the National Academy of Sciences*, 100(13):7931–7936.

[Robbe et al., 2006] Robbe, D., Montgomery, S. M., Thome, A., Rueda-Orozco, P. E., McNaughton, B. L., and Buzsaki, G. (2006). Cannabinoids reveal importance of spike timing coordination in hippocampal function. *Nature Neuroscience*, 9(12):1526–1533.

[Robinson et al., 2017] Robinson, N. T., Priestley, J. B., Rueckemann, J. W., Garcia, A. D., Smeglin, V. A., Marino, F. A., and Eichenbaum, H. (2017). Medial entorhinal cortex selectively supports temporal coding by hippocampal neurons. *Neuron*, 94(3):677–688.e6.

[Rotstein et al., 2006] Rotstein, H. G., Oppermann, T., White, J. a., and Kopell, N. (2006). The dynamic structure underlying subthreshold oscillatory activity and the onset of spikes in a model of medial entorhinal cortex stellate cells. *Journal of Computational Neuroscience*, 21(2006):271–292.

[Rotstein et al., 2008] Rotstein, H. G., Wechselberger, M., and Kopell, N. (2008). Canard induced mixed-mode oscillations in a medial entorhinal cortex layer ii stellate cell model. *SIAM Journal on Applied Dynamical Systems*, 7(4):1582–1611.

[Rowland et al., 2018] Rowland, D. C., Obenhaus, H. A., Skytøen, E. R., Zhang, Q., Kentros, C. G., Moser, E. I., and Moser, M.-B. (2018). Functional properties of stellate cells in medial entorhinal cortex layer II. *eLife*, 7:1–17.

[Royer et al., 2012] Royer, S., Zemelman, B. V., Losonczy, A., Kim, J., Chance, F., Magee, J. C., and Buzsáki, G. (2012). Control of timing, rate and bursts of hippocampal place cells by dendritic and somatic inhibition. *Nature Neuroscience*, 15(5):769–775.

[Samsonovich and McNaughton, 1997] Samsonovich, A. and McNaughton, B. L. (1997). Path integration and cognitive mapping in a continuous attractor neural network model. *The Journal of Neuroscience*, 17(15):5900–5920.

[Sargolini et al., 2006] Sargolini, F., Fyhn, M., Hafting, T., McNaughton, B. L., Witter, M. P., Moser, M.-B., and Moser, E. I. (2006). Conjunctive representation of position, direction, and velocity in entorhinal cortex. *Science*, 312(5774):758–762.

[Schmidt et al., 2017] Schmidt, H., Gour, A., Straehle, J., Boergens, K. M., Brecht, M., and Helmstaedter, M. (2017). Axonal synapse sorting in medial entorhinal cortex. *Nature*, 549(7673):469–475.

[Schmidt et al., 2009] Schmidt, R., Diba, K., Leibold, C., Schmitz, D., Buzsaki, G., and Kempter, R. (2009). Single-trial phase precession in the hippocampus. *Journal of Neuroscience*, 29(42):13232–13241.

[Schmidt-Hieber et al., 2017] Schmidt-Hieber, C., Toleikyte, G., Aitchison, L., Roth, A., Clark, B. A., Branco, T., and Häusser, M. (2017). Active dendritic integration as a mechanism for robust and precise grid cell firing. *Nature Neuroscience*, 20(8):1114–1121.

[Schönfeld and Wiskott, 2015] Schönfeld, F. and Wiskott, L. (2015). Modeling place field activity with hierarchical slow feature analysis. *Frontiers in computational neuroscience*, 9:51–51. 26052279[pmid].

[Scoville and Milner, 1957] Scoville, W. B. and Milner, B. (1957). Loss of recent memory after bilateral hippocampal lesions. *Journal of Neurology, Neurosurgery & Psychiatry*, 20(1):11–21.

[Selverston et al., 1998] Selverston, A., Elson, R., Rabinovich, M., Huerta, R., and Abarbanel, H. (1998). Basic principles for generating motor output in the stomatogastric ganglion. *Annals of the New York Academy of Sciences*, 860(1 NEURONAL MECH):35–50.

[Shay et al., 2016] Shay, C. F., Ferrante, M., Chapman 4th, G. W., and Hasselmo, M. E. (2016). Rebound spiking in layer II medial entorhinal cortex stellate cells: Possible mechanism of grid cell function. *Neurobiology of learning and memory*, 129:83–98.

[Shilnikov and Maurer, 2016] Shilnikov, A. L. and Maurer, A. P. (2016). The art of grid fields: geometry of neuronal time. *Frontiers in Neural Circuits*, 10(March):1–16.

[Shipston-Sharman et al., 2016] Shipston-Sharman, O., Solanka, L., and Nolan, M. F. (2016). Continuous attractor network models of grid cell firing based on excitatory–inhibitory interactions. *The Journal of Physiology*, 594(22):6547–6557.

[Shouval et al., 2002] Shouval, H. Z., Bear, M. F., and Cooper, L. N. (2002). A unified model of NMDA receptor-dependent bidirectional synaptic plasticity. *Proceedings of the National Academy of Sciences*, 99(16):10831–10836.

[Siegle and Wilson, 2014] Siegle, J. H. and Wilson, M. A. (2014). Enhancement of encoding and retrieval functions through theta phase-specific manipulation of hippocampus. *eLife*, 3.

[Skaggs et al., 1996] Skaggs, W. E., McNaughton, B. L., Wilson, M. A., and Barnes, C. A. (1996). Theta phase precession in hippocampal neuronal populations and the compression of temporal sequences. *Hippocampus*, 6(2):149–172.

[Skinner, 1974] Skinner, B. (1974). *About behaviorism.* Alfred A. Knopf.

[Skinner et al., 1994] Skinner, F. K., Gramoll, S., Calabrese, R. L., Kopell, N., and Marder, E. (1994). Frequency control in biological half-center oscillators. In *Computation in Neurons and Neural Systems*, pages 223–228. Springer US.

[Solanka et al., 2015] Solanka, L., van Rossum, M. C., and Nolan, M. F. (2015). Noise promotes independent control of gamma oscillations and grid firing within recurrent attractor networks. *eLife*, 4:e06444.

[Solstad et al., 2008] Solstad, T., Boccara, C. N., Kropff, E., Moser, M.-b., and Moser, E. I. (2008). Representation of geometric borders in the entorhinal cortex. *Science*, 1109(December):1865–1869.

[Song, 2005] Song, P. (2005). Angular path integration by moving "hill of activity": A spiking neuron model without recurrent excitation of the head-direction system. *Journal of Neuroscience*, 25(4):1002–1014.

[Stangl et al., 2018] Stangl, M., Achtzehn, J., Huber, K., Dietrich, C., Tempelmann, C., and Wolbers, T. (2018). Compromised grid-cell-like representations in old age as a key mechanism to explain age-related navigational deficits. *Current Biology*, 28(7):1108–1115.e6.

[Stensola et al., 2012] Stensola, H., Stensola, T., Solstad, T., FrØland, K., Moser, M. B., and Moser, E. I. (2012). The entorhinal grid map is discretized. *Nature*, 492(7427):72–78.

[Steriade, 2001] Steriade, M. (2001). Impact of Network Activities on Neuronal Properties in Corticothalamic Systems. *Journal of Neurophysiology*, 86(1):1–39.

[Takehara-Nishiuchi et al., 2012] Takehara-Nishiuchi, K., Maal-Bared, G., and Morrissey, M. D. (2012). Increased entorhinal–prefrontal theta synchronization parallels decreased entorhinal–hippocampal theta synchronization during learning and consolidation of associative Memory. *Frontiers in Behavioral Neuroscience*, 5(January):1–13.

[Tendler and Wagner, 2015] Tendler, A. and Wagner, S. (2015). Different types of theta rhythmicity are induced by social and fearful stimuli in a network associated with social memory. *eLife*, 4:e03614.

[Tiesinga et al., 2004] Tiesinga, P. H., Fellous, J.-M., Salinas, E., José, J. V., and Sejnowski, T. J. (2004). Synchronization as a mechanism for attentional gain modulation. *Neurocomputing*, 58-60:641–646.

[Tocker et al., 2015] Tocker, G., Barak, O., and Derdikman, D. (2015). Grid cells correlation structure suggests organized feedforward projections into superficial layers of the medial entorhinal cortex. *Hippocampus*, 25(12):1599–1613.

[Tolman, 1948] Tolman, E. C. (1948). Cognitive maps in rats and men. *Psychological review*, 55(4):189.

[Tremblay et al., 2016] Tremblay, R., Lee, S., and Rudy, B. (2016). GABAergic interneurons in the neocortex: From cellular properties to circuits. *Neuron*, 91(2):260–292.

[Tsanov, 2017] Tsanov, M. (2017). Speed and oscillations: Medial septum integration of attention and navigation. *Frontiers in Systems Neuroscience*, 11.

[Tsodyks et al., 1996] Tsodyks, M. V., Skaggs, W. E., Sejnowski, T. J., and McNaughton, B. L. (1996). Population dynamics and theta rhythm phase precession of hippocampal place cell firing: A spiking neuron model. *Hippocampus*, 6(3):271–280.

[Unal et al., 2015] Unal, G., Joshi, A., Viney, T. J., Kis, V., and Somogyi, P. (2015). Synaptic targets of medial septal projections in the hippocampus and extrahippocampal cortices of the mouse. *Journal of Neuroscience*, 35(48):15812–15826.

[Valerio and Taube, 2012] Valerio, S. and Taube, J. S. (2012). Path integration: how the head direction signal maintains and corrects spatial orientation. *Nature Neuroscience*, 15(10):1445–1453.

[van der Meer and Redish, 2011] van der Meer, M. A. A. and Redish, A. D. (2011). Theta phase precession in rat ventral striatum links place and reward information. *Journal of Neuroscience*, 31(8):2843–2854.

[Vanderwolf, 1969] Vanderwolf, C. (1969). Hippocampal electrical activity and voluntary movement in the rat. *Electroencephalography and Clinical Neurophysiology*, 26(4):407–418.

[Varela et al., 2013] Varela, C., Kumar, S., Yang, J. Y., and Wilson, M. A. (2013). Anatomical substrates for direct interactions between hippocampus, medial prefrontal cortex, and the thalamic nucleus reuniens. *Brain Structure and Function*, 219(3):911–929.

[Vertes and Kocsis, 1997] Vertes, R. P. and Kocsis, B. (1997). Brainstem – diencephalo-septohippocampal systems controlling the theta rhythm of the hippocampus. *Neuroscience*, 81(4):893–926.

[Wahlstrom et al., 2018] Wahlstrom, K. L., Huff, M. L., Emmons, E. B., Freeman, J. H., Narayanan, N. S., McIntyre, C. K., and LaLumiere, R. T. (2018). Basolateral amygdala inputs to the medial entorhinal cortex selectively modulate the consolidation of spatial and contextual learning. *The Journal of Neuroscience*, 38(11):2698–2712.

[Wang, 1996] Wang, X.-J. (1996). Gamma oscillation by synaptic inhibition in a hippocampal interneuronal network model. *Journal of Neuroscience*, 16(20):6402–6413.

[Wang and Rinzel, 1992] Wang, X.-J. and Rinzel, J. (1992). Alternating and synchronous rhythms in reciprocally inhibitory model neurons. *Neural Computation*, 4(1):84–97.

[Weber and Sprekeler, 2018] Weber, S. N. and Sprekeler, H. (2018). Learning place cells, grid cells and invariances with excitatory and inhibitory plasticity. *eLife*, 7.

[Weimann et al., 1991] Weimann, J. M., Meyrand, P., and Marder, E. (1991). Neurons that form multiple pattern generators: identification and multiple activity patterns of gastric/pyloric neurons in the crab stomatogastric system. *Journal of Neurophysiology*, 65(1):111–122.

[Weiss et al., 2017] Weiss, S., Talhami, G., Gofman-Regev, X., Rapoport, S., Eilam, D., and Derdikman, D. (2017). Consistency of spatial representations in rat entorhinal cortex predicts performance in a reorientation task. *Current Biology*, 27(23):3658–3665.e4.

[Wernle et al., 2018] Wernle, T., Waaga, T., Mørreaunet, M., Treves, A., Moser, M. B., and Moser, E. I. (2018). Integration of grid maps in merged environments. *Nature Neuroscience*, 21(1):92–105.

[Wilent and Nitz, 2007] Wilent, W. B. and Nitz, D. A. (2007). Discrete place fields of hippocampal formation interneurons. *Journal of Neurophysiology*, 97(6):4152–4161.

[Wilson et al., 2013] Wilson, D. I. G., Langston, R. F., Schlesiger, M. I., Wagner, M., Watanabe, S., and Ainge, J. A. (2013). Lateral entorhinal cortex is critical for novel object-context recognition. *Hippocampus*, 23(5):352–366. 23389958[pmid].

[Wilson and McNaughton, 1993] Wilson, M. and McNaughton, B. (1993). Dynamics of the hippocampal ensemble code for space. *Science*, 261(5124):1055–1058.

[Wilson et al., 2015] Wilson, M. A., Varela, C., and Remondes, M. (2015). Phase organization of network computations. *Current Opinion in Neurobiology*, 31:250–253.

[Winterer et al., 2017] Winterer, J., Maier, N., Wozny, C., Beed, P., Breustedt, J., Evangelista, R., Peng, Y., D'Albis, T., Kempter, R., and Schmitz, D. (2017). Excitatory microcircuits within superficial layers of the medial entorhinal cortex. *Cell Reports*, 19(6):1110–1116.

[Witter et al., 2017] Witter, M. P., Doan, T. P., Jacobsen, B., Nilssen, E. S., and Ohara, S. (2017). Architecture of the entorhinal cortex: a review of entorhinal anatomy in rodents with some comparative notes. *Frontiers in Systems Neuroscience*, 11(June):1–12.

[Womelsdorf et al., 2007] Womelsdorf, T., Schoffelen, J.-M., Oostenveld, R., Singer, W., Desimone, R., Engel, A. K., and Fries, P. (2007). Modulation of neuronal interactions through neuronal synchronization. *Science*, 316(5831):1609–1612.

[Wouterlood et al., 1995] Wouterlood, F. G., Härtig, W., Brückner, G., and Witter, M. P. (1995). Parvalbumin-immunoreactive neurons in the entorhinal cortex of the rat: localization, morphology, connectivity and ultrastructure. *Journal of Neurocytology*, 24(2):135–153.

[Yamaguchi et al., 2007] Yamaguchi, Y., Sato, N., Wagatsuma, H., Wu, Z., Molter, C., and Aota, Y. (2007). A unified view of theta-phase coding in the entorhinal–hippocampal system. *Current Opinion in Neurobiology*, 17(2):197–204.

[Yartsev et al., 2011] Yartsev, M. M., Witter, M. P., and Ulanovsky, N. (2011). Grid cells without theta oscillations in the entorhinal cortex of bats. *Nature*, 479(7371):103–107.

[Yoon et al., 2016] Yoon, K., Lewallen, S., Kinkhabwala, A. A., Tank, D. W., Fiete, I. R., Yoon, K., Lewallen, S., Kinkhabwala, A. A., Tank, D. W., and Fiete, I. R. (2016). Grid cell Responses in 1D environments assessed as slices through a 2D Lattice. *Neuron*, 89(5):1086–1099.

[Zhang and Abbott, 2000] Zhang, J. and Abbott, L. F. (2000). Chapter 84 - gain modulation of recurrent networks. In Bower, J., editor, *Computational neuroscience: Trends in research 2000*, pages 623 – 628. Elsevier, The Netherlands, first edition edition.

[Zhang, 1996] Zhang, K. (1996). Representation of spatial orientation by the intrinsic dynamics of the head-direction cell ensemble: a theory. *The Journal of Neuroscience*, 16(6):2112–2126.

[Zilli, 2012] Zilli, E. A. (2012). Models of grid cell spatial firing published 2005–2011. *Frontiers in Neural Circuits*, 6.

[Zilli and Hasselmo, 2010] Zilli, E. A. and Hasselmo, M. E. (2010). Coupled noisy spiking neurons as velocity-controlled oscillators in a model of grid cell spatial firing. *Journal of Neuroscience*, 30(41):13850–13860.

[Zutshi et al., 2018] Zutshi, I., Fu, M. L., Lilascharoen, V., Leutgeb, J. K., Lim, B. K., and Leutgeb, S. (2018). Recurrent circuits within medial entorhinal cortex superficial layers support grid cell firing. *Nature Communications*, 9(1).

[Ólafsdóttir et al., 2018] Ólafsdóttir, H. F., Bush, D., and Barry, C. (2018). The role of hippocampal replay in memory and planning. *Current Biology*, 28(1):R37 – R50.